

AMERICAN UNIVERSITY OF BEIRUT

EFFECTIVE INCORPORATION OF ASPHALT MIXTURE
PROPERTIES IN THE STRUCTURAL DESIGN OF
ASPHALT PAVEMENTS AS A PRECURSOR FOR
IMPLEMENTING PERFORMANCE-BASED DESIGN

by
YARA SALIM HAMDAR

A thesis
submitted in partial fulfillment of the requirements
for the degree of Master of Engineering
to the Department of Civil and Environmental Engineering
of the Faculty of Engineering and Architecture
at the American University of Beirut

Beirut, Lebanon
April 2016

AMERICAN UNIVERSITY OF BEIRUT

EFFECTIVE INCORPORATION OF ASPHALT MIXTURE
PROPERTIES IN THE STRUCTURAL DESIGN OF
ASPHALT PAVEMENTS AS A PRECURSOR FOR
IMPLEMENTING PERFORMANCE-BASED DESIGN

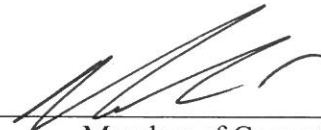
by
YARA SALIM HAMDAR

Approved by:



Dr. Ghassan Chehab, Associate Professor
Department of Civil and Environmental Engineering

Advisor



Dr. Mohamed-Asem Abdul Malak, Professor
Department of Civil and Environmental Engineering

Member of Committee



Dr. Ibrahim Alameddine, Assistant Professor
Department of Civil and Environmental Engineering

Member of Committee

AMERICAN UNIVERSITY OF BEIRUT

thesis, dissertation, project release form

Student Name: Hamdar Yara Salim
Last First Middle

Master's Thesis

Master's Project

Doctoral Dissertation

I authorize the American University of Beirut to: (a) reproduce hard or electronic copies of my thesis, dissertation, or project; (b) include such copies in the archives and digital repositories of the University; and (c) make freely available such copies to third parties for research or educational purposes.

I authorize the American University of Beirut, **three years after the date of submitting my thesis, dissertation, or project**, to: (a) reproduce hard or electronic copies of it; (b) include such copies in the archives and digital repositories of the University; and (c) make freely available such copies to third parties for research or educational purposes.

Mara Hamdar May 4, 2016
Signature Date

ACKNOWLEDGMENTS

First and foremost, thanks and praise to God. Looking back at the past two years, His work in my personal and professional life has manifested through all the ‘coincidences’, pleasant or otherwise, without which the work presented in this thesis would not have been possible.

To my family: you have been my daily companions in this journey. You dealt with all my ups and downs with unmatched grace. You listened fervently to my long enthusiastic talks about asphalt and pavements when, really, who wants to hear about pavement distresses and the theory of viscoelasticity over dinner? You suffered with me, and you rejoiced with me. Mom, Dad, Shadi, Rayan and Jad, I could not have stayed sane without you. Although I do not express it often, thank you...

To my advisor and mentor, Dr. Ghassan Chehab: being your student was like being in a pressure-aging vessel. We are talking lots and lots of condensed pressure! You had me juggle at least seven tasks at a time, while maintaining the highest possible standard for each. And that is exactly what happened: I aged.... I learned, I stumbled and I stood back up, I matured, I got to value the effort and perseverance it takes to achieve superior quality work and the ethics it takes to be a trustworthy researcher, and I gained excellent research experience intertwined with a practical vision. None of this would have happened had you not invested your time, effort, and experience, in being the toughest yet best and most dedicated teacher I know. I cannot say it enough: thank you...

To my committee members: Dr. Mohamed-Asem Abdul Malak and Dr. Ibrahim Alameddine, your input has helped me better develop my research. Thank you for the time and effort you put in serving on my committee.

Hussein Kassem and Dima Hassanieh, my colleagues and friends, you were both generous in sharing with me your experience, your valuable data, and your support. You both contributed directly and indirectly towards my research. I am grateful to you both. Jad Khalil, thank you with your help with the MEPDG runs over the past few months. You were exceptionally reliable, and your enthusiasm was contagious.

To my friends: you have all been amazing support. I cannot but name Amal Bakshan and Lynn Farran. Your daily company and encouragement kept me motivated.

Finally, to those who have contributed to this research through providing me with data-support and sharing their knowledge and expertise with me: Dr. Mohamed El-Basyouny, Mr. Nadim Haddad, and Mr. Bryan Smith, I am grateful for your help.

AN ABSTRACT OF THE THESIS OF

Yara Salim Hamdar for Master of Engineering
Major: Civil Engineering

Title: Effective Incorporation of Asphalt Mixture Properties in the Structural Design of Asphalt Pavements as a Precursor for Implementing Performance-Based Design

Despite its numerous limitations and its empirical nature, the 1993 AASHTO Design Guide for Pavement Structures is, to date, the most widely used pavement design manual by highway agencies and consultants around the world. As defined in the 1993 design guide, the structural coefficient of a pavement layer is an abstract measure of the relative ability of a unit thickness of a given material to function as a structural component of the pavement. The structural coefficient of the asphalt layer ' a_1 ' is typically assumed to be 0.44 for dense graded asphalt mixes, or is acquired from a relationship that ties ' a_1 ' to the resilient modulus (M_R). The main shortcoming of the design guide is that the assumed ' a_1 ' value of 0.44 and the relationship between ' a_1 ' and the resilient modulus (M_R) relationship do not account for the effect of mix type and properties, traffic volume and speed, layer thicknesses (thin versus thick pavements), climate, and unbound layer properties. Recently, pavement design needs have prominently evolved, owing to significant changes in traffic volumes and truck configurations, materials, material characterization models, performance prediction models, mix design methods, mix fabrication and construction procedures. These developments have rendered the 1993 design guide unsuitable in numerous design scenarios.

The objective of this research is to enhance the design methodology for asphalt pavements incorporated in the 1993 AASHTO design guide by integrating asphalt mixture properties in the design process. The aim is to provide a more accurate estimate of the structural coefficient ' a_1 ' of the asphalt layer by establishing a new relationship between the structural coefficient and the effective dynamic modulus ($|E^*|_{\text{eff.}}$) of the asphalt mix. The methodology employed to develop the relationship entails back-calculating the structural layer coefficient of the asphalt layer for a number of design scenarios (mix type, traffic volume and speed, climate, unbound layer properties) based on the equations of the 1993 design guide, but with thicknesses calculated using the Mechanistic-Empirical Pavement Design Guide (Pavement-ME). The research resulted in the development of a multi-linear relationship between the structural layer coefficient ' a_1 ', the effective dynamic modulus of the asphalt mix ($|E^*|_{\text{eff.}}$), and the resilient modulus of the aggregate base layer (E_{base}). Acquiring the structural number from the developed relationship is proven to yield design thicknesses that are generally close to those acquired using the Pavement-ME. A Microsoft-Excel-based pavement structural design tool was also built to support the developed a_1 - $|E^*|_{\text{eff.}}$ - E_{base} relationship, and simplify calculations. The tool can be used for (1) more accurate structural design of asphalt pavements, (2) improving asphalt concrete mix selection, and (3) serving as a precursor for performance-based specifications.

CONTENTS

ACKNOWLEDGMENTS	V
TABLES	XIII
ILLUSTRATIONS	XV
1. INTRODUCTION	1
1.1 Introduction.....	1
1.2 Background.....	1
1.3 Research Problem	3
1.4 Research Motive	6
1.5 Research Objective	7
1.6 Outline of Presented Research	7
2. LITERATURE REVIEW	8
2.1 Introduction.....	8
2.2 Evolution of Pavement Structural Design Methods Developed in the USA	9
2.3 Overview of AASHTO’s Empirical and Mechanistic-Empirical Design Guides .	11
2.3.1 AASHTO’s 1993 Pavement Design Guide	11
i. Design Methodology	12
ii. Development of the Structural Layer Coefficient	13
iii. Limitations	15
iv. Initiatives to Adjust the Structural Layer Coefficients.....	16
2.3.2 AASHTO’s Mechanistic-Empirical Pavement Design Guide.....	18
i. Design Methodology	18

ii. Limitations.....	21
2.4 State of the Practice of Pavement Design	21
2.4.1 Design Procedures Adopted In the USA	22
2.4.2 Design Procedures Adopted In Countries Outside the USA	24
i. Challenges for Implementing MEPDG in Countries Outside USA ..	24
2.5 Research Needs for Improvement of Pavement Design and Implementation	27
3. THEORETICAL BACKGROUND	28
3.1 Introduction.....	28
3.2 Classical Pavement Distresses and their Relation to Structural Design	28
3.3 1993 AASHTO Design Guide	29
3.3.1 Design Procedure.....	30
3.3.2 Fundamental Design Equation.....	30
3.3.3 Sensitivity of Design Thickness to Design Inputs.....	32
3.4 Mechanistic-Empirical Pavement Design Guide.....	34
3.4.1 Design Procedure.....	34
3.4.2 Performance Prediction Models	34
i. Reliability	37
3.4.3 Sensitivity of MEPDG Predictions to Input Parameters	38
3.5 Comparison of 1993 AASHTO Guide and MEPDG.....	40
3.5.1 Design Processes	40
3.5.2 Design Parameters	42
i. General Inputs	42
ii. Traffic Inputs	43
iii. Performance Criteria and Pavement Roughness Indices.....	43

iv. Reliability	46
3.5.3 Design Outputs	47
3.6 Effect of Pavement Thickness on Stress, Strain, and Fatigue Cracking.....	47
3.7 Dynamic Modulus of Asphalt Concrete and Its Use in Pavement Design	49
3.8 Conclusion	56
4. RESEARCH SCOPE AND METHODOLOGY.....	57
4.1 Introduction.....	57
4.2 Research Scope	57
4.3 Research Methodology	61
4.4 Assumptions.....	62
5. RESULTS AND ANALYSIS	65
5.1 Introduction.....	65
5.2 Structural Layer Coefficient of Different Asphalt Mix Categories	65
5.3 Relationship between Asphalt Layer Coefficient ' a_1 ' and $ E^* _{\text{eff}}$	68
i. Mixes with Unmodified Binder.....	70
ii. Mixes with Polymer-Modified Binder	73
5.3.2 Statistical Justification	74
5.3.3 Analytical Discussion	75
5.4 Sensitivity Analysis and Interpretation.....	76
i. Sensitivity to Fatigue- Δ PSI Correlation	77
ii. Sensitivity to Traffic Volume.....	80
iii. Sensitivity to Thickness of Base	80
iv. Sensitivity to Resilient Modulus of Subgrade	81
v. Sensitivity to Resilient Modulus of Aggregate Base.....	82

5.5	$a_1- E^* _{\text{eff.}}-E_{\text{base}}$ Relationship and Discussion	83
5.6	Implications of Research Findings	85
5.7	Conclusions.....	87
6.	DESIGN SUPPORT TOOL	88
6.1	Introduction.....	88
6.2	Features of Design Support Tool	88
6.3	Comparison of Developed Tool Against 1993 AASHTO and MEPDG	95
6.4	Limitations	96
6.5	Potential Applications of the Design Support Tool	99
6.5.1	Airfield Pavement Design	99
i.	Case Study	100
6.5.2	Performance-Based Specifications	102
7.	CONCLUSIONS AND FUTURE WORK	104
7.1	Conclusions.....	104
7.2	Limitations and Future Work.....	105
	REFERENCES	107
	APPENDIX	116

TABLES

Table 2.1: Asphalt Layer Coefficients From AASHO Road Test	14
Table 2.2: Conditions and Limitations of the AASHO Road Test	16
Table 2.3: Main Findings of Studies to Improve the Estimate of Structural Layer Coefficient for Asphalt Layers	17
Table 2.4 Main Findings of Studies to Improve the Estimate of the Structural Layer Coefficient for Aggregate Layers	18
Table 2.5: MEPDG Implementation and Local Calibration Studies	22
Table 3.1: Inputs of the 1993 AASHTO Design Equation	31
Table 3.2: Criterion for Establishing Serviceability Level According to the AASHTO 1993 Pavement Design Guide.....	32
Table 3.3: Correlation Between HMA Thickness and Other Inputs.....	33
Table 3.4: Sensitivity of MEPDG Predictions base on Literature	39
Table 3.5: Differences in Design Inputs of MEPDG and 1993 AASHTO.....	42
Table 3.6: Performance Criteria in MEPDG vs. 1993 AASHTO Guides	44
Table 3.7: Suggested Reliability Levels by MEPDG and 1993 AASHTO for Various Functional Classifications	46
Table 4.1: Summary of Asphalt Mixes Included in Scope	58
Table 5.1: Statistical Summary of Linear Models	75
Table 5.2: Design Thicknesses Using $a_1- E^* _{\text{eff}}$. Curves Compared to Design Thicknesses Using $a_1=0.44$	86

Table 6.1: Comparison of output of design tool to design thicknesses using 1993

AASHTO and MEPDG* 97

Table 7.1: Damage ratio and EALF for fatigue for B777, B737 and A330 101

ILLUSTRATIONS

Figure 2.1: Typical three-layered pavement cross-section.	13
Figure 2.2: 1993 AASHTO Design Nomograph	13
Figure 2.3: Relationship between resilient modulus of asphalt and structural layer coefficient	15
Figure 2.4: Mechanistic-empirical design methodology.	20
Figure 2.5: The three levels of analysis in the MEPDG (Pavement-ME).	20
Figure 2.6: Design procedures and asphalt layer coefficient adopted by the various states in the USA.....	23
Figure 2.7: The time it will take each state in the USA to implement the MEPDG.....	24
Figure 3.1: Trend in asphalt layer design thickness with change in asphalt structural coefficient	33
Figure 3.2: M-E pavement design procedure.....	36
Figure 3.3: Design reliability concept for smoothness (IRI).	37
Figure 3.4: Typical differences between empirical design procedures and an integrated M-E design system (adapted from MEPDG manual [34]).	41
Figure 3.5: Constant stress vs. constant strain phenomena [106].....	48
Figure 3.6: Constructing dynamic modulus mastercurve.	52
Figure 4.1: Dynamic modulus mastercurves of mixes included in scope: (a) polymer modified and fiber modified mixes, (b) WMA with PMB, (c) WMA with neat binder, (d) RAP, (e) Virginia DOT surface mixes, (f) Virginia DOT base mixes, (g) Virginia DOT SMA mixes.	59
Figure 4.2: Methodology adopted to develop the $a_1- E^* _{\text{eff}}$ relationship.....	64

Figure 5.1: Average structural layer coefficient of different asphalt mix categories.	66
Figure 5.2: Box-plot showing effect of mix type on the structural layer coefficient (U: unmodified, M: polymer-modified).	66
Figure 5.3: Universal $a_I- E^* _{\text{eff}}$ relationship (based on database considered in scope)..	69
Figure 5.4: $a_I- E^* _{\text{eff}}$ relationship for mixes with polymer-modified binder versus unmodified binder.	70
Figure 5.5: $a_I- E^* _{\text{eff}}$ relationship for conventional HMA and unmodified WMA mixes, separated by NMAAS.	71
Figure 5.6: $a_I- E^* _{\text{eff}}$ relationship for mixes with RAP, separated by NMAAS.	72
Figure 5.7: $a_I- E^* _{\text{eff}}$ relationship for SMA mixes and mixes with fibers.	73
Figure 5.8: $a_I- E^* _{\text{eff}}$ relationship for mixes with polymer-modified binder.	74
Figure 5.9: General initial $a_I- E^* _{\text{eff}}$ relationship based on the research scope.	76
Figure 5.10: Sensitivity of structural layer coefficient to assumed change in PSI in cold climate (Chicago) (left), and moderate to hot climate (Dallas) (right).	78
Figure 5.11: Sensitivity of structural layer coefficient to % fatigue cracking in cold climate (Chicago) (left), and moderate to hot climate (Dallas) (right).	79
Figure 5.12: Sensitivity of structural layer coefficient to traffic volume in cold climate (Chicago, left), and moderate to hot climate (Dallas, right).	80
Figure 5.13: Sensitivity of structural layer coefficient to base thickness in cold climate (Chicago, left), and moderate to hot climate (Dallas, right).	81
Figure 5.14: Sensitivity of structural layer coefficient to subgrade modulus in cold climate (Chicago, left), and moderate to hot climate (Dallas, right).	82
Figure 5.15: Sensitivity of structural layer coefficient to aggregate base modulus in cold climate (Chicago, left), and moderate to hot climate (Dallas, right).	83

Figure 5.16: Sample nomograph for calculating the structural layer coefficient of an average conventional HMA mix bas based on $ E^* _{\text{eff}}$ and E_{base}	85
Figure 6.1: Interface of structural design tool.....	89
Figure 6.2: Computation methodology adopted in design tool.	91
Figure 6.3: Climatic data inputs for structural design tool.	92
Figure 6.4: Design tool material inputs: (a) Level 1, (b) Level 2, (c) Level 3.	93
Figure 6.5: Effective conditions for fatigue and rutting.	94
Figure 6.6: Sample input and output.....	95
Figure 6.7: Design thicknesses acquired using the 1993 design guide compared to those acquired using MEPDG (Level 1) based on scenarios in Table 6.1.	96
Figure 6.8: Design thicknesses acquired using developed tool (new a_1) compared to those acquired using MEPDG (Level 1) based on scenarios in Table 6.1... ..	96

To the strongest woman I have ever known; to my constant source of inspiration;

To my mom...

Chapter 1

INTRODUCTION

1.1 Introduction

Despite its numerous limitations and its empirical nature, the 1993 AASHTO Design Guide for Pavement Structures is, to date, the most widely used pavement design manual by highway agencies and consultants around the world. The research presented herein proposes an enhancement to the design methodology incorporated in the 1993 design guide by integrating asphalt mixture properties in the design process. This chapter briefly discusses the most notable advances made in the pavement field over the course of the past few decades, highlights the wide gap between research and practice in the context of pavement structural design as well as the shortcomings of the currently used design methods, and introduces the research motive and objective.

1.2 Background

The 1980's onwards witnessed a remarkable and fundamental shift in research on and understanding of the behavior of the constitutive materials of asphalt mixes, and asphalt pavement structures in general. Perhaps the first leap in pavement-related research came in the form of the first Strategic Highway Research Program (SHRP) and the corresponding Long Term Pavement Performance test sections (LTPP), launched in 1984, and the results of which were reaped on the level of asphalt binder specifications and mix design methodology through the development of the Superpave system [1]. In the 1990's, a series of National Cooperative Highway Research (NCHRP) projects, most notably NCHRP 9-19, led to the formulation of new asphalt mix characterization techniques and simple performance tests [2]. The developments in mix characterization

testing and the advancements in computer technology resulted in the development of the mechanistic-empirical pavement design guide (MEPDG) and its corresponding software (currently Pavement-ME) through NCHRP 1-37 [3].

Research has been progressing in the arena of mechanistic pavement structural analysis and design. Various highway agencies have funded research projects to develop advanced mechanistic techniques and tools for comprehensive structural analysis and design of pavements. Of the most notable are the Layered Visco-Elastic Continuum Damage (LVECD) by North Carolina State University [4]–[7], Computer Aided Pavement Analysis (CAPA-3D) by the Delft University of Technology [8], [9], and Pavement Analysis Using Nonlinear Damage (PANDA) by Texas A&M [10]–[12]. However, these tools remain too complex for practice, and are thus currently restricted to research level tasks.

Over the past few decades, and on the level of mix materials, new technologies have been employed to improve conventional hot mix asphalt (HMA) and develop novel mixes and mix designs. These nonconventional mixes include, rubber-modified mixes, mixes with reclaimed asphalt pavement (RAP) and recycled asphalt shingles (RAS), warm mix asphalt (WMA), stone matrix/mastic asphalt (SMA), fiber-modified asphalt mixes, and mixes with polymer modified bitumen (PMB). New material characterization models, mix design methods, and production recommendations for these nonconventional mixes have been undergoing continuous development and improvement [13], [14].

It is reasonable to conclude that research and knowledge in the area of asphalt pavements have been on the rise, though still restricted on many facets and levels due to the complex nature of the asphalt as a material. In fact, practice in many realms has not progressed with research, especially in the area of pavement structural design. Pavement structural design procedures adopted by many agencies around the world have not kept up with the new advances in asphalt mix constituents and paving technologies, leaving many agencies restricted to using old methods, such as those based on the empirical 1993 AASHTO design guide, that do not accommodate the modifications in mixes, addition of additives, and corresponding advances in characterizing their properties.

1.3 Research Problem

The empirical design procedures of the 1972 and subsequent AASHTO Design Guides of 1986 and 1993 incorporate design data from the AASHO road test sections that were constructed in the late 1950's in Ottawa, Illinois [15]. The initial motive behind those test sections was to develop a fair tax scheme for different truck types based on damage caused by loading. The design equations incorporated in the guide are predominantly restricted by the original AASHO road test conditions. These equations and procedures, being empirical in nature, were developed using statistical regression models, performance measurements, or observations rather than using fundamental material properties and constitutive mathematical relationships. However, since the inception of the AASHO Road Test, design needs have prominently evolved owing to significant changes in traffic volumes and truck configurations, materials, material characterization models, performance prediction models, in addition to new mix design methods, mix fabrication and construction procedures [16].

The above limitations, compounded by the relatively poor performance of the existing roadways, led to the establishment of the NCHRP project 1-37a, with a main goal of achieving a more realistic and reliable design. The new design guide [3], [17] presents a fundamental shift in the analysis and design philosophy of asphalt pavements from an empirical approach towards one that is based on a mechanistic-empirical procedure. This procedure utilizes conditions that could be national, state, or site-specific, such as a detailed climatic profile and traffic characterization, and relates, to different extents, to the basic material properties to be used in construction. The model is termed mechanistic-empirical due to the mechanistic calculation of stresses, strains, and deflections of a pavement structure, which are the fundamental pavement responses under repeated traffic loadings, and the empirical relationships, widely known as transfer functions, used to relate these responses to field distresses and performance.

A key added value of the mechanistic-empirical pavement design guide (MEPDG, or recently Pavement-ME) is that it accommodates mix-specific material characterization through inputs such as the dynamic modulus ($|E^*|$) mastercurve, the binder shear modulus ($|G^*|$) and phase angle ($|\delta|$) mastercurves, in addition to volumetric properties such as effective binder content and percent air voids. The implementation of the MEPDG in the USA started in 2004, and throughout the past decade, the departments of transportation (DOTs) of most states in the USA have adopted and started implementing it for the design of expressways and arterials [16], [18]–[20]; nevertheless, the 1993 AASHTO Design Guide for Pavement Structures (or its earlier counterparts) is still, to date, the most widely used design guide by highway agencies and consultants around the world, particularly in Latin America, Asia, and Africa [21], [22], as well as in many states in the USA [23]. States in the USA that did

implement the MEPDG still use the 1993 guide for the design of low-volume roads.

Many of these highway agencies around the world have come across major obstacles when attempting to implement the MEPDG. Additionally, some are refusing to invest in it, while others are simply unaware of the benefits behind using it. The main challenges behind implementing in the MEPDG are attributed to: lack of input data (mainly traffic and climate), unavailability of Superpave and Simple Performance Testing equipment, difficulties in locally calibrating the prediction models due to the absence of test sections, poor training and minimal know-how of highway agency personnel, lack of financial resources and/or economic justification to invest in Pavement-ME, and resistance to change [24], [25].

The 1993 AASHTO design method relies on the concept of structural number. The structural number is an abstract number that roughly represents the overall structural requirement needed to sustain traffic loading for a given soil structure and serviceability [15], [26]. The design thicknesses of the asphalt and aggregate layers depend on the structural number as well as the layers' respective structural layer coefficient ' a_i '. By definition, the structural layer coefficient is a measure of how much a unit thickness of a given material is able to function as a structural component in the pavement [15], [26]. Similar to the structural number, the structural layer coefficient is also an abstract value that does not represent tangible or measurable mechanistic property of the material.

Typical structural numbers and structural layer coefficients used are reasonable for conventional mixes and design scenarios (climate, traffic loading, and soil

properties) that are close to those present at the AASHO road test. These structural numbers and structural layer coefficients, however, may not be suitable for nonconventional mixes, and for design scenarios different than those present at the road test. An enhancement to the 1993 AASHTO design guide is thus essential and warranted to cater for non-conventional mixes that are used around the world, albeit with empirical and simplistic structural design procedures.

1.4 Research Motive

The structural coefficient of a pavement layer is a measure of the relative ability of a unit thickness of a given material to function as a structural component of the pavement [15], [26]. The structural coefficient of the asphalt layer ' a_1 ' is typically assumed to be 0.44 for dense graded asphalt mixes, or is acquired from a relationship that ties ' a_1 ' to the resilient modulus (M_R) [15], [26]. Asphalt concrete is viscoelastic, and its structural layer coefficient must theoretically depend on its stiffness, which in turn depends on pavement temperature and frequency of traffic loading (speed). The assumed ' a_1 ' value of 0.44 and the relationship between ' a_1 ' and the resilient modulus (M_R) relationship do not account for the effect of mix type and properties, traffic volume or speed, layer thickness (thin versus thick pavement), or climate. To overcome these shortcomings, this research proposes a new relationship that relates ' a_1 ' to the effective dynamic modulus of the asphalt mix, $|E^*|_{\text{eff}}$. The dynamic modulus ($|E^*|$) is the ratio of stress to strain obtained at a range of temperature and loading frequency combinations. The effective dynamic modulus $|E^*|_{\text{eff}}$ is the $|E^*|$ value of the mix that corresponds to a specific combination of frequency (F_{eff}) and temperature (T_{eff}) that is prevalent for the roadway pavement under design [27]–[29] (Section 3.7). As such,

$|E^*|_{\text{eff}}$ can be considered a more reliable and realistic indicator of material behavior than M_R for structural design purposes.

1.5 Research Objective

The objective of this research is to enhance the design methodology for asphalt pavements incorporated in the 1993 AASHTO design guide by integrating asphalt mixture properties in the design process. The aim is to provide a more accurate estimate of the structural coefficient ' a_1 ' of the asphalt layer by establishing a new relationship between the structural coefficient and the effective dynamic modulus ($|E^*|_{\text{eff}}$).

Ultimately, the goal is to develop a design support tool that incorporates the newly developed a_1 - $|E^*|_{\text{eff}}$ relationship, and that can be used for: (1) more accurate structural design of asphalt pavements, (2) improving asphalt concrete mix selection, and (3) serving as a precursor for performance-based specifications.

1.6 Outline of Presented Research

While Chapter 2 presents a synthesis of the literature review, with an emphasis on design methods and tools developed and used in the USA, Chapter 3 discusses the theoretical background required for the conducting the research. Details of the adopted research scope and methodology are included in Chapter 4. Chapter 5 is dedicated to presenting and discussing the developed analytical model that relates the asphalt layer coefficient to ' a_1 ' to the effective dynamic modulus ($|E^*|_{\text{eff}}$). Chapter 6 includes a primer of the pavement structural design support tool built to complement the analytical model. Chapter 7 sheds light on possible applications of the developed tool. Finally, Chapter 8 presents an overview of the conclusions drawn from the work presented in Chapters 5, 6 and 7, and highlights suggestions for future work.

Chapter 2

LITERATURE REVIEW

2.1 Introduction

An asphalt pavement, also termed flexible pavement, is a structure made up of multiple layers, namely the subgrade (natural soil), aggregate sub-base, aggregate base, and a bituminous wearing course. Pavement structural design entails estimating the appropriate thickness of each of these layers such that the pavement withstands the stresses and strains induced by traffic loading and climatic conditions, while exhibiting reliable performance over its service life, i.e., limiting types and severity of distresses (cracking and permanent deformation). Pavement design is a challenging process, given the complexity of the viscoelastic asphalt material properties, as well as the probabilistic nature of design inputs such as traffic and climate, which greatly influence the design.

The synthesis of literature review in the subsequent sections focuses on areas that are deemed necessary for understanding the currently used pavement design methods as well as the challenges associated with them. The emphasis is on design methods and tools developed and used in the USA, and that are widely used around the world. There are numerous and notable methods that have been developed in other parts of the world and that are commonly used (e.g. Austroads [30] and the South African Pavement Design Guide [31]), but that are outside the scope of this thesis. A study conducted by Das (2015) investigated the different design principles of various pavement design methods [32].

The aim of the literature review presented in this chapter is to better understand the state-of-the-practice of pavement structural design and identify areas of potential improvement. The topics covered include (1) a brief historic overview of the progression of pavement structural design, (2) focus on the AASHTO's empirical (1993) pavement design guide, and on the newly released mechanistic empirical design guide (MEPDG), (3) research initiatives conducted to improve and/or implement AASHTO's design methodologies, (4) the state-of-the-practice in the USA and other parts of the globe, and (5) research needs for improving pavement design methods.

2.2 Evolution of Pavement Structural Design Methods Developed in the USA

Up until the 1950's, pavement structural design methods adopted in the USA and in other parts of the world were based primarily on experience [15]. In the late 1950's, the AASHO Road Test was initiated in Ottawa, Illinois in an attempt to develop a fair tax scheme for different vehicle types based on damage caused by loading. The AASHO Road Test included various test sections that were constructed of similar pavement structures but subjected to different traffic levels, loads, and axle types [23]. An interim pavement design guide was established by AASHTO in 1961 based on empirical equations relating traffic, pavement performance, and structure from data measured or gathered at the Road Test [33]. Successive versions of the AASHTO Design Guide were released in 1972, 1986 and 1993, introducing new concepts in the pavement design process.

The 1972 Interim Design Guide attempted to extend the findings of the 1961 guide to include guidelines for estimating materials and environmental conditions different than those of the AASHO Road Test [33]. The subsequent 1986 Guide further

refined material input parameters and introduced reliability and drainage factors, as well as procedures for overlay design [33]. Main additions to the 1993 version of the AASHTO Pavement Design Guide [26] involved overlay design. In addition, the 1993 Guide highlighted the importance of nondestructive deflection testing for evaluating existing pavements and back calculating layer moduli [33]. A computer software (DARWin) was also developed to support the design process.

The major shortcoming of AASHTO's 1993 Pavement Design Guide and its predecessor versions is their empirical nature. This means that the design equations are strictly limited to the conditions of AASHO Road Test. The limitations encompass soil type, climate, asphalt mix type, pavement structure, and traffic. Most designs conducted today using AASHTO's 1993 Guide are based on extrapolations from the original conditions [23], which reduces the reliability of the design.

In the 1990's, and in an effort to overcome the shortcomings of the empirical design method, AASHTO made a fundamental leap towards improved pavement design and analysis, and shift in design philosophy, by launching the development of the mechanistic-empirical design procedure. The National Cooperative Highway Research Program (NCHRP) sponsored Project 1-37A, entitled "Development of the 2002 Guide for the Design of New and Rehabilitated Pavement Structures: Phase II" which began in 1998 and spanned through 2004. It culminated with the development of the Mechanistic Empirical Pavement Design Guide (MEPDG) [3], [34]. The main advantage of the mechanistic-empirical design method is its ability to incorporate advanced material characterization and detailed traffic and climatic conditions.

The Beta version of the MEPDG software (Version 0.7) was released in 2004 for testing by agencies, researchers and practitioners. Since then, the software has been updated under other NCHRP projects several times. In year 2007, Version 1.0 of the MEPDG was adopted as an interim AASHTO pavement design procedure. The differences among the different MEPDG software versions are discussed in detail in the NCHRP Project 1-40D project report [35]. The software became commercially available in 2013 under the name AASHTOWare™ Pavement ME Design. Following the commercial release of the MEPDG and Pavement-ME, AASHTO withdrew its support of the DARWin software and 1993 Design Guide. Many agencies are thus faced with the challenge of transitioning from their existing empirical design methodology into mechanistic-empirical design.

2.3 Overview of AASHTO's Empirical and Mechanistic-Empirical Pavement Design Guides

The following sections cover a brief overview of AASHTO's 1993 Pavement Design Guide, and the relatively new Mechanistic-Empirical Pavement Design Guide. The overview highlights design methodology, limitations, and relevant research initiatives to compare, improve and/or implement each of the two guides. More detail about the fundamentals of the two design methodologies can be found in Chapter 3.

2.3.1 AASHTO's 1993 Pavement Design Guide

The main objective of the AASHO Road Test was to determine the relationship between pavement loading and deterioration in order to develop a tax scheme based on the damage to the pavement that a loaded truck would induce. The correlation between loading and damage was found to be approximately a fourth power relationship, which

means that a unit increase in axle weight causes pavement damage to increase by four times [15]. In addition to the primary objective, observations from the road test led to the development of an empirical pavement design guide. The design methodology, background, limitations, and research initiatives to enhance the guide are discussed below.

i. Design Methodology

The 1993 Pavement Design Guide and its predecessors are empirical in nature, and are based on the concept of structural number (SN), which is an abstract value that represents the overall structural requirement needed to sustain traffic loading (in equivalent single axle loads (ESALs)) for a given soil structure and serviceability. The structural number of a pavement is a function of layer thicknesses (D_i), layer coefficients (a_i), and drainage coefficients (m_i) (Equation 2.1). The subscripts represent the relative locations of the layers in the pavement. For a three-layered pavement (

Figure 2.1), the subscripts 1, 2 and 3 represent the asphalt, base, and subbase pavement layers respectively.

$$SN = a_1D_1 + a_2D_2m_2 + a_3D_3m_3 + \dots + a_nD_nm_n \quad (2.1)$$

The layer coefficient (a_i), is a measure of the relative ability of a unit thickness of a given material to function as a structural component of the pavement [15], [26]. Given the design reliability, traffic volume (ESALs), subgrade resilient modulus, and change in serviceability, the designer can acquire the structural number of the pavement using a nomograph provided by the 1993 guide (Figure 2.2).



Figure 2.1: Typical three-layered pavement cross-section.

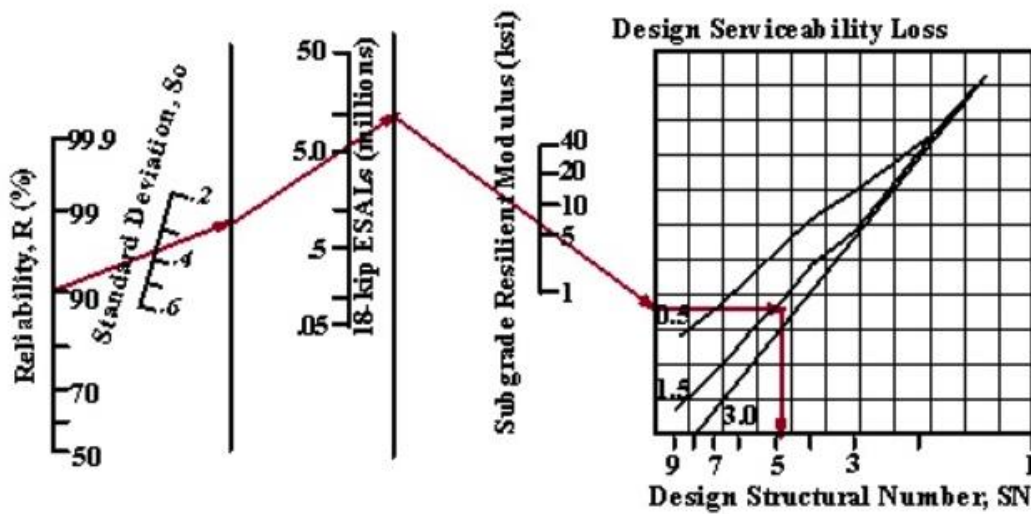


Figure 2.2: 1993 AASHTO Design Nomograph [26], [36].

ii. Development of the Structural Layer Coefficient

The notion of pavement capacity originated from the fourth-power relationship between loading and damage. Researchers at the AASHTO Road Test established a design parameter termed “thickness index” [37]. The thickness index (Equation 4) is similar to the structural number (SN), and is a function of layer thicknesses (D_i) and layer coefficients (a_i). The subscripts 1, 2 and 3 represent the asphalt, base, and subbase pavement layers respectively.

$$D = a_1 D_1 + a_2 D_2 + a_3 D_3 \quad (2.2)$$

If all layer coefficients are equal to one, the thickness index would be the total thickness of the pavement cross section. However, each layer has a unique structural contribution to the capacity of the pavement, depending on its material properties. An asphalt layer, for example, would contribute more to the pavement capacity than a subbase layer of the same thickness. To account for the difference in structural capacity between the pavement layers, researchers at the AASHO Road Test developed the concept of structural coefficient, an empirical value that expresses a layer's contribution to the pavement. Data from the road test was used to determine the structural layer coefficients of the different pavement sub-layers. The analysis resulted in different layer coefficients for the asphalt layer (Table 2.1). By weighing the layer coefficients in Table 2.1, the value of 0.44 was recommended for use as the layer coefficient for dense graded asphalt mixes. It is unclear, however, how this value was selected [38].

Table 2.1: Asphalt Layer Coefficients From AASHO Road Test [37]

Loop*	Layer Coefficient 'a _l '	Test Sections	R ²
2	0.83	44	0.80
3	0.44	60	0.83
4	0.44	60	0.90
5	0.47	60	0.92
6	0.33	60	0.81

**Loop 1 is not included because it was never trafficked. It was used to evaluate environmental impacts.*

In 1972, a relationship that links the layer coefficient of asphalt to the elastic (resilient) modulus (M_R) was developed (Figure 2.3) [39]. The resilient modulus may be acquired using triaxial testing (ASTM D7369-11) or indirect tension testing (ASTM D4123-82). By definition, M_R is the ratio of applied axial stress to recoverable axial strain. The resilient modulus (M_R) does not account for the effect of traffic volume or

speed, layer thickness (thin versus thick), and most importantly climate. Therefore, M_R is not a fundamental material property and is currently an outdated indicator, with the resilient modulus test being no longer commonly performed.

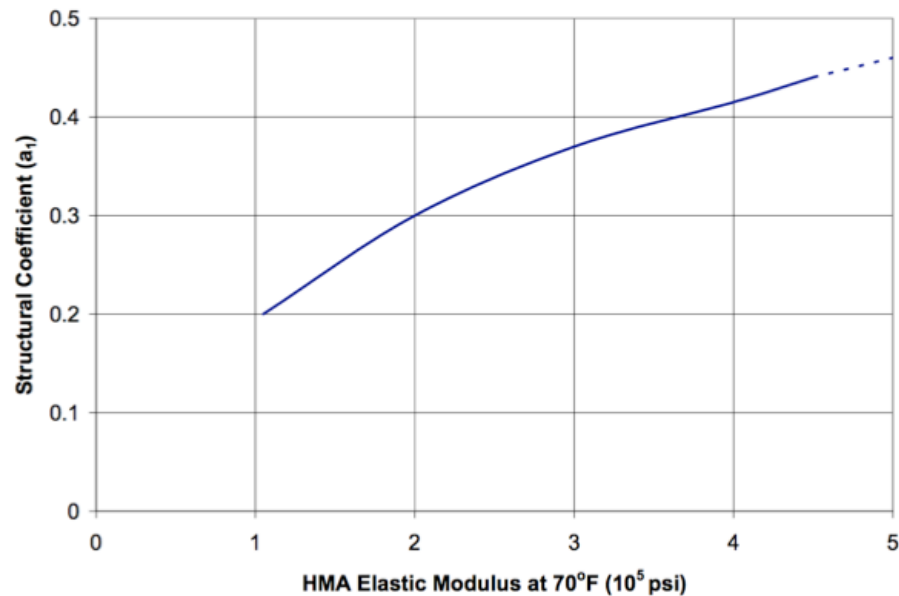


Figure 2.3: Relationship between resilient modulus of asphalt and structural layer coefficient [15], [26], [38]

iii. Limitations

The most basic limitation of the 1993 AASHTO Design Guide is its vastly empirical nature. It fails to account for mechanistic responses (stresses and strains) of the pavement structure to loading and unloading, and does not incorporate inputs that are essential for design such as material properties, traffic characteristics, and climatic factors. Moreover, AASHTO's empirical design methodology is based on the limited parameters used at the AASHO Road Test. These parameters are displayed in Table 2.2. The most notable shortcoming is the fact that the empirical method does not cater for the properties of the numerous new mixes developed since the inception of the road test that provide better performance against rutting, fatigue cracking, and other distresses. It

seems reasonable that these improved asphalt mixes would have a higher structural capacity, and layer coefficient, which is not reflected in empirical design.

Table 2.2: Conditions and Limitations of the AASHO Road Test [37]

Category	Parameter	AASHO Condition/Limitation
Time	Time frame	2 years
Traffic	Truck types	Bias-ply (No triple or quad axes; no super singles)
	Tire pressure	~ 70 psi
	Traffic volume	≤ 2 million ESALs
	Asphalt material	One type of HMA (No Superpave, open-graded friction courses, stone-matrix asphalt, reclaimed asphalt pavements, warm-mix asphalt, or other advanced materials)
Materials	Aggregate base material	One type
	Subgrade	One type
Structure	Pavement structure	Limited number of cross-sections
	Asphalt layer thickness	≤ 6 inches
Climate	Climate	Northern Illinois

iv. Initiatives to Adjust the Structural Layer Coefficients

The 1972 AASHTO Design Guide states, “because of widely varying environments, traffic, and construction practices, it is suggested that each design agency establish layer coefficients applicable to its own experience. Careful consideration should be given before adoption of values developed by others”. Nevertheless, currently, thirty-eight states in the USA use a structural coefficient value for the asphalt layer that is equal to or less than the value of 0.44 originally recommended by AASHTO in 1962 [23]. This means that all the advances made in the asphalt paving industry since then are not accounted for when determining the required thickness. Two states, Alabama and Washington, have recently revised their structural coefficients to reflect actual flexible pavement performance in their states. Alabama [38] increased its

value to 0.54 while Washington [17] increased its value to 0.50, which translates to 18.5% and 12% thinner cross-sections, respectively [23]. The Vermont Agency of Transportation (VTrans) found that layer coefficients estimated for asphalt concrete were generally 25 to 35% higher than AASHTO's implied maximum of 0.44 [40].

Research initiatives have also taken place to estimate the structural coefficient of various asphalt layers as well as aggregate base and subbase layers to account for advances in technologies and materials used. The methodology that is commonly adopted to back calculate the structural layer coefficients relies on measurements of the falling weight deflectometer (FWD). This methodology is based on recommendations of the 1993 AASHTO guide as well as NCHRP Project 10-48 [41]. Findings of such studies are summarized in Table 2.3 and Table 2.4 below

. Table 2.3: Main Findings of Studies to Improve the Estimate of Structural Layer Coefficient for Asphalt Layers

Reference	Technology	Main Finding(s)
Qi et al. (1995) [42]	Polymer modified asphalt	Layer coefficients of the polyethylene-modified mixtures were 75-85% higher than the layer coefficients of the unmodified ones
Hossain et al. (1997) [43]	Crumb-rubber modified (CRM) asphalt	For CRM asphalt mix overlays, the average surface layer coefficients were found to vary between 0.11 and 0.46, with most values falling around 0.3 For newly constructed CRM pavements, the structural layer coefficients varied from 0.25 to 0.48, with the average around 0.35
Marquis et al. (2003) [44]	Foamed asphalt	The layer coefficient of foamed asphalt ranged between 0.22 and 0.35
Davis and Timm (2009) [38]	Hot mix asphalt (HMA)	The average recalibrated layer coefficient was found to be 0.54, with a standard deviation of 0.08

Table 2.4 Main Findings of Studies to Improve the Estimate of the Structural Layer Coefficient for Aggregate Layers

Reference	Technology	Main Finding(s)
MacGregor et al. (1999) [45]	Reclaimed asphalt pavement (RAP)	The layer coefficient of the base and subbase layers increase with an increase in percentage of RAP of up to 50%
Bin-Shafique et al. (2004) [46]	Fly ash stabilization	Assigning layer coefficients for fly-ash stabilized soils based on correlations for granular subbase materials appears reasonable until layer coefficients specific to fly ash stabilized soils become available
Romanoschi et al. (2004) [47]	Full-depth reclamation material stabilized with foamed asphalt	Average structural layer coefficient of FAS-FDR was found to be 0.18
Misra et al. (2007) [48]	Fly ash stabilized recycled asphalt base	Recommended value for the structural layer coefficient was found to be 0.18-0.2
Puppala et al. (2011) [49]	Cement-treated reclaimed asphalt pavement (RAP)	Structural layer coefficients ranged from 0.16 to 0.22.

2.3.2 AASHTO's Mechanistic-Empirical Pavement Design Guide (Pavement-ME)

The fundamental shortcomings of the empirical pavement design methodology led to a paradigm shift in the approach towards pavement analysis and design. The pavement industry came to the realization that a mechanistic component is inevitable for reliable structural design. Relatively recent advancements in computer technology enabled the development of the mechanistic-empirical pavement design method.

i. Design Methodology

The mechanistic-empirical pavement design procedure relies on advanced material characterization, comprehensive traffic characterization, and detailed climatic data to simulate the response of the pavement under close-to-reality conditions. The model predicts pavement responses, i.e., stresses, strains and deflections, using

mechanistic analysis, and relates these responses to distresses and performance, i.e., cracking, rutting, and IRI, using empirical mathematical functions known as transfer functions. Designing a pavement using the mechanistic-empirical method is an iterative procedure that eventually leads to levels of pavement distresses that are acceptable by the design engineer based on the reliability level selected. The AASHTO Pavement-ME software, also known as MEPDG, is the most widely used tool to perform such a design.

In the MEPDG, the performance prediction model consists of four sub-models: (1) environmental effects model, (2) pavement response model, (3) material characterization model, and (4) performance prediction model. The interaction between those models, which ultimately yields the pavement performance prediction, is shown in Figure 2.4. As seen in the figure, there are four major inputs to the design and analysis processes: (1) the pavement structure, (2) traffic data, (3) local climatic, and (4) materials related inputs. Traffic parameters involve considerations of traffic volume, axle load spectrum, tire contact pressure, wheel and axle configuration, lateral wander of wheel path, and traffic growth rate. The MEPDG makes use of the enhanced integrated climatic model (EICM) to forecast future pavement temperatures and moisture contents as a function of historical weather records. An important feature of the MEPDG approach is the establishment of three levels of design inputs as shown in Figure 2.5. The reliability of each of the analysis levels as well as the sensitivity of MEPDG outputs to design inputs have been the subject of many research initiatives and investigations [24], [50]–[52].

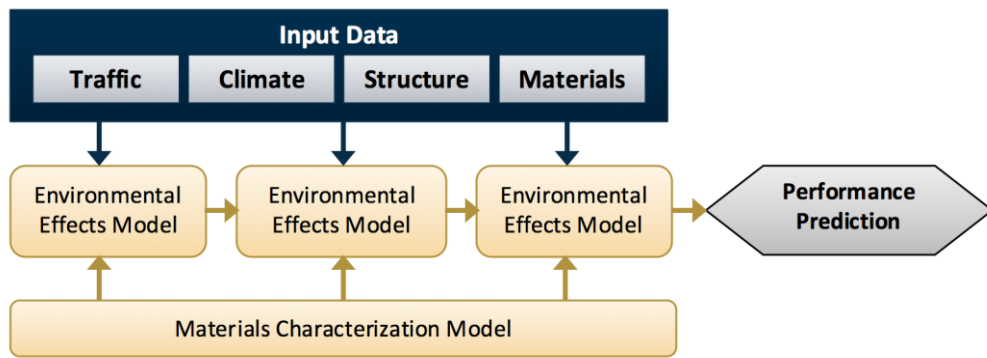


Figure 2.4: Mechanistic-empirical design methodology.

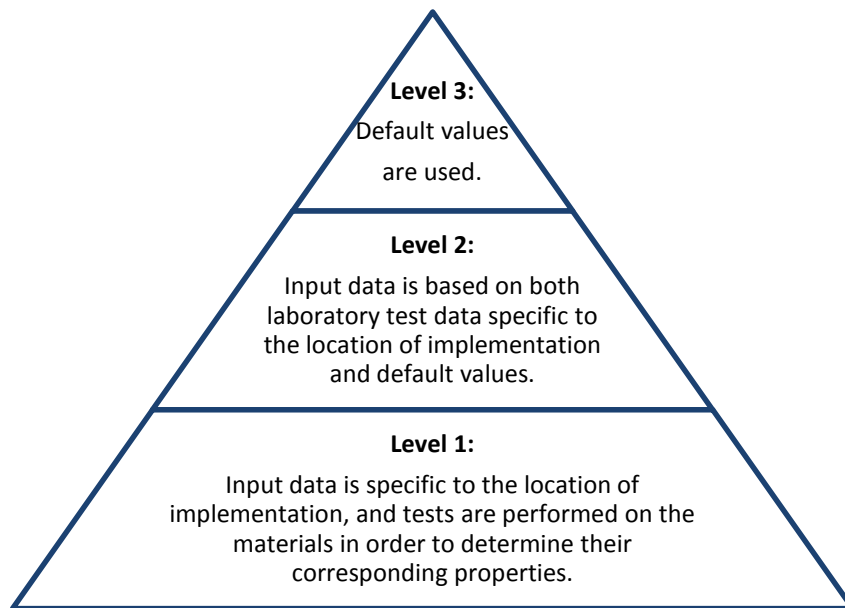


Figure 2.5: The three levels of analysis in the MEPDG (Pavement-ME).

It is important to note that the distress models of the MEPDG require the dynamic modulus ($|E^*|$) as input. The $|E^*|$ can be obtained from simple performance testing (for level 1 analysis), or from Witczak predictive equations [53], [54] that predict the $|E^*|$ based on the volumetrics and binder properties of the mix (for level 3 analysis). More on the dynamic modulus is discussed in Chapter 3.

ii. Limitations

The MEPDG has been criticized for a number of shortcomings, most importantly:

- There is an underlying assumption that the asphalt material remains in its linear elastic range, and the mechanistic models are thus relatively simplistic.
- The reliability model incorporated in the MEPDG is restricted to the uncertainty of the performance prediction model and does not consider any specific uncertainty from individual input parameters.
- The MEPDG does not tie the hourly traffic data to the hourly climatic data. Instead, the temperatures in each asphalt layer are combined into five quintiles for each month of the analysis period, and the truck traffic is assumed to be equal within each these temperature quintiles [34].

Moreover, implementing the MEPDG is challenging, the reasons for which can be summed up in three main points: (1) its prediction models were calibrated for the United States and therefore local calibration is required for reliable results, (2) it is data intensive, and the data is sometimes not readily available, and (3) the software (Pavement-ME) is expensive. However, despite its limitations, the MEPDG remains, to date, the most reliable and practical pavement design tool.

2.4 State of the Practice of Pavement Design

Understanding the state of the practice is essential, since pavement structural design, though often tackled in research, is directly associated with practice. Pavement design procedures adopted by many agencies around the world have not kept up with

new advances in the research realm, leaving many agencies restricted to old methods, such as those based on the empirical 1993 AASHTO design guide and its predecessor versions, that do not account for mixes properties, traffic speeds, and climatic conditions.

2.4.1 Design Procedures Adopted In the USA

In a recently conducted survey [23], it was found that forty-four states in the USA still use empirical design methods, though some have incorporated mechanistic-empirical methods as well (Figure 2.6). Following a series of implementation studies [24], [50], [52], [55], and as of the first of January 2009, Indiana DOT mandated the use of MEPDG as design methodology for all new state highway and interstate pavement design. Indiana is, to date, the only state that has fully and officially adopted the MEPDG.

Apart from Indiana, many states have initiated official or research-driven MEPDG implementation and local calibration studies (Table 2.5). However, not all of these states have actually implemented the MEPDG nor plan to implement it in the near future (Figure 2.6 and Figure 2.7).

Table 2.5: MEPDG Implementation and Local Calibration Studies

State	Reference	State	Reference
Florida	[56]	New Jersey	[57]
Indiana	[55]	North Carolina	[58]
Maryland	[59]	Virginia	[60]
Minnesota	[61]	Washington	[62]
Montana	[63]	Wisconsin	[64]

Some states are looking into implementing the MEPDG in the near future (Figure 2.7), while others do not envision implementing the MEPDG anytime soon and will thus continue relying on empirical design methods. Some state highway agencies acknowledge that many pavement design decisions do not require individual analysis using the MEPDG, and that 1993 AASHTO guide could in some cases be a more viable option. On such example is Washington State DOT that developed a new pavement design catalogue based on the 1993 design guide, MEPDG, and its own historical records [17].

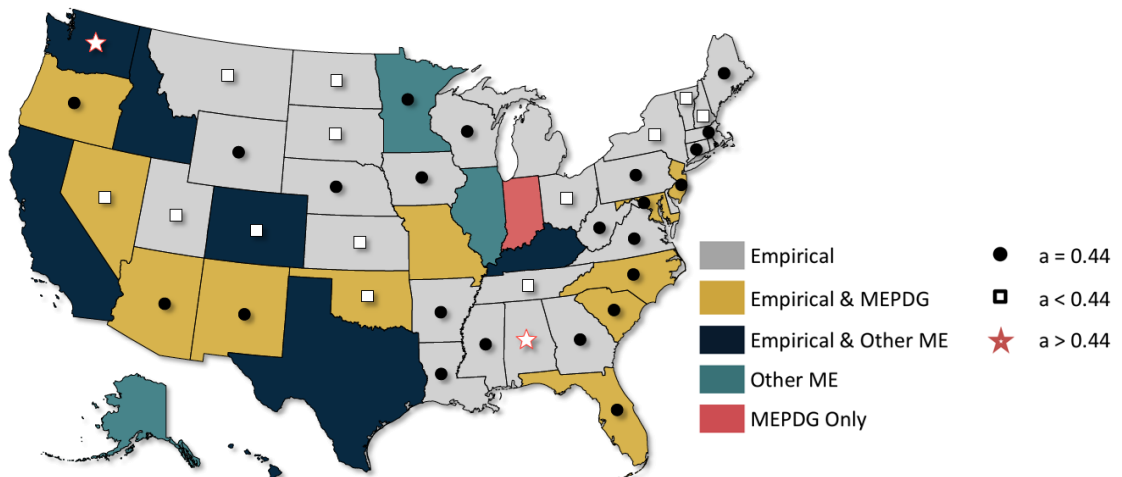


Figure 2.6: Design procedures and asphalt layer coefficient adopted by the various states in the USA [23].

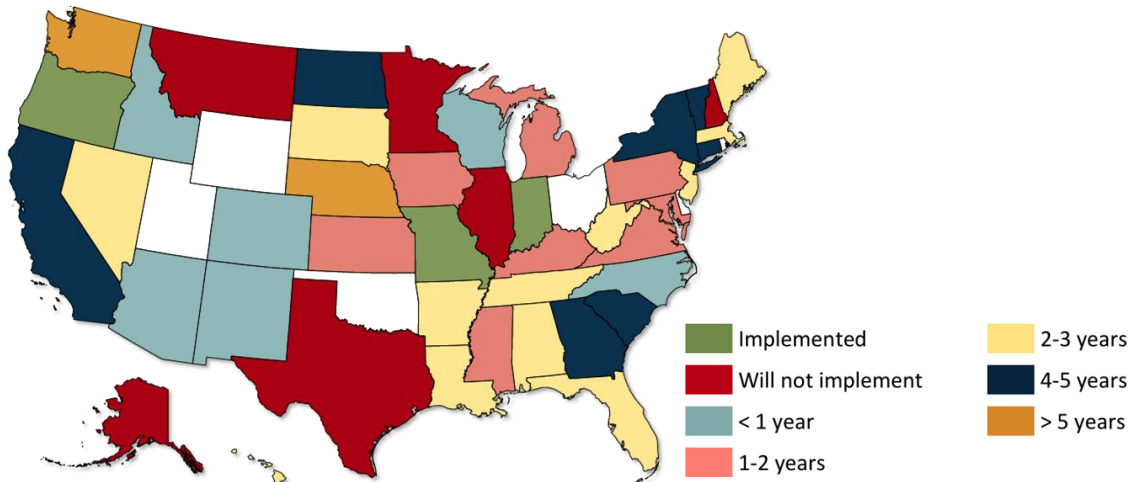


Figure 2.7: The time it will take each state in the USA to implement the MEPDG [23].

2.4.2 Design Procedures Adopted In Countries Outside the USA

Outside the USA, the 1993 AASHTO Design Guide is still the primary design methodology adopted in many countries, including all those of the MENA region. In the UAE, Abu Dhabi is aiming to shift to mechanistic-empirical procedures, but is shying away from the MEPDG due to the extensive level of detail of its inputs as well as its high cost. Saudi Arabia is gearing towards implementing the MEPDG [65], and research has been conducted about the implementation of the MEPDG in Qatar [66]. The highway agencies of other countries and cities do not plan on diverting away from the 1993 AASHTO Guide soon.

i. Challenges for Implementing the MEPDG in Countries Outside the USA

There are apparent challenges and concerns for implementing the MEPDG in regions outside the United States, particularly in developing countries. These challenges

primarily relate to the intricate level of detail of the various inputs required for accurate and reliable pavement design:

- **Climate files:** All climatic files embedded in the MEPDG are particular to regions in the United States and Canada. Although it is possible to develop climate files for any region outside the USA, many countries lack the needed hourly climatic data, and it could take significant time for countries planning to adopt the guide to compile the proper climatic database. Oftentimes, to overcome the constraint relating to unavailability of climatic data, design engineers use climate files of USA regions that have similar climatic conditions to those present in the project location, but the effect of such an assumption on the reliability of outputs is often questionable.
- **Traffic level and vehicle classification:** Similar to the case of climate data, traffic data is not readily available in many countries and could hinder adopting the MEPDG until the required records are obtained. Traffic data required for MEPDG (Pavement-ME) includes detailed truck fleet characteristics (truck types, axle distributions, weights), traffic speed, and time and lane distribution of traffic. Presently, inaccurate assumptions in traffic characterization can skew the results and undermine the significance of using the MEPDG in these countries.
- **Material properties and testing:** Some countries have not yet adopted certain advanced asphalt materials testing, such as the simple performance test, and Superpave binder grading tests. Moreover, material testing standards could be different than those required for the MEPDG, such as British Standards, Russian Standards, Chinese Standards, and other country specific standards [16].

- **Model calibration:** The performance prediction models and the dynamic modulus prediction model (Witczak model) used in the MEPDG have been regressed based on data that is specific to the USA. Although the MEPDG offers the option of inputting local calibration coefficients, many countries do not have the means (test sections and/or periodic performance measurements) to locally calibrate these equations.

In addition to the above limitations, design firms in developing countries often lack the financial resources required to purchase and maintain mechanistic-empirical design guide software licenses. Moreover, education, awareness, training and willingness are crucial. Designers in these countries need to gain enough familiarity with the new mechanistic-empirical software and knowledge of the incorporated design methodology, design inputs and levels, and their relationships to key distresses and performance [16].

While implementation of Pavement-ME in some US States and in countries outside the USA is progressing, full implementation will require significant time and effort [8, 9]. In the meantime, it is thus of benefit to build on and improve currently used design methods, namely the AASHTO 1993 design guide. The need to improve currently adopted design methods is evidenced by the numerous recent high profile failures that occurred in multiple major roadways, runways, and taxiways in several of the MENA [67]–[69]. Pavement failures may be attributed to poor structural design that does not adequately account for material properties. Therefore, improving the estimate of the asphalt layer's structural coefficient is potentially a prominent step forward towards more reliable pavement design.

2.5 Research Needs for Improvement of Pavement Design and Implementation

Based on the discussion in the previous section, the 1993 AASHTO design guide is still an inevitable option for numerous highway agencies worldwide. This is evidenced by the state of the practice in the United States [23] and other parts of the world, as well as by the multiple studies that have been conducted, some of which are fairly recent [38], in order to improve the structural coefficients for the 1993 guide. However, the main shortcoming of these studies (Table 2.3 and Table 2.4) is that they rely on Falling Weight Deflectometer (FWD) back-calculations, which means that the back-calculated structural coefficients are limited by the temperature under which the test was performed, the material types with which the pavements were constructed, the thicknesses of the layers in the pavement structure, and the traffic loadings which the pavement was subjected to. The back-calculated structural layer coefficients in these cases, though very likely more accurate than AASHTO's estimate of 0.44, still do not account for a wide range of mix types, climatic conditions, and traffic volumes and speeds. Improving the estimate of the structural layer coefficient of the asphalt layer is therefore a pressing need for agencies that still rely on the 1993 design guide.

Chapter 3

THEORETICAL BACKGROUND

3.1 Introduction

Pavement design is a combined structures and materials exercise, and design thicknesses are associated not only with the type and characteristics of the asphalt used, but also with truck fleet classification, traffic volume and speed, climatic conditions, and subgrade and aggregate base properties. Understanding the basics of pavement structural analysis methods and relevant fundamental material properties is essential for the sound development of the research work presented in this thesis. However, the theories of pavement design and asphalt viscoelasticity are wide and cannot be entirely covered within the scope of this thesis. As a result, this chapter covers the knowledge that is deemed to be essential for conducting the research, which includes: (1) standard pavement distresses, (2) fundamentals of the 1993 AASHTO guide and the MEPDG, and the differences between them (3) basics of pavement structural design, i.e., stresses, strains, and their relation to pavement distresses and design thicknesses, (4) fundamental asphalt material properties, namely the dynamic modulus, and (5) the concept of effective dynamic modulus.

3.2 Classical Pavement Distresses and their Relation to Structural Design

Repetitive and heavy traffic loading, and environmental factors such as heat and rain, induce stresses and strains in the various pavement layers (Figure 2.1). These stresses and strains eventually exceed the capacity of the materials in the different layers (asphalt, aggregate base, and subgrade), leading to the formation of distresses and failures in the pavement. The two classical distresses are rutting and fatigue cracking.

Rutting, also termed permanent deformation, is a phenomenon that is exhibited through surface depression under the wheel path [70]. There are two types of rutting: asphalt rutting, and subgrade rutting. Asphalt rutting is directly related to material properties of the asphalt mixture at the surface of the pavement, and is thus independent of structural design. It typically results from poor materials selection, deficient compaction, and sub-optimal mix design, among other constructability problems. Rutting typically occurs at high temperatures and low loading frequency (slow vehicle speed). Subgrade rutting, on the other hand, is a structural problem that occurs when stresses on top of the subgrade exceeds the bearing capacity of the soil. It is caused by weak subgrade soil, and inadequate asphalt and/or aggregate base layer thickness and/or moduli.

Fatigue cracking is manifested through the formation of a series of interconnected cracks, caused by failure of the asphalt pavement under repetitive traffic loading [71]. A fatigue crack initiates at the bottom of the asphalt layer due to repetitive bending caused by stresses and strains, and makes its way to the surface of the pavement. The severity of fatigue cracks and the speed at which they develop depends on the stiffness and thickness of the asphalt layer, and the modulus and thickness of the aggregate base layer. Therefore, fatigue cracking is primarily a structural failure, as well as a material-related distress. More on fatigue cracking is discussed in Section 3.6.

3.3 1993 AASHTO Design Guide

The 1993 design guide is based on the concept of structural number (SN) (Equation 2.1), which is an abstract value that represents the overall structural

requirement needed to sustain traffic loading (in equivalent single axle loads (ESALs)) for a given soil structure and serviceability.

3.3.1 Design Procedure

For a two-layered pavement consisting of an asphalt layer and an aggregate base layer, the design procedure of the 1993 guide is as follows [15], [26]:

1. Assume that the subgrade resilient modulus is equal to the modulus of the aggregate base layer, and get the structural number (SN_1) from the nomograph in Figure 2.2. Acquire the design thickness of the asphalt layer necessary to protect the aggregate base using Equation 3.1.

$$D_1 = \frac{SN_1}{a_1} \quad (3.1)$$

2. Using the subgrade resilient modulus, get the structural number (SN_2) from the nomograph in Figure 2.2. Acquire the design thickness of the aggregate base layer necessary to protect the subgrade using Equation 3.2.

$$D_2 = \frac{SN_2 - a_1 D_1}{a_2} \quad (3.2)$$

3.3.2 Fundamental Design Equation

The main design equation of the 1993 AASHTO design method is shown in Equation 3.3 below [15], [26].

$$\begin{aligned} \log(W_{18}) = & Z_R S_o + 9.36 \log(SN + 1) - 0.2 + \frac{\log(\Delta PSI / (4.2 - 1.5))}{0.4 + 1094 / (SN + 1)^{5.19}} \\ & + 2.32 \log M_R - 8.07 \end{aligned} \quad (3.3)$$

This equation determines the amount of traffic (in equivalent single axle loads (ESALs)) that a pavement can withstand, given its structural number (SN), the resilient modulus of the soil (M_R), and the expected change in serviceability (ΔPSI), at a specified reliability level ($Z_R S_o$). Table 3.1 briefly explains each of these inputs.

Table 3.1: Inputs of the 1993 AASHTO Design Equation

Design Input	Appearance in Design Equation	Brief Overview
Performance Period	Through expected traffic volume	Time that a new pavement will last before requiring major rehabilitation
Traffic	W_{18}	Cumulative expected 18-kip equivalent single axle load (ESAL) during the analysis period
Unbound Layer Properties	M_R	Resilient modulus (i.e. strength) of unbound layers (subgrade and aggregate base)
Reliability	Reliability factor (Z_R) and overall standard deviation (S_o)	Degree of certainty to account for variations in traffic prediction and performance prediction
Serviceability	PSI	Pavement's ability to serve the traffic (i.e. the resulting loss in performance at W_{18})
Environmental Effects	Through loss of serviceability	Loss of serviceability loss over time for different environmental effects such as changes in temperature and moisture levels

In the 1993 guide, serviceability is the main performance criterion for design. Serviceability (or pavement serviceability index (PSI) is defined as the pavement's ability to serve the traffic. The parameter was conceptualized during the AASHTO Road Test, where a panel of raters made routine inspections of each section and rated their best estimate of the road's performance on a scale of zero (impossible road) to five (perfect road) following the criterion shown in Table 3.2. The pavement is typically designed to experience a predetermined loss in serviceability over its design period. The loss or change in serviceability (ΔPSI) is defined as the change between terminal

serviceability (p_i) (the lowest index that will be tolerated before rehabilitation) and initial serviceability (p_o). The serviceability loss is a function of roadway classification, and is recommended to be 1.7 for major highways, and 2.2 for roads with lower traffic volumes [3, 10].

Table 3.2: Criterion for Establishing Serviceability Level According to the AASHTO 1993 Pavement Design Guide [26]

Terminal Serviceability Level	Percent of People Stating Unacceptable
3.0	12
2.5	55
2.0	85

3.3.3 *Sensitivity of Design Thickness to Design Inputs*

Over the years, design inputs have been subject to scrutiny, with interest and focus on the sensitivity of the design thicknesses to the various parameters. It has been observed that inference could be made about the sensitivity of design thicknesses to the input parameters by looking at the design nomograph (Figure 2.2) [38]. For instance, the higher the reliability level (90 to 99%), the more sensitive the design thickness will be to a slight change in design reliability compared to lower reliability levels (50 to 70%). The same can be deduced in regards to the standard deviation, the resilient modulus, and the structural number.

A sensitivity analysis was conducted to come up with conclusive and tangible results on the design parameters that are most influential on the resulting thickness of the asphalt layer, and revealed that the layer coefficient has the greatest influence on the thickness of the asphalt layer, followed by traffic level [38].

Table 3.3: Correlation Between HMA Thickness and Other Inputs [38]

Parameter	Correlation Coefficient
Layer coefficient (a_1)	-0.518
Traffic level (W_{18})	0.483
Resilient modulus (M_R)	-0.425
Reliability (R)	0.157
Change in serviceability (ΔPSI)	-0.141
Variability (S_o)	0.083

Figure 3.1 illustrates the general trend in variation of asphalt layer thickness with change in structural coefficient. The conditions used to obtain this graph are traffic level of 10^8 ESALs, resilient modulus of 20,000 psi, variability of 0.4, reliability of 80%, and change in serviceability of 2.0 [38]. In this case, changing the magnitude of the structural coefficient from 0.44 to 0.6 would save two inches in design thickness.

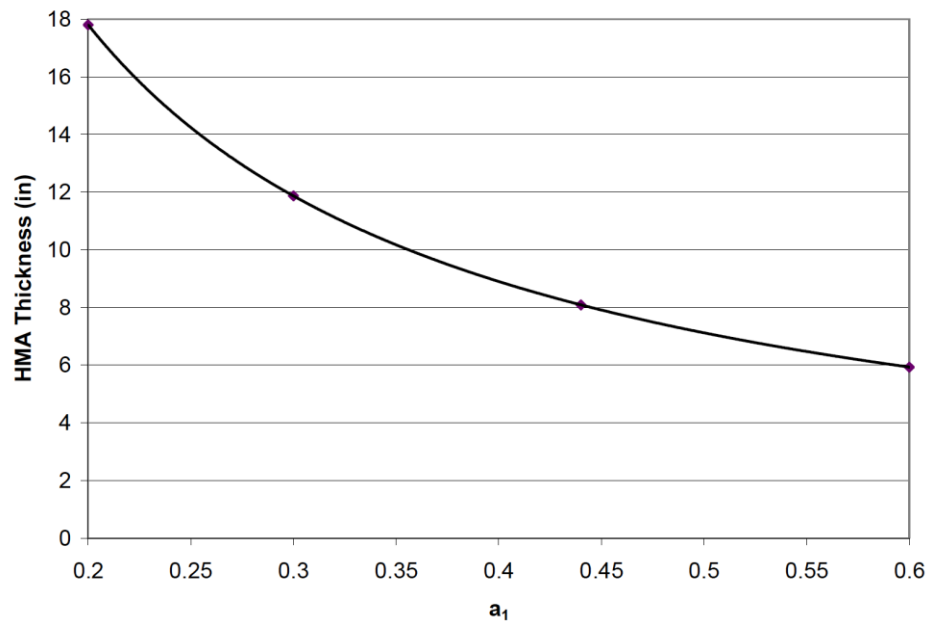


Figure 3.1: Trend in asphalt layer design thickness with change in asphalt structural coefficient [38].

3.4 Mechanistic-Empirical Pavement Design Guide

3.4.1 Design Procedure

Mechanistic-empirical design is an iterative, performance-based process. The design process is described in the flowchart in Figure 3.2. For the mechanistic module, the critical pavement responses are calculated using the elastic layer theory program identified as JULEA [72], which is embedded in the MEPDG. The modulus of the asphalt layer is determined by using the integrated climatic model (ICM).

3.4.2 Performance Prediction Models

The performance prediction models of the MEPDG were calibrated using data from the Long Term Pavement Performance (LTPP) database. These rutting and fatigue models are also known as transfer functions, and are empirical by nature. The asphalt concrete (AC) rutting prediction model is shown in Equation 3.4 [34], [35].

$$\Delta_p (AC) = \varepsilon_p (AC) h_{(AC)} = \beta_{1r} k_z \varepsilon_r (AC) 10^{k_{1r}} n^{k_{2r}} \beta_{2r} T^{k_{3r}} \beta_{3r} \quad (3.4)$$

where: $\Delta_p (AC)$ = accumulated permanent vertical deformation in the AC layer (in),

$\varepsilon_p (AC)$ = accumulated permanent vertical strain in the AC layer (in),

$\varepsilon_r (AC)$ = resilient (elastic) strain at middepth of the AC layer (in),

$h_{(AC)}$ = thickness of the asphalt layer (in),

n = number of axle load repetitions,

T = mix or pavement temperature (°F),

k_z = depth confinement factor,

$k_{1r,2r,3r}$ = global field calibration parameters,

= -3.35412, 0.4781, and 1.5606 respectively (NCHRP 1 – 40D), and

$\beta_{1r,2r,3r}$ = local or mixture field calibration constants.

The MEPDG assumes that fatigue cracks initiate at the bottom of the HMA layers and propagate to the surface with continued truck traffic. The fatigue cracking prediction model is shown in Equation 3.5 [34][35].

$$N_f = k_{f1}(C)\beta_{f1}(\varepsilon_t)^{k_{f2}\beta_{f2}}(E)^{k_{f3}\beta_{f3}} \quad (3.5)$$

where:

- N_f = allowable number of axle load applications,
- ε_t = tensile strain at critical locations (in./in.),
- E = dynamic modulus of the asphalt measured in compression (psi),
- $k_{f1,f2,f3}$ = global field calibration parameters,
= 0.007566, -3.9492, and -1.281 respectively (NCHRP 1 – 40D), and
- $\beta_{ir,2r,3r}$ = local or mixture field calibration constants.

$$C = 10^M$$

$$M = 4.84\left(\frac{V_{be}}{V_a + V_{be}} - 0.69\right)$$

where:

- V_{be} = effective asphalt content by volume (%),
- V_a = percent air voids in the asphalt mixture, and
- C_H = thickness correction term, dependent on the type of cracking.

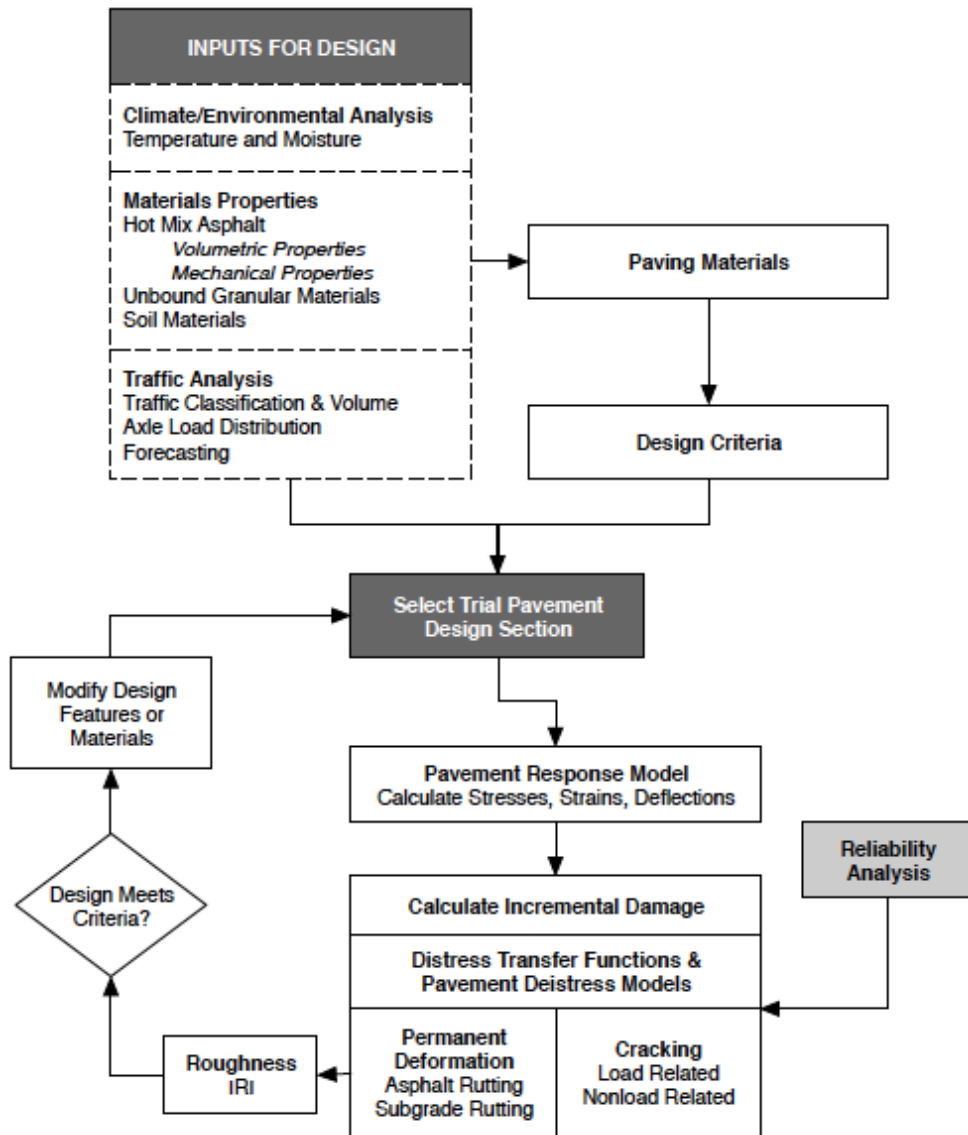


Figure 3.2: M-E pavement design procedure [34].

i. Reliability

In the MEPDG methodology and the Pavement-ME software, reliability is defined as the probability that the predicted distress will be less than the critical level for the design period (Equation 3.6) [34]. Reliability is dependent on the model prediction error (standard error) of the distress prediction equations. Therefore, the mean distress value is increased by the number of standard errors that apply to the reliability level selected (e.g. ~2 for 95% reliability). This is based on a principal assumption that distresses are normally distributed over the ranges of distress that are of interest in the design [34].

$$R = P [\text{Distress over design period} < \text{critical distress level}] \quad (3.6)$$

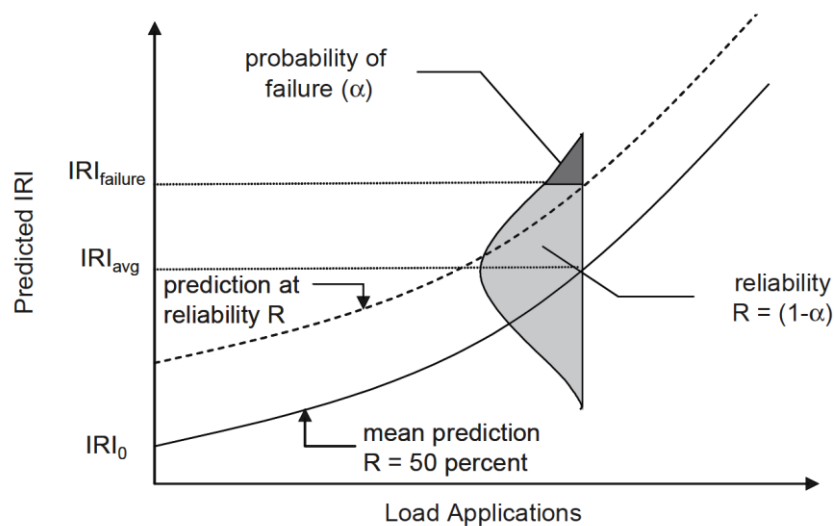


Figure 3.3: Design reliability concept for smoothness (International Roughness Index (IRI)) [34].

3.4.3 Sensitivity of MEPDG Predictions to Input Parameters

An extensive study on the sensitivity of MEPDG predictions to input parameters was conducted through NCHRP project 01-47 (“Sensitivity Evaluation of MEPDG Performance Prediction”) [73] [76]. Prior to this project, numerous research studies investigated the sensitivity of MEPDG for asphalt pavements. The earlier studies were conducted using Version 0.7 of the MEPDG or other versions prior to the release of Version 1.0 in year 2007 [74]–[91]. With the modifications and recalibrations of the MEPDG prediction models since, sensitivity to some of the input parameters may have significantly changed rendering the results of these studies restricted to the older versions of the software. More recent studies have been conducted using Versions 1.0 or 1.1 of the MEPDG software [25], [61], [92]–[100]. The findings of these studies (until year 2010) are summarized in Table 3.4. More information can be found in the report of NCHRP 01-47 [73].

The results of the NCHRP study concluded that the most sensitive input parameters for fatigue are (by order of most to least sensitive) $|E^*|$ parameters, asphalt concrete (AC) layer thickness, traffic volume, air voids, and resilient moduli of the aggregate base and subgrade layers, and asphalt content. The most sensitive parameters for asphalt rutting are $|E^*|$ parameters, shortwave absorptivity, AC thickness, AC Poisson ratio, AC thickness, and traffic volume.

Table 3.4: Sensitivity of MEPDG Predictions base on Literature (adapted from NCHRP 01-47 [73])

HMA Pavement Inputs		Levels of Sensitivity for Flexible Pavement Outputs*				
Group	Parameter	HMA Rutting	Total Rutting	Alligator Cracking	Long. Cracking	Thermal Cracking
General	Traffic open month	NS	NS	NS	NS	NS
Traffic	Volume	VS	VS	VS	VS	NS
	Speed	VS	VS	S	S	NS
Climate	Location	VS	S	S	S	S
	Depth to groundwater table	NS	S	NS	NS	NS
Layer/General	Surface shortwave absorptivity	VS	VS	S	VS	NS
Layer/AC	Thickness	VS	VS	VS	S	NS
	Dynamic Modulus	S	S	S	S	NS
	Binder grade/stiffness	VS	S	S	S	NS
	Poisson's ratio	NS	NS	NS	NS	NS
	Thermal conductivity	NS	NS	NS	NS	S
	Heat capacity	NS	NS	NS	NS	S
	Creep compliance	NS	NS	NS	NS	VS
	Tensile strength at 14 F	NS	NS	NS	NS	VS
	Aggregate coefficient of thermal contraction	NS	NS	NS	NS	VS
	Layer/Base (Subbase)	Thickness	S	S	S	S
Resilient modulus		S	S	S	VS	NS
Poisson's ratio		NS	NS	NS	NS	NS
Soil-water characteristic curve		NS	NS	NS	NS	NS
Permeability		NS	NS	NS	NS	NS
Compacted/uncompacted		NS	NS	NS	NS	NS

*VS = very sensitive, S = sensitive, NS = nonsensitive.

3.5 Comparison of 1993 AASHTO Guide and MEPDG

3.5.1 Design Processes

Fundamental differences in the design philosophy and process exist between the MEPDG and the 1993 AASHTO design guide (Figure 3.4). The empirical design procedure does not integrate fundamental asphalt material properties in the design process. The recommended structural layer coefficient and its relationship with the resilient modulus do not accommodate differences in the constituents of the asphalt mixes (asphalt content, percent air voids, aggregate gradation, additives). Moreover, the empirical method does not correlate material properties and layer thicknesses to distresses. The mechanistic-empirical design procedure, on the other hand, incorporates advanced material properties (dynamic modulus ($|E^*|$) mastercurve, binder shear modulus $|G^*|$ and phase angle ($|\delta|$) mastercurves) as well as volumetric properties (effective binder content and percent air voids), and relates these properties to design criteria (e.g. maximum allowable total rutting or fatigue cracking) through prediction of performance.

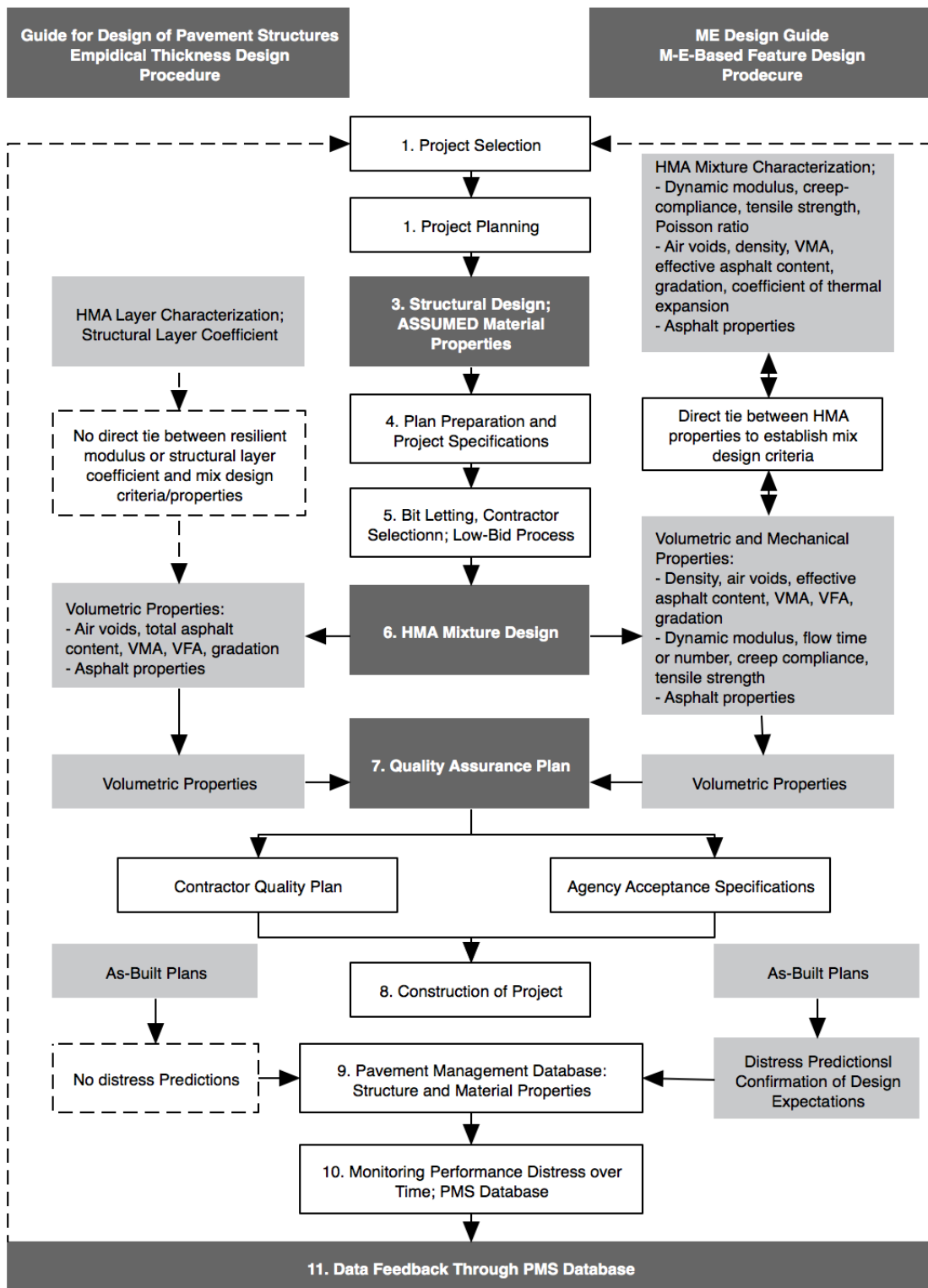


Figure 3.4: Typical differences between empirical design procedures and an integrated M-E design system (adapted from MEPDG manual [34]).

3.5.2 Design Parameters

The depth and breadth of design inputs differ significantly between the empirical and mechanistic-empirical design approaches.

i. General Inputs

The differences in design inputs between the AASHTO's empirical and mechanistic-empirical design guides are highlighted in Table 3.5. Traffic, climate, and material properties are incorporated in significantly greater detail in the MEPDG as compared to the 1993 guide.

Table 3.5: Differences in Design Inputs of MEPDG and 1993 AASHTO

Category	MEPDG Design Inputs	1993 AASHTO Design Inputs
Traffic	Volume Speed Truck fleet characteristics Tire wander	Equivalent single axle load (ESAL)
Climate	Hourly climatic data Location (latitude, longitude) Depth to groundwater table	No direct consideration
Layer/HMA	Thickness Dynamic modulus Binder grade/stiffness Poisson's ratio Thermal conductivity Heat capacity Creep compliance Tensile strength at 14 F Aggregate coefficient of thermal contraction	Layer structural coefficient
Layer/Base (Subbase)	Thickness Resilient modulus Poisson's ratio Soil-water characteristic curve Permeability Compacted/ uncompacted	Layer structural coefficient Resilient modulus

ii. Traffic Inputs

The traffic volume input required by the 1993 design guide is in the form of equivalent single axle loads (ESALs). By definition, the ESALs of a vehicle (truck) fleet is the ratio of the damage caused to the pavement from wheel loads of various vehicle types (loads and axle configurations) and loading repetitions, to the damage of an equivalent number of standard (or equivalent) load [101]. The most commonly used equivalent load is the 18-kip single axle load [101].

The MEPDG, on the other hand, accommodates full characterization of the design truck traffic fleet, which includes truck types, loads, tire wander, design speed, and operating hours (truck loading in midday when the temperature is elevated and the asphalt material is soft has a different effect on the pavement than truck loading at night when the temperature is low). Traffic volume in the MEPDG is expressed through average annual daily truck traffic (AADTT). It is possible to convert the AADTT of a vehicle fleet to ESALs using the conventional AASHTO truck damage factors [15], [26].

iii. Performance Criteria and Pavement Roughness Indices

As shown in the flowchart in Figure 3.4, the mechanistic-empirical design procedure is performance-based, meaning that prediction of key pavement distresses (permanent deformation and cracking) is an integral part design process. Therefore, in the MEPDG, pavements are designed to meet a predefined distress limit. In the empirical design guide, on the other hand, pavements are designed to meet a certain serviceability criterion. Serviceability, as defined in Section 3.3.2, does not correlate to primary pavement distresses. This is further evidenced by research study which proved

that there is inconsistency between serviceability criteria and performance [81]. For the serviceability loss criterion, different pavement designs conducted with 1993 AASHTO guide yielded varying distress rates when analyzed using the MEPDG. Table 3.6 shows the performance and serviceability criteria recommended by the MEPDG and the 1993 AASHTO guide for different roadway classes.

Table 3.6: Performance Criteria in MEPDG vs. 1993 AASHTO Guides

Roadway Functional Classification	MEPDG Recommended Performance Criteria [34]	1993 AASHTO Recommended Serviceability Loss Criteria [26]
Interstate	Alligator cracking: 10% lane area	1.2
	Total rut depth: 0.4 in.	
	IRI: 160 in./mi	
Primary	Alligator Cracking: 20% lane area	1.7
	Total rut depth: 0.5 in.	
	IRI: 200 in./mi	
Secondary	Alligator cracking: 35% lane area	2.2
	Total rut depth: 0.65 in.	
	IRI: 200 in./mi	

The roughness of an asphalt pavement expresses irregularities in the pavement structure that affect rideability (ride quality of the vehicle and comfort of the passenger), vehicle fuel consumption, and vehicle and pavement maintenance costs [102]. Poor construction quality (uneven pavement surface) as well as pavement distresses contribute to these irregularities. There are two main methods to quantify pavement roughness: international roughness index (IRI) and pavement serviceability index (PSI). Pavement serviceability index is incorporated in the 1993 AASHTO Pavement Design Guide, and is explained in Section 3.3.2. International roughness index (IRI) represents the longitudinal profile of a road (pavement), and is defined as the ratio of a standard vehicle's interrupted motion (in. or mm) divided by the total distance traveled (mi or

km), and multiplied by 1000. Thus, the lower the IRI, the better the performance of the pavement. IRI is incorporated in the MEPDG through Equation 3.7 [34]. This relationship is empirical and lacks consensus among researchers and practitioners.

$$IRI = IRI_0 + 0.015(SF) + 0.4(FC_{total}) + 0.008(TC) + 40(RD) \quad (3.7)$$

where:

- IRI* = IRI at any given time (in/mi),
IRI₀ = initial IRI (after construction) (in/mi),
SF = site factor (includes pavement age, soil plasticity index, average annual freezing index, and average annual precipitation index),
FC_{total} = area fatigue cracking (% of total lane area) (%),
TC = total length of transverse cracks (ft/mi), and
RD = average rut depth (in).

Several models have been developed to relate pavement serviceability index (PSI) to the international roughness index (IRI) [103]–[105]. However, the model represented by Equation 3.8 is based on the largest case database and is the most commonly used in literature [82].

$$PSI = 5e^{(-0.0038.IRI)} \quad (3.8)$$

The relationship between IRI and PSI shown in Equation 3.8 was used in studies that aim to adjust the structural layer coefficient of asphalt [38].

iv. Reliability

The MEPDG manual states “reliability values recommended for use in previous AASHTO guide should not be used with the MEPDG” [34]. There is a conceptual difference between the reliability considered in the MEPDG and the reliability considered in 1993 AASHTO guide. In the empirical guide, reliability is defined as the probability that the traffic prediction will be less than the actual traffic at the end of the design life. In the mechanistic-empirical guide, reliability is defined as the probability that the predicted distress will be less than the critical level for the design period (Equation 2.8), and is therefore dependent on the model prediction error of the distress prediction equations (see Section 3.3.2). It is thus reasonable that each guide recommends different reliability levels for each road class (Table 3.7).

Table 3.7: Suggested Reliability Levels by MEPDG and 1993 AASHTO for Various Functional Classifications

Roadway Functional Classification	MEPDG [34]		1993 AASHTO [26]	
	Urban	Rural	Urban	Rural
Interstate/Freeway	95	95	85-99.9	80-99.9
Principal Arterial	90	85	80-99	75-95
Collector	80	75	80-95	75-95
Local	75	70	50-80	50-80

3.5.3 Design Outputs

The 1993 AASHTO design guide over-predicts performance, i.e., underestimates distresses, for pavements in warm locations and at high traffic levels compared to mechanistic-empirical design [81]. This is mainly because the AASHTO Road Test was completed in Illinois, which has fairly a cold climate. Despite this fact, the 1993 guide is commonly used in hot climates worldwide without modification and without accounting for areas with warm temperatures.

3.6 Effect of Pavement Thickness on Stress, Strain, and Fatigue Cracking

Pavement structures exhibit two loading response phenomena associated with fatigue cracking. Cyclic loading can be characterized either by constant stress or by constant strain, depending on the thickness of the pavement. Under constant stress, the repetitive load (stress) causes damage to the pavement asphalt layer, leading to a decrease in the stiffness of the mix and an increase in tensile strain. Conversely, under constant strain, the strain (deformation) remains constant and leads to a reduced stiffness. In a laboratory test, this is achieved by reducing the stress with time to obtain a constant strain. The constant stress and constant strain phenomena are represented graphically in Figure 1.

Constant stress type of loading is generally considered to be applicable to thick asphalt pavements, where the asphalt layer is the main load-carrying component. Even though repetitive loading decreases the stiffness of the layer, the changes in stress due to traffic loading are not significant, i.e. stress is constant, because of the relatively large thickness. Constant strain type of loading is considered applicable to thin pavements, where the asphalt layer is not the main load-carrying component. Here, the underlying

layers govern the strain in the asphalt layer. Any decrease in the stiffness of the asphalt in time will not reflect significantly on the strain.

There is no consensus on the definition of thin and thick pavements. It is, however, common to consider pavements thicker than 8" as thick and those 2" as thin, as adopted in the MEPDG [106]. For intermediate thickness (2" to 8"), fatigue life is generally governed by a combination of constant stress and constant strain.

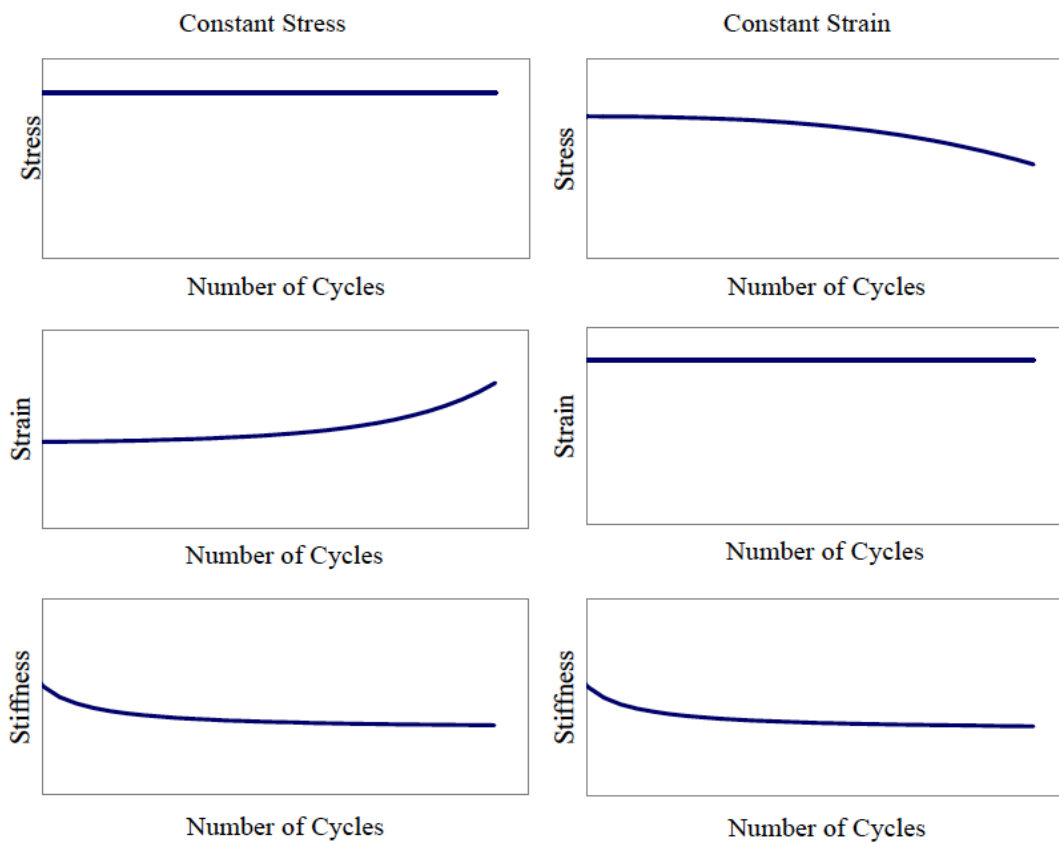


Figure 3.5: Constant stress vs. constant strain phenomena [106].

3.7 Dynamic Modulus of Asphalt Concrete and Its Use in Pavement Structural Design

NCHRP Report 456 recommends a set of laboratory tests to determine asphalt material properties that address three primary distresses: (1) asphalt rutting through the dynamic modulus and phase angle, (2) fatigue cracking through the dynamic modulus, and (3) thermal cracking through creep compliance [2]. Furthermore, NCHRP Project 1-37A which culminated in the development of the MEDPG indicates that the dynamic modulus is the main asphalt material property needed for pavement structural design [107].

The dynamic modulus represents the stiffness of an asphalt mix. The same asphalt mix has different values of stiffness for different combinations of temperature and loading frequency. Unlike concrete whose compressive strength can be accurately acquired from a simple, quick and cheap test for the purposes of material characterization and QA/QC, measuring the stiffness of asphalt at different temperature and frequency combinations is an intricate, costly and time-consuming process that requires skilled workmanship.

The complex modulus (E^*) is measured by conducting a test called simple performance test (SPT) [108]. The SPT is defined as a “test that accurately and reliably measures the mixture response characteristics or parameter that is highly correlated to the occurrence of pavement distress over a diverse range of traffic and climatic conditions” [2]. The test mainly consists of subjecting an unconfined cylindrical asphalt specimen to a uniaxial sinusoidal compressive load at different combinations of loading frequency (to reflect traffic speed) and temperature (to reflect climate). It represents the

stress strain relationship of the asphalt material in the linear viscoelastic range. Due to the viscoelastic nature of asphalt, the complex modulus is a function of the mix properties, testing frequency, testing temperature, and specimen geometry [107]. The complex modulus consists of two components: a real part (the storage modulus), and an imaginary part (the loss modulus) (Equation 3.9).

$$E^* = E' + iE'' \quad (3.9)$$

where:

E^* = complex modulus,

E' = storage modulus,

E'' = loss modulus, and

i = $\sqrt{-1}$.

The dynamic modulus is defined as the magnitude of the complex modulus (Equation 3.10). The storage and loss moduli are related to the dynamic modulus by the phase angle (ϕ) (Equation 3.11 and Equation 3.12). An elastic asphalt specimen has a low phase angle ($\phi = 0^\circ$ for a purely elastic material). As the viscous component of the asphalt specimen increases, the phase angle increases as well ($\phi = 90^\circ$ for a purely viscous material).

$$|E^*| = \sqrt{(E')^2 + (E'')^2} \quad (3.10)$$

$$E' = |E^*| \cos \phi \quad (3.11)$$

$$E'' = |E^*| \sin \phi \quad (3.12)$$

Time-temperature superposition principles characterize the linear viscoelastic behavior of asphalt concrete. As a result, the same dynamic modulus value can be acquired at a range of temperature-frequency combinations. Low temperature is equivalent to high frequency, i.e., high loading speed, and vice versa. By measuring the dynamic modulus at a number of temperature and frequency combinations, measured values can be shifted by a shift factor (a_T) to obtain a reduced frequency at a reference temperature (Equation 3.13), resulting in a dynamic modulus mastercurve, represented by a sigmoidal fit (Equation 3.14), as illustrated in Figure 3.6. The dynamic modulus mastercurve of an asphalt mix is required by Pavement-ME for Level 1 analysis.

$$a_T = \frac{f_r}{f} \quad (3.13)$$

where a_T = *shift factor at a given temperature*,

f_r = *reduced frequency at the reference temperature (Hz)*, and

f = *frequency at a given temperature (Hz)*.

$$\log(|E^*|) = a + \frac{b}{c + f / \exp^{d+e(\log(f_r))}} \quad (3.14)$$

where $|E^*|$ = *dynamic modulus*,

a, b, c, d, e, f = *fitting parameters*, and

f_r = *reduced frequency (Hz)*.

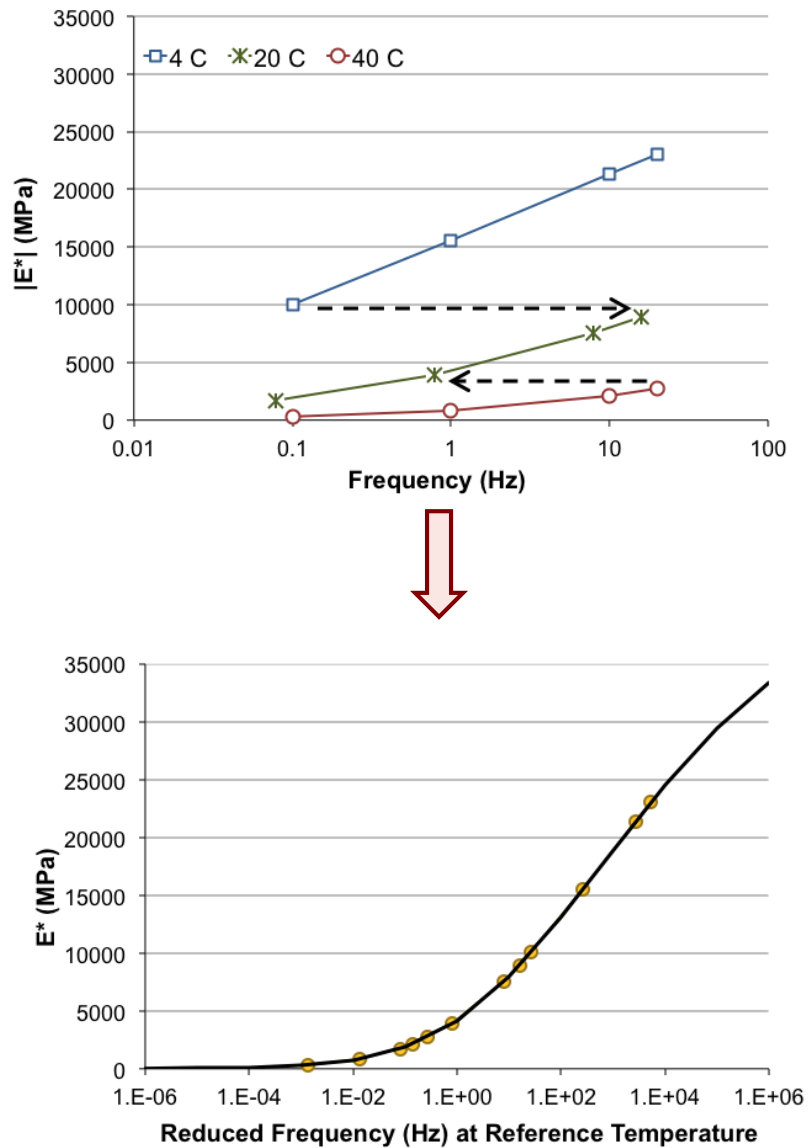


Figure 3.6: Constructing dynamic modulus mastercurve.

Predictive Models:

Due to the complexity of the simple performance test required to measure the dynamic modulus ($|E^*|$), prediction models were developed and enhanced over the years. These models generally rely on mix volumetrics to predict the $|E^*|$ of the mix at a given temperature and frequency. The most commonly used model is the one developed

by Witczak [53], [54], [65], [109], [110]. The Witczak model is incorporated in the MEPDG for level 2 and level 3 analyses. The latest version of the Witczak equation (2005) is based on 7400 data points from 346 HMA mixtures, and is presented in Equation 3.15. Kahil et al. have examined the reliability and variability in the prediction of the Witczak model [111].

$$\begin{aligned}
 \log(|E^*|) = & -0.349 + 0.754(|G^*|_b^{-0.0052})[6.65 - 0.032p_{200} + 0.0027(p_{200})^2 \\
 & + 0.011p_4 - 0.0001(p_4)^2 \\
 & + 0.006p_{3/8} - 0.00014(p_{3/8})^2 - 0.08V_a - 1.06\left(\frac{V_{b\,eff}}{V_{b\,eff} + V_a}\right)] \quad (3.15) \\
 & + \frac{2.558 + 0.032V_a + 0.713\left(\frac{V_{b\,eff}}{V_{b\,eff} + V_a}\right) + 0.0124p_{3/8} - 0.0001(p_{3/8})^2 - 0.0098p_{3/4}}{1 + \exp(-0.7814 - 0.5785 \log |G^*|_b + 0.8834 \log \delta_b)}
 \end{aligned}$$

where:

- $|E^*|$ = dynamic modulus,
- p_{200} = percentage of aggregate passing #200 sieve,
- p_4 = cumulative percentage of aggregate retained in #4 sieve,
- $p_{3/8}$ = cumulative percentage of aggregate retained in #3/8 sieve,
- $p_{3/4}$ = cumulative percentage of aggregate retained in #3/4 sieve,
- V_a = percentage of air voids (by volume of mix),
- $V_{b\,eff}$ = percentage of effective asphalt content (by volume of mix),
- $|G^*|_b$ = dynamic shear modulus of asphalt binder (psi), and
- δ_b = binder phase angle associated with $|G^*|_b$ (degrees).

Effective Conditions:

A dynamic modulus mastercurve represents the stiffness of an asphalt mix over a wide range of temperature-frequency combinations. However, for a pavement structure in a specific climatic location (mainly temperature), subjected to traffic at a

specific speed (frequency), the dynamic modulus of the asphalt layer is characterized by a portion of the mastercurve that best represents the given temperature and frequency conditions. The terms “effective temperature” and “effective frequency” represent those conditions that best represent the prevalent climate and traffic speed that a given pavement is subjected to. The “effective dynamic modulus ($|E^*|_{\text{eff}}$)” is the value on the mastercurve that corresponds to the prevalent temperature-frequency combination. The concept of effective $|E^*|$ is commonly used in knowledge-based tools such as the E* SPT Specification Criteria Program [110], the Quality Related Specifications Software (QRSS) [29], [112], and the Program for Integrated Analysis of HMA Mix And Structural Designs [113], [114]. The effective conditions are a function of the type of distress in question, which means there are effective conditions for fatigue cracking, and effective conditions for asphalt rutting.

- Effective Temperature:

The concept of effective temperature, and its development, calibration and evolution over the years is explained in detail by Basyouny and Jeong (2010) [115]. They define effective temperature as “a single test temperature at which an amount of distress would be equivalent to that which occurs from the seasonal temperature fluctuations throughout the annual temperature cycle” [115]. By this definition, it seems logical that different failure mechanisms (distresses) would have different effective temperatures. The latest calibrated effective temperature equations for rutting and fatigue are represented in Equation 3.7 and Equation 3.8 respectively [115].

$$T_{eff.fat.} = -13.995 - 2.332(Freq)^{0.5} + 1.006(MAAT) + 0.876(\sigma_{MAAT}) - 1.186(wind) + 0.549(sunshine) + 0.071(rain) \quad (3.16)$$

where:

$T_{eff.fat.}$ = effective temperature for fatigue ($^{\circ}F$),

$Freq$ = effective frequency (Hz)(see equation 3.9),

σ_{MAAT} = mean monthly air temperature ($^{\circ}F$),

$wind$ = wind speed (mph),

$sunshing$ = % sunshine, and

$rain$ = annual cumulative rainfall depth (in).

$$T_{eff.rut} = 14.62 - 3.36 \ln(Freq) - 10.94(z) + 1.121(MAAT) + 1.718(\sigma_{MAAT}) - 0.431(wind) + 0.333(sunshine) + 0.08(rain) \quad (3.17)$$

where:

$T_{eff.rut.}$ = effective temperature for rutting ($^{\circ}F$),

$Freq$ = effective frequency (Hz)(see equation 3.10), and

z = critical depth (in).

- Effective Frequency

The effective frequency of an asphalt layer can be defined as a single frequency at which an amount of distress would be equivalent to that which occurs from the speed of truck loading and unloading. The effective frequency equations for rutting and fatigue are represented in Equation 3.9 and Equation 3.10 respectively [29].

$$F_{eff.fat.} = \frac{17.6 v}{2(h_{ac}+r)} \quad (3.18)$$

where:

$F_{eff.fat.}$ = effective temperature for fatigue (Hz),

v = design speed (mph), and

h_{ac} = depth of asphalt layer (in).

$$F_{eff.rut.} = \frac{17.6 v}{2(Z_{eff}+r)} \quad (3.19)$$

where

$F_{eff.rut.}$ = effective temperature for fatigue (Hz), and

$Z_{eff.}$ = critical depth (in).

Finding the effective temperature for fatigue cracking is somewhat straight forward, whereas that of rutting involves iterations to find the critical depth, and is therefore more complex. More information can be found in [29], [110], [112]–[114].

3.8 Conclusion

This chapter covered the background theory that was believed to be essential for conducting the research in this thesis. Important highlights of this chapter include the basics of the 1993 AASHTO guide and the MEPDG design methodologies and the differences between them, fundamental asphalt material properties, namely the dynamic modulus, and the concept of effective dynamic modulus.

Chapter 4

RESEARCH SCOPE AND METHODOLOGY

4.1 Introduction

Based on the findings from Chapter 2 and Chapter 3, the proposed research targets the improvement of structural coefficient of the asphalt layer in the AASHTO 1993 Design Guide to accommodate various mixes and mix properties under different climatic conditions, traffic volumes, and traffic speeds. This chapter sets forth the research scope and methodology adopted to accomplish the stated objective.

4.2 Research Scope

The scope of the research entails developing an analytical model that relates the structural layer coefficient of asphalt ' a_1 ' to the effective dynamic modulus ($|E^*|_{\text{eff}}$), and investigating the sensitivity of the model to various design inputs. The scope also involves the development of a Microsoft-Excel-based design support tool that relies on the a_1 - $|E^*|_{\text{eff}}$ relationship to generate the asphalt layer coefficient and the resultant design thickness for a set of material (asphalt and unbound), traffic, and climate related input parameters. Details of the tool are included in Chapter 6.

Developing the Analytical Model:

- **Asphalt mixes:** 33 mixes belonging to five main mix type categories are considered:
(1) conventional hot mix asphalt, (2) asphalt with polymer modified binder (PMB),
(3) warm mix asphalt (WMA), (4) mixes with reclaimed asphalt pavement (RAP),
and (5) stone matrix asphalt (SMA) (Table 4.1 and Figure 4.1).

Table 4.1: Summary of Asphalt Mixes Included in Scope

Mix Designation	Mix Description	NMAS* (mm)	Source**
M-HMA-1	Highly modified HMA mix	19	1
M-HMA-2	Highly modified HMA mix	19	1
HMA-1	Conventional HMA	19	1
HMA-Fib	HMA + fibers	19	1
M-HMA-3	Polymer-modified HMA	19	1
M-WMA-O	Polymer-modified WMA, organic additive	19	1
M-WMA-C	Polymer-modified WMA, chemical additive	19	1
M-WMA-F	Polymer-modified WMA, foaming agent	19	1
HMA-2	Conventional HMA	25	1
WMA-O	WMA, organic additive	25	1
WMA-C	WMA, chemical additive	25	1
WMA-F	WMA, foaming agent	25	1
HMA-3	Conventional HMA	12.5	1
HMA-RA-1	HMA + 10% recycled concrete aggregate	12.5	2
HMA-RA-2	HMA + 20% recycled concrete aggregate	12.5	2
HMA-RA-3	HMA + 30% recycled concrete aggregate	12.5	2
HMA-4	Conventional HMA	12.5	3
HMA-RAP-1	HMA + 10%RAP	12.5	3
HMA-RAP-2	HMA + 25%RAP	12.5	3
HMA-RAP-3	HMA + 40%RAP	12.5	3
SM-1	HMA + 15%RAP	9.5	4
SM-2	Polymer-modified HMA + 12%RAP	12.5	4
SM-3	HMA + 25%RAP	12.5	4
SM-4	Polymer-modified HMA + 15%RAP	12.5	4
BM-1	HMA + 15%RAP	25	4
BM-2	HMA + 15%RAP	25	4
BM-3	HMA + 15%RAP	25	4
BM-4	HMA + 25%RAP	25	4
BM-5	HMA + 25%RAP	25	4
BM-6	HMA + 25%RAP	25	4
SMA-1	Polymer-modified SMA	12.5	4
SMA-2	Polymer-modified SMA	12.5	4
SMA-3	SMA	12.5	4

*Nominal Maximum Aggregate Size

**Source 1: Ongoing Testing at the American University of Beirut.

Source 2: [116]

Source 3: [117], [118]

Source 4: [119]

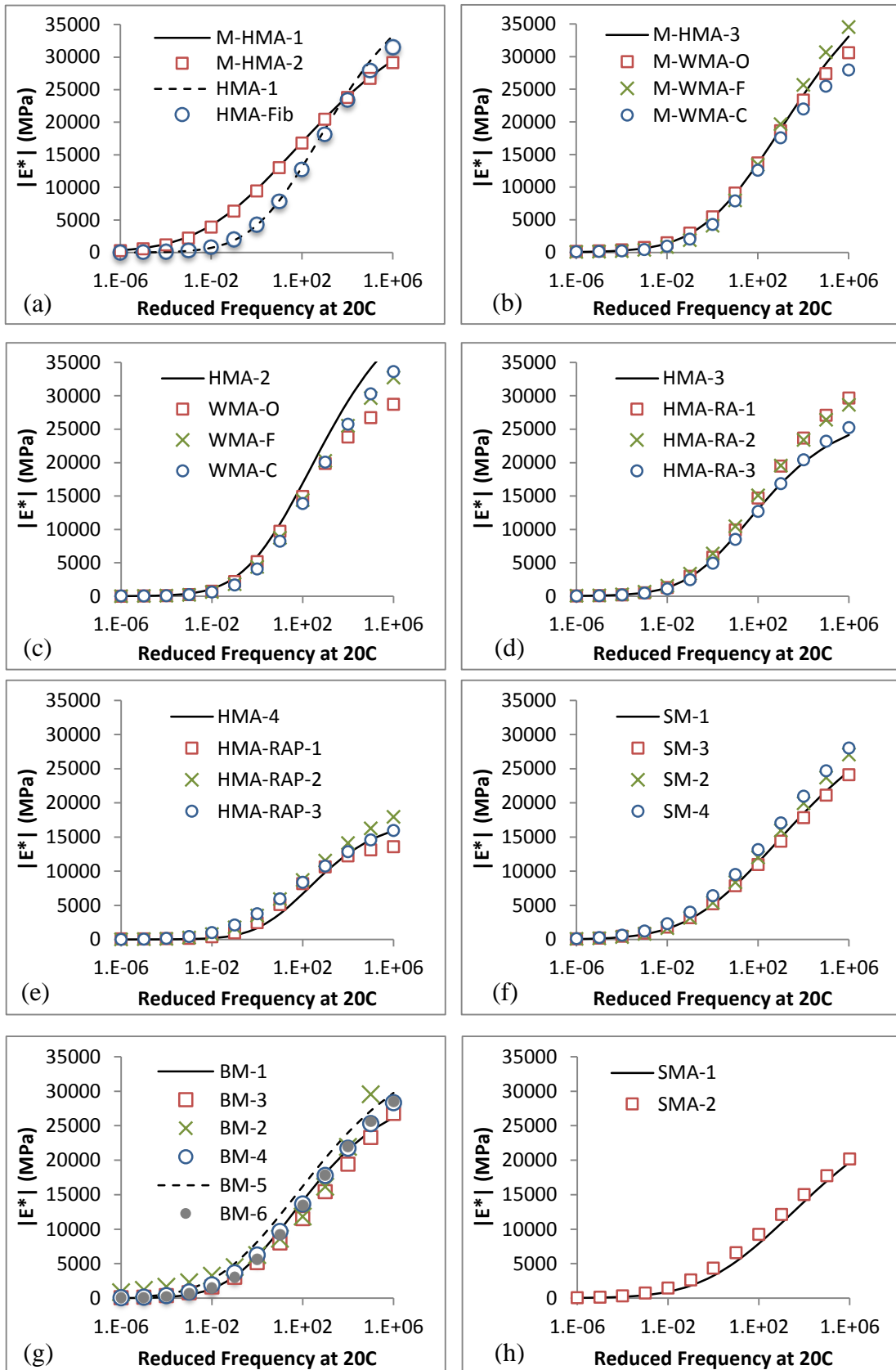


Figure 4.1: Dynamic modulus mastercurves of mixes included in scope: (a) polymer modified and fiber modified mixes, (b) WMA with PMB, (c) WMA with neat binder, (d) RAP, (e) Virginia DOT surface mixes, (f) Virginia DOT base mixes, (g) Virginia DOT SMA mixes.

- Climatic conditions:** To develop the $a_I-|E^*|_{\text{eff}}$ relationship, four climatic regions are considered: cold (represented by Chicago, IL, mean annual air temperature (MAAT) $\sim 52^\circ\text{F}$ (11°C)), moderate (represented by St. Louis, MO, MAAT $\sim 56^\circ\text{F}$ (13.5°C)), moderate to hot (represented by Dallas, TX, MAAT $\sim 66^\circ\text{F}$ (19°C)), and hot (represented by Phoenix, AZ, MAAT $\sim 75^\circ\text{F}$ (24°C)). In addition, two traffic levels are studied: low volume (1,500 AADTT) and high volume (15,000 AADTT), where AADTT is the average annual daily truck traffic. It is known that temperature and frequency (speed) have similar effects on fundamental asphalt material properties due to the applicability of time-temperature superposition. Therefore, traffic speed is held constant at 60 mph (~ 96 km/h) and is not varied, as its effect can be mapped from that of temperature.
- Unbound layer properties:** The moduli of the aggregate base layer and the subgrade layer are assumed to be 30,000 psi (~ 200 MPa) and 25,000 psi (~ 172 MPa) respectively. The thickness of the aggregate base taken to be 12 inches (~ 30 cm) for the low volume scenarios and 15 inches (~ 38 cm) for the high volume scenarios.
- Design life and failure criterion:** The proposed model addresses fatigue cracking as the main mode of failure. The failure limit is set at 15% fatigue cracking at the end of a 10-year design life.

Based on the above, the analytical model that relates the structural layer coefficient of asphalt ' a_I ' to the effective dynamic modulus ($|E^*|_{\text{eff}}$) is based on 264 data points, each representing a distinct structural design scenario (Equation 4.1). All statistical analysis of the data was conducted using R through the R-Studio platform [120].

$$\text{Number of Scenarios} = 33 \text{ mixes} \times 4 \text{ climates} \times 2 \text{ traffic volumes} = 264 \quad (4.1)$$

Studying the Sensitivity of the a_1 - $|E^*|_{eff}$ relationship to Design Inputs:

The sensitivity study includes investigating the effect of changing the traffic, unbound layer properties, and performance criteria, on the a_1 - $|E^*|_{eff}$ relationship. The analysis encompasses three mixes (one belonging to each of the main mix categories: conventional HMA, HMA with polymer-modified binder, and WMA) and two climatic regions (Chicago (cold) and Dallas (moderate-hot)). The input parameters included in the sensitivity study were selected based on findings from the literature review (Table 3.4), and include performance limits (10%, 15%, and 20% fatigue cracking), traffic level (10,000, 12,500, 15,000, 17,500, and 20,000 AADTT), aggregate base thickness (13, 15, and 17 inches (~33, 38, and 43 cm respectively)), subgrade modulus (15,000, 20,000, and 25,000 psi (~103, 138, and 172 MPa respectively)), and aggregate base modulus (20,000, 22,500, 25,000, 27,500, 30,000, and 35,000 psi (138, 155, 172, 190, 207, and 241 respectively)).

4.3 Research Methodology

The research methodology entails three distinct steps: (1) establishing the analytical model that relates the structural coefficient ' a_1 ' to the effective dynamic modulus ($|E^*|$), (2) conducting a sensitivity analysis, and (3) comparing the design thicknesses obtained using the model to those acquired using the 1993 design guide and the MEPDG for a given fatigue failure of 15%. Details of each step are summarized below.

- I. Establishing the a_1 - $|E^*|_{eff}$ relationship: The methodology specific to establishing the relationship is presented in Figure 4.2 and entails:

- a. Conducting runs using Pavement-ME to find design thicknesses (by using increments of 0.05 inches) for the 264 scenarios,
 - b. Back-calculating the structural layer coefficient of the asphalt layer based on the equations of the 1993 design guide but with thicknesses calculated using Pavement-ME,
 - c. Finding the effective dynamic modulus ($|E^*|_{\text{eff.}}$) for each mix under each of the climatic conditions, and
 - d. Establishing a relationship between the structural coefficient ' a_1 ' and the effective dynamic modulus ($|E^*|_{\text{eff.}}$) using statistical regression.
- II. Studying the sensitivity of a_1 - $|E^*|_{\text{eff.}}$ relationship to design inputs by running Pavement-ME for the different sensitivity conditions specified in the scope, and comparing them to the default values that were selected to develop the model, and updating the model according to findings, and
- III. Studying the implications of the research model by comparing the design thicknesses obtained using the model to those acquired using the 1993 design guide, and the subsequent effect on economic and environmental costs.

4.4 Assumptions

The methodology is based on an underlying assumption that the MEPDG (Pavement-ME) is more reliable than the 1993 design guide, and generates design thicknesses that are closer to optimal. Other assumptions include the following:

- As built design air voids range between 6 and 8% depending on the mix type,

- 15% fatigue cracking is equivalent to a change in pavement serviceability index (PSI) of 1.2 (Table 3.6),
- Reliability is assumed to be 90% in both, the MEPDG and 1993 guide. Although the concept of reliability is different in each of the two design guides, change in reliability is assumed to have a similar effect on design thickness in both [81].
- Conversion of traffic from AADTT to ESALs is based on calculations conducted by Pavement-ME, which assumes a structural number of 5 and a terminal serviceability of 2.5.

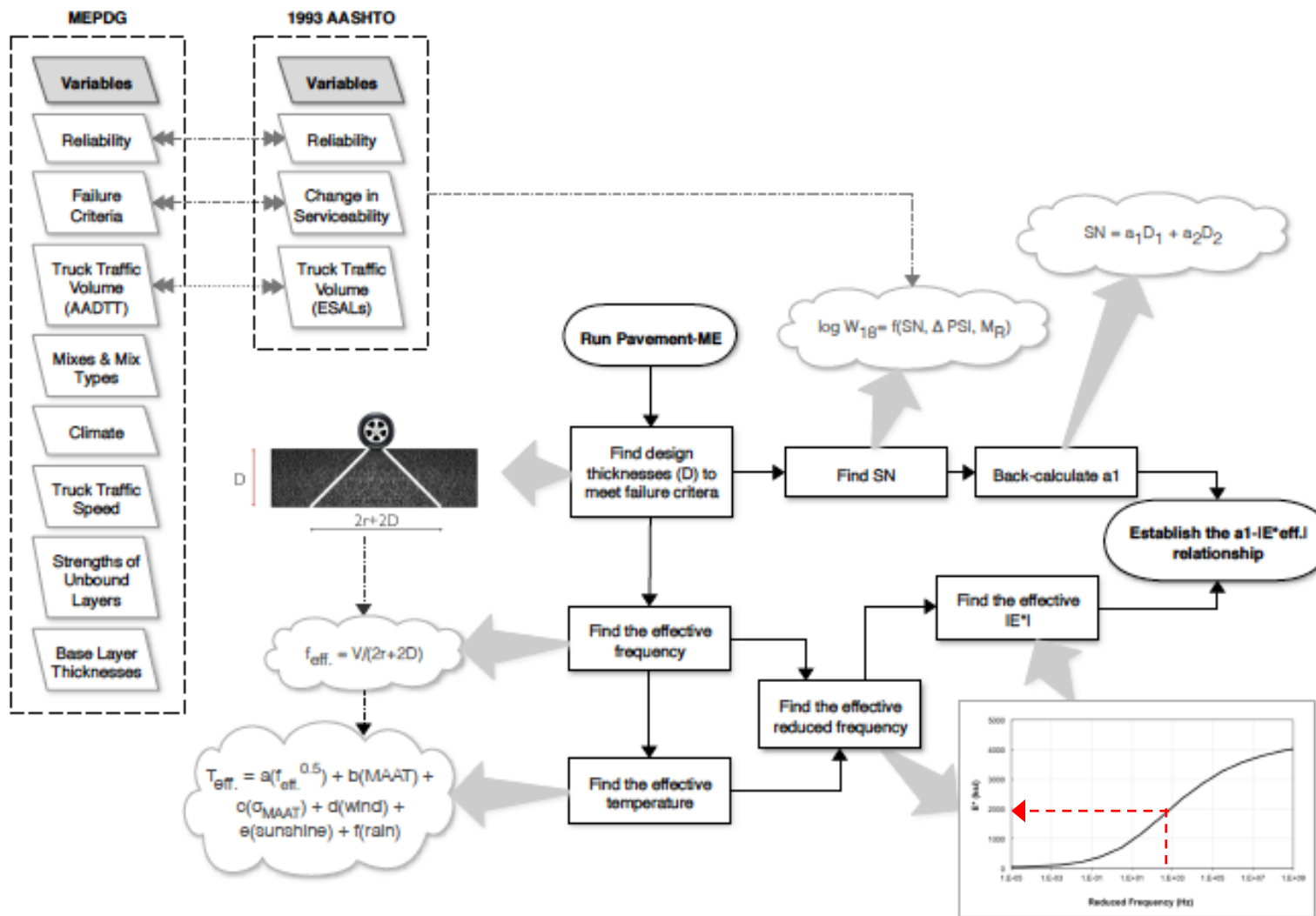


Figure 4.2: Methodology adopted to develop the $a_1-|E^*|_{\text{eff}}$ relationship.

Chapter 5

RESULTS AND ANALYSIS

5.1 Introduction

It has been established from the discussions in Chapter 2 and Chapter 3 that AAHSTO's 1993 pavement design method has serious limitations, one of which being the fact that the structural layer coefficient of the asphalt layer is an abstract value that does not represent the properties of the material in question. Studies aiming at improving the estimate of the structural layer coefficients of asphalt mixes and that relied on using FWD results to back-calculate ' a_l ' (Table 2.3) failed to capture the effect of climate and traffic speed, and only targeted a limited number of material types. This chapter presents the findings of the study conducted to provide a more accurate estimate of the structural coefficient ' a_l ' of the asphalt layer by establishing a relationship between the structural coefficient and the effective dynamic modulus ($|E^*|_{\text{eff}}$). The effective dynamic modulus was selected as a representative indicator, since it captures the effect of mix type (unique viscoelastic response) as well as climate (temperature), and traffic speed (frequency).

5.2 Structural Layer Coefficient of Different Asphalt Mix Categories

The structural layer coefficient for each of the material-climate-traffic scenarios defined in the scope (Chapter 4) was acquired based on the methodology presented in Figure 4.2. The structural layer coefficient was found to be dependent on the three variables: mix type (e.g. polymer modified asphalt versus conventional asphalt), climate (mainly temperature), and traffic speed, as evidenced by Figure 5.1. The figure distinguishes between the structural layer coefficients of each mix type under

the different climatic conditions considered in this study. The effect of traffic speed is not portrayed directly, but is represented by the effect of climate due to the applicability of time-temperature superposition in the asphalt material's linear viscoelastic range.

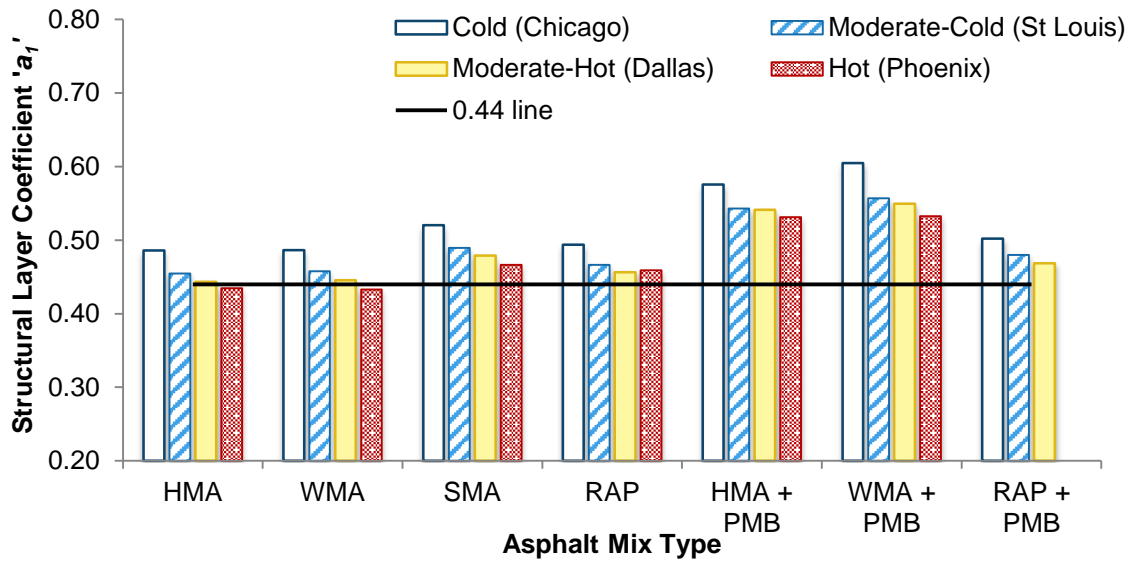


Figure 5.1: Average structural layer coefficient of different asphalt mix categories.

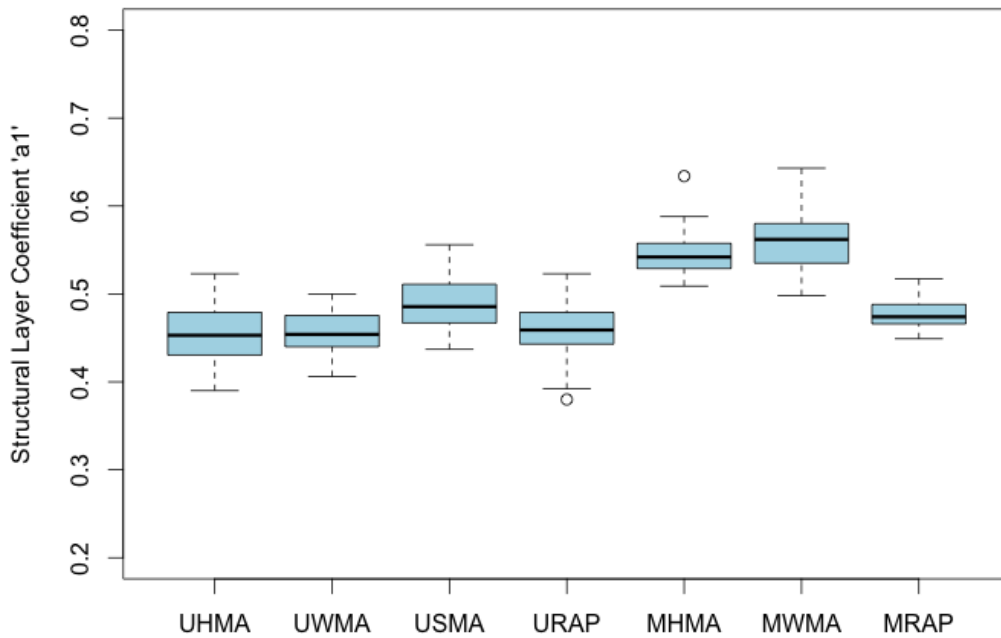


Figure 5.2: Box-plot showing effect of mix type on the structural layer coefficient (U: unmodified, M: polymer-modified).

A one-way ANOVA was conducted to validate statistically the effect of mix type on the average structural layer coefficient for the six mixes types. The ANOVA showed a significant effect of mix type on the average structural layer coefficient at the 95% confidence level [$F(9, 228) = 43.87, p\text{-value} < 2E-16$]. The difference in the mean layer coefficient and corresponding variance between the mix types can be visualized in the boxplot in Figure 5.2. A post hoc Tukey HSD test was conducted to evaluate the statistical significance of the difference between the average structural layer coefficients among the mixes at $p\text{-value} < 0.05$. The results of the Tukey HSD test showed no significant difference among: HMA and WMA (for both conventional and polymer-modified binder), RAP with polymer-modified binder and conventional HMA, and all HMA mixes with unmodified binder.

Based on the results that are summarized in Figure 5.1, the following can be concluded:

- For all mix types, as temperature increases, i.e., traffic speed decreases, the structural layer coefficient decreases. This is expected since at higher temperatures, asphalt mixes, irrespective of their type, become softer, and thus their structural capacity decreases.
- Polymer-modified asphalt mixes have, on average, higher layer coefficients, i.e., higher structural capacity than conventional mixes or other mixes with unmodified binder, which agrees with the literature (Table 2.3).
- The layer coefficient tends to decrease, i.e., design thickness increases due to the presence of reclaimed asphalt pavement (RAP) in the asphalt mixes.
- The effect of WMA additives on the structural capacity of the asphalt layer is not pronounced.

- Stone matrix asphalt (SMA) mixes tend to have better structural capacity (higher layer coefficient) than conventional HMA.
- All average structural layer coefficients fall relatively close to or above the value of 0.44 recommended by the 1993 AASHTO Design Guide.

5.3 Relationship between Asphalt Layer Coefficient ‘ a_1 ’ and $|E^*|_{\text{eff}}$.

The research methodology presented in Figure 4.2 culminated in establishing a *linear* relationship (Equation 5.1) between the structural layer coefficient of the asphalt layer and the effective dynamic modulus $|E^*|_{\text{eff}}$ of the asphalt mix.

$$a_1 = m|E^*_{\text{eff}}| + \text{int.} + \varepsilon \quad (5.1)$$

where a_1 = structural coefficient of the asphalt layer,
 $|E^*_{\text{eff}}|$ = effective dynamic modulus of the asphalt mix,
 m = slope (unit change in a_1 for every unit change in $|E^*_{\text{eff}}|$),
 int. = intercept, and
 ε = $N(0, \sigma^2)$.

Figure 5.3 shows the universal a_1 - $|E^*|$ relationship. Note that the term “universal” is used to refer to the general a_1 - $|E^*|$ curve established based on the scope of the thesis, and thus cannot be regarded as a generic curve. The linear fit shown in Figure 5.3 is significant at the 95% confidence level (p -value for the regression = 3.45E-13), and accounts for more than 27.6% of the variability in the data (R^2) (Table 5.1). The model indicates that, on average, an increase in asphalt stiffness by 5000 MPa leads to an increase of approximately 0.02 in the layer coefficient.

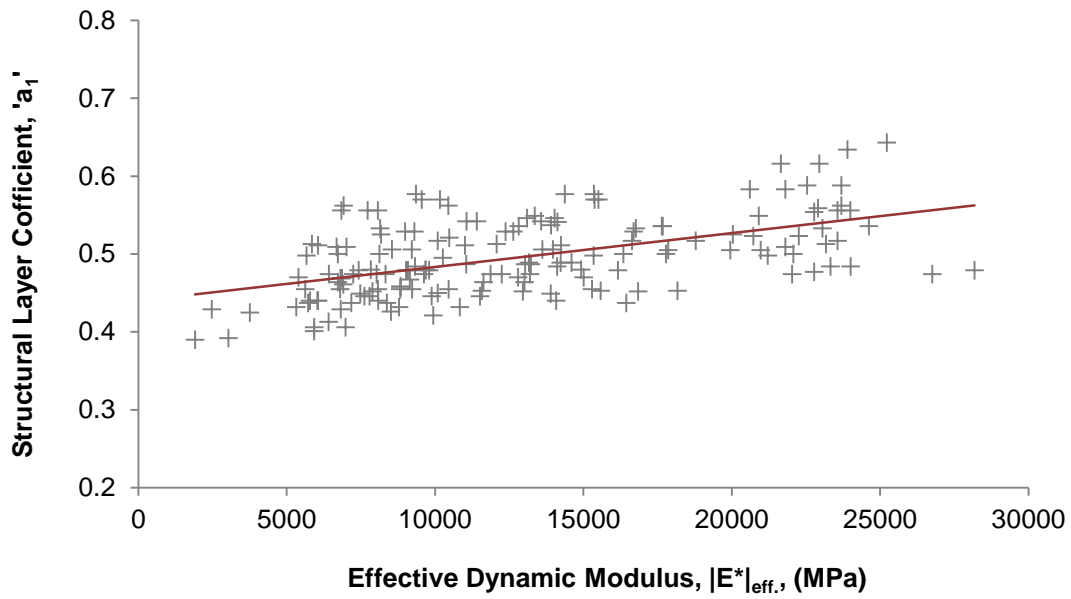


Figure 5.3: Universal a_1 - $|E^*|_{\text{eff.}}$ relationship (based on database considered in scope).

Further inspection of the data and the universal a_1 - $|E^*|_{\text{eff.}}$ relationship revealed that the regression can be improved by segregating the data points according to mix category and fitting a linear model for each separately. As such, it is anticipated that the (virtual) intercept would be a function of mix type. The mixes were separated into two broad categories: mixes with polymer-modified binder, and those with unmodified binder. As shown in Figure 5.4, the regression improves due to the fact that polymer-modified mixes have, on average, higher structural layer coefficients than mixes with unmodified binders. The new linear models for unmodified and polymer-modified binders are both statistically significant at the 95% confidence level (p -value = 2.97E-14 and 3.25E-8 respectively), and account for greater variability in the data than the universal curve shown Figure 5.3 (29.8% and 35.6% respectively).

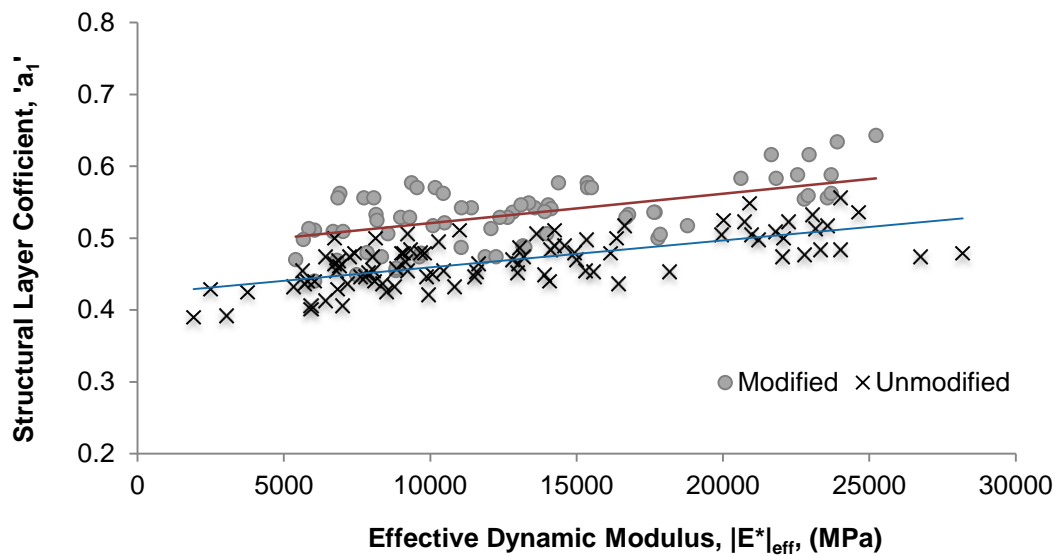


Figure 5.4: a_1 - $|E^*|_{\text{eff}}$ relationship for mixes with polymer-modified binder versus unmodified binder.

Each of these two categories (modified and unmodified) was further divided into sub-categories based on mix type and aggregate gradation through nominal maximum aggregate size (NMAS). Mixes with lower NMAS, which typically correspond to surface mixes, are theoretically meant to have superior performance (higher structural capacity) compared to those with higher NMAS (usually base mixes). Therefore, NMAS reflects not only the quality of the mix, but also its location in the pavement structure. It would thus be expected that base mixes have lower structural layer coefficients than surface mixes for the same mix type.

i. Mixes with Unmodified Binder

For asphalt mixes with unmodified binder, which constitute a larger set of data points in the scope of this study compared to mixes with modified binder, nominal maximum aggregate size (NMAS) was a variable alongside mix type. Some of the

asphalt mixes constitute surface mixes, and have a NMAS of 9.5mm, 12.5mm and 19mm. Other mixes constitute mixes for asphalt base layers and have a NMAS of 25mm. Unmodified WMA mixes were combined with unmodified HMA mixes because of an unapparent effect of the WMA additive on the structural capacity of the asphalt layer. Figure 5.5 shows two $a_1-|E^*|_{\text{eff}}$ relationships for these mixes, separated by NMAS, with surface mixes having slightly higher structural layer coefficients than asphalt base mixes. The linear models for the surface and asphalt base mixes are both statistically significant at the 95% confidence level, and account for greater variability in the data than the general curve (Table 5.1) for unmodified mixes shown in Figure 5.4.

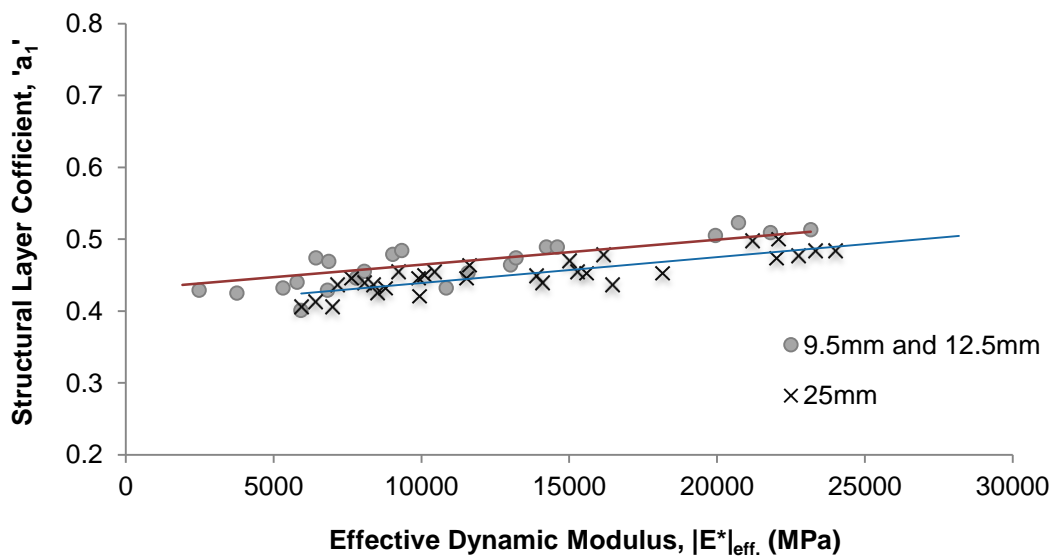


Figure 5.5: $a_1-|E^*|_{\text{eff}}$ relationship for conventional HMA and unmodified WMA mixes, separated by NMAS.

A similar effect of NMAS is observed for the mixes with RAP (Figure 5.6). The linear models for the surface and base mixes are both statistically significant at the 95% confidence level, and account for greater variability in the data (Table 5.1) than the curve shown Figure 5.5.

Similarly, nonconventional HMA mixes (Figure 5.7), namely SMA mixes, mixes with fibers, and mixes with fine RCEA, resulted in a significant linear fit at the 95% confidence level and a large variability in 'a' captured by the model (Table 5.1).

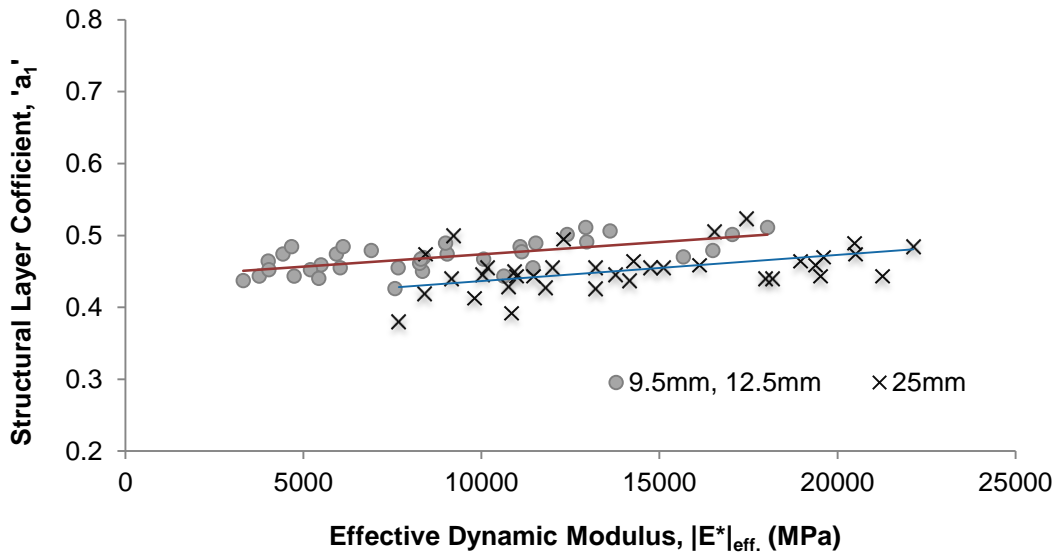


Figure 5.6: a_1 - $|E^*|_{\text{eff.}}$ relationship for mixes with RAP, separated by NMAS.

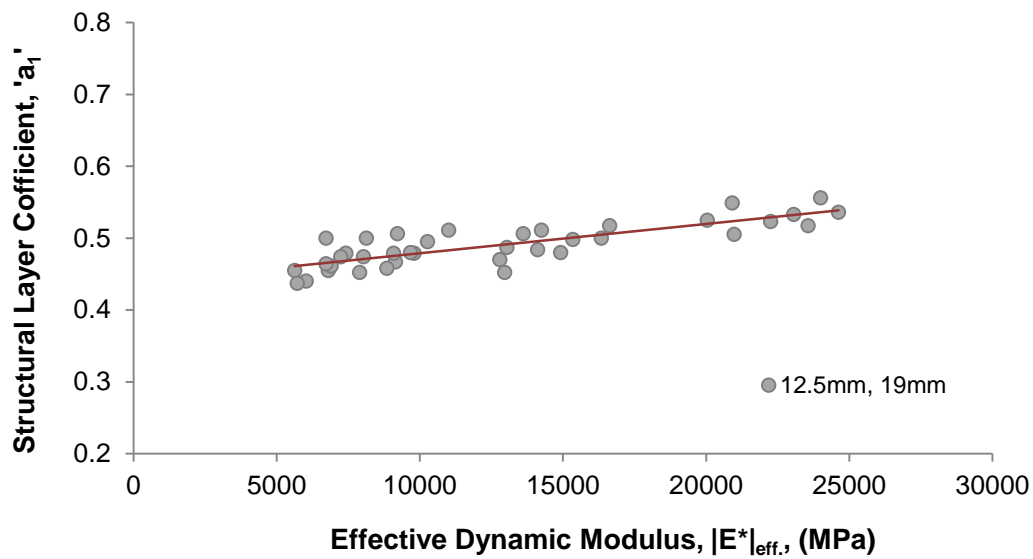


Figure 5.7: a_1 - $|E^*|_{\text{eff.}}$ relationship for SMA mixes and mixes with fibers.

ii. Mixes with Polymer-Modified Binder

The mixes with polymer-modified binder were subdivided into two categories: one for HMA and WMA, and one for RAP. It is clear that mixes with RAP have lower structural layer coefficients, as expected (Figure 5.8). The HMA and WMA mixes and the mixes with RAP constitute surface mixes and have a NMAS of 19mm 12.5mm respectively. Therefore, the effect of NMAS cannot be not directly observed, since it is masked by mix type. The linear relationships for the HMA/WMA and RAP mixes are both statistically significant at the 95% confidence level (Table 5.1).

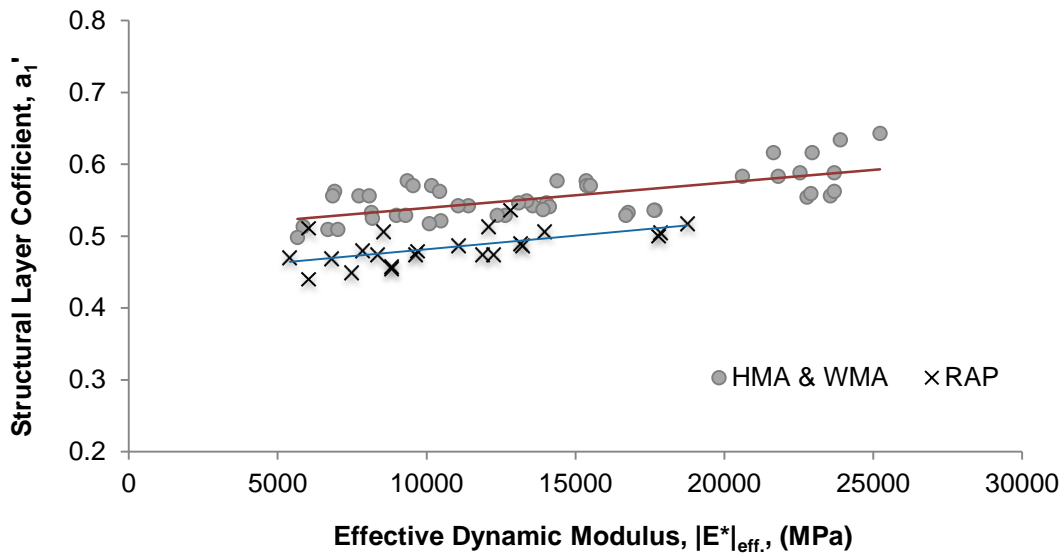


Figure 5.8: a_1 - $|E^*|_{\text{eff.}}$ relationship by mix type for mixes with polymer-modified binder.

5.3.2 Statistical Justification

All linear fits presented above were examined statistically, and their slopes and intercepts were found to be significant at the 95% confidence level. The structural layer coefficients (y-axis) were found to be normally distributed about the effective dynamic modulus (x-axis), and the residuals were well scattered for all fits. All linear regressions yielded satisfactory R^2 values. The regression parameters and the results of the statistical analysis for all fits are summarized in Table 5.1. By taking a look at the intercept for each mix category, it can be inferred that in general, polymer-modified mixes surface have the highest layer coefficients, as one would expect, and unmodified mixes have the lowest layer coefficients.

Table 5.1: Statistical Summary of Linear Models

Mix Category*	(Virtual) Intercept	<i>p</i> -value (Intercept)	Slope	<i>p</i> -value (Slope)	R ²	Adjusted R ²
All mixes (universal)	0.434	<2E-16	4.35E-6	3.45E-13	0.276	0.272
All mixes with unmodified binder	0.422	<2E-16	3.70E-6	2.97E-14	0.298	0.293
All polymer-modified mixes	0.468	<2E-16	4.77E-6	3.25E-8	0.356	0.347
U-Sur	0.405	2.14E-8				
U-Bas	0.413	1.30E-7				
U-SMA	0.438	7.72E-4				
RAP-Sur	0.441	1.68E-4	3.0E-6	9.53E-4	0.791	0.773
RAP-Bas	0.410	1.73E-7				
M-HMA-WMA	0.505	<2E-16				
M-RAP	0.440	9.32E-3				

*U: unmodified, M: modified

5.3.3 Analytical Discussion

By examining the $a_I-|E^*|_{\text{eff}}$ plots, it is obvious that the same $|E^*|_{\text{eff}}$ can yield different values of ‘ a_I ’, depending on the mix type. Although it is analytically justifiable that polymer-modified mixes have, on average, higher structural layer coefficients than mixes with unmodified binder, it may seem counterintuitive that the *same* $|E^*|_{\text{eff}}$ can yield different values of ‘ a_I ’, depending on the mix type. However, this can be explained by the fact that, although two mixes can have the same $|E^*|$ value at their respective effective reduced frequencies, their overall response function (mastercurve) may be different. For example, for the case of polymer-modified mixes, the entire mastercurve is often higher, i.e., mix is stiffer compared to conventional HMA (Figure 4.1).

Figure 5.9 demonstrates a summarized $a_I-|E^*|_{\text{eff}}$ relationship. The plot shows three broad zones pertaining to the y-axis: zone 1 for polymer-modified mixes, zone 2 for unmodified mixes, and zone 3 for mixes with RAP. The color gradient represents

the effect of climate (temperature) on the E^*_{eff} . and accordingly the structural layer coefficient ' a_1 '. Hotter temperatures (red, left) yield lower effective dynamic modulus, and thus lower ' a_1 ', whereas colder temperatures (blue, right) yield higher effective dynamic modulus, and thus higher ' a_1 '.

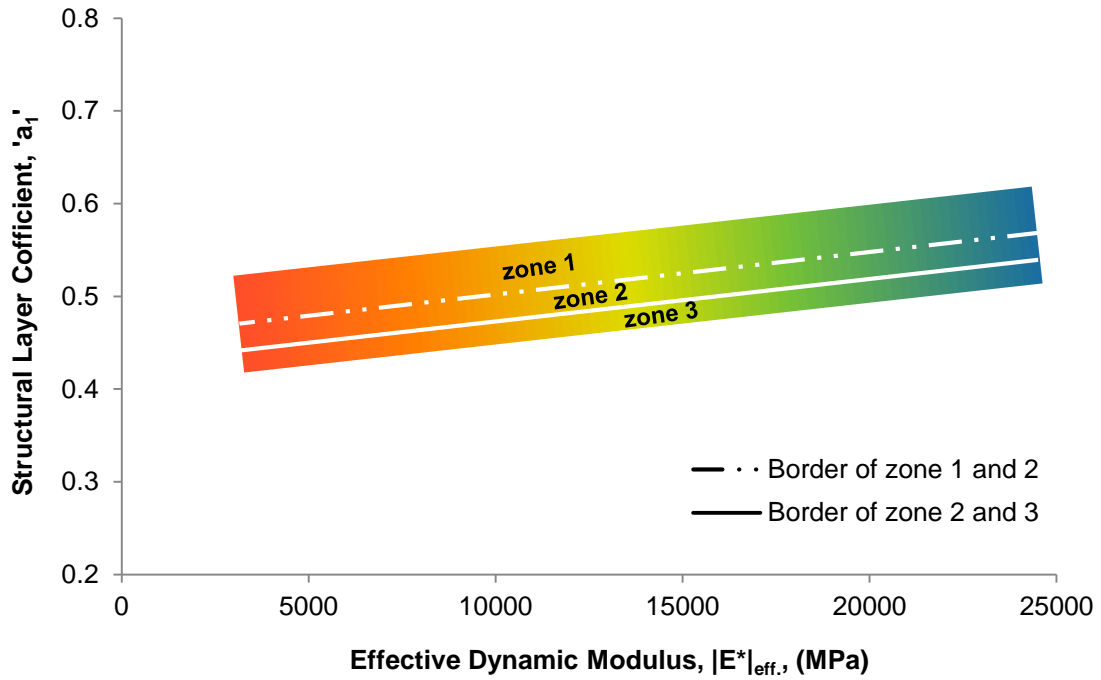


Figure 5.9: General initial a_1 - $|E^*|_{\text{eff}}$ relationship based on the research scope.

5.4 Sensitivity Analysis and Interpretation

Design inputs, such as the failure criterion, thickness and modulus of the aggregate base layer, and traffic volume (Chapter 4), were initially assumed for the back-calculation of the structural layer coefficient. These inputs may affect the output of the MEPDG (Pavement-ME) runs, and in turn, may affect the back-calculated structural layer coefficient. Therefore, a sensitivity analysis was conducted to examine the sensitivity of the back-calculated ' a_1 ', and subsequently the a_1 - $|E^*|_{\text{eff}}$ relationship to

each of the input parameters. Since fatigue cracking was used as the basis for structural design, it was essential to select the inputs that have the greatest effect on fatigue cracking for the sensitivity analysis. Based on the literature review (Table 3.4), four main parameters were selected for investigation: traffic volume, modulus of aggregate base layer, thickness of aggregate base layer, and modulus of subgrade. These represent the design inputs that most affect fatigue-cracking predictions in the MEPDG. An additional parameter was investigated that also relates to the 1993 design guide, and that is the assumption that 15% fatigue cracking is equivalent to change in serviceability (Δ PSI) of 1.2.

i. Sensitivity to Fatigue- Δ PSI Correlation

A main assumption in the back-calculation of the structural layer coefficients was that 15% fatigue cracking is equivalent to a Δ PSI of 1.2. The sensitivity of the structural layer coefficient to that assumption was investigated in two steps. Initially, the change in PSI was varied between 1.1 and 1.3, by increments of 0.1, keeping fatigue cracking at 15%. It was found that the back-calculated ' a_1 ' is slightly sensitive to the assumed Δ PSI, but the effect may be neglected since the assumed value of 1.2 yields a reasonable average ' a_1 ' (Figure 5.10).

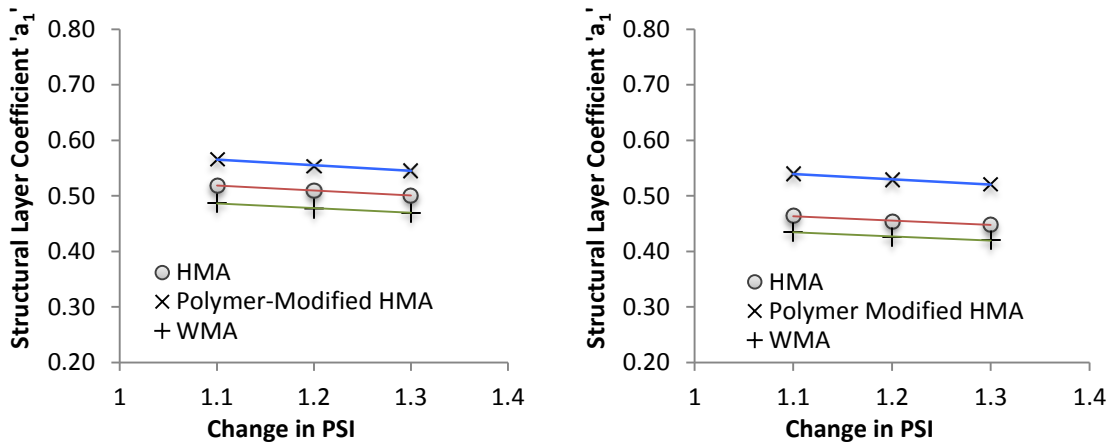


Figure 5.10: Sensitivity of structural layer coefficient to assumed change in PSI in cold climate (Chicago) (left), and moderate to hot climate (Dallas) (right).

Second, both Δ PSI and the failure limit of fatigue cracking were varied simultaneously. Fatigue cracking limits of 10%, 15% and 20% were considered. The challenge here was to associate the fatigue limit with a representative Δ PSI. Although empirical relationships that relate PSI to IRI do exist (e.g. Equation 3.7), however, the correlation between PSI and IRI lacks a fundamental comparative basis. PSI includes rideability parameters that are not considered in IRI calculations, such as longitudinal and transverse variations in slope. Moreover, no consensus exists on the extent of contribution of fatigue cracking to IRI. Therefore, the PSI-IRI correlation was dismissed, and Table 3.6 was used as a benchmark instead. In order to make the correlation between fatigue cracking and PSI as representative as possible, it was important to isolate the effect of fatigue cracking on the change in PSI. To do so, it was essential to look at other distresses, mainly total rutting (asphalt and subgrade).

A pilot study revealed that beyond an asphalt layer thickness of 5.5 inches (14 cm) (which represents the thicknesses in the scope of this research), fatigue cracking has a close to linear relationship with layer thickness, whereas thickness increases,

fatigue cracking decreases in a uniform fashion. Total rutting, however, has an exponential relationship with thickness, and subsequently with fatigue cracking. Therefore, it can be generally stated that, as the pavement deteriorates and fatigue cracking increases, total rutting increases exponentially. As a result, “serviceability” decreases exponentially. Moreover, rutting has a more pronounced effect on serviceability.

Accounting for the above discussion, it was assumed that 10% fatigue cracking is equivalent to Δ PSI of 1.1, and 20% fatigue cracking to Δ PSI of 1.7 (Table 3.6). Accordingly, almost no effect on the back-calculated ‘ a_1 ’ was observed (Figure 5.11).

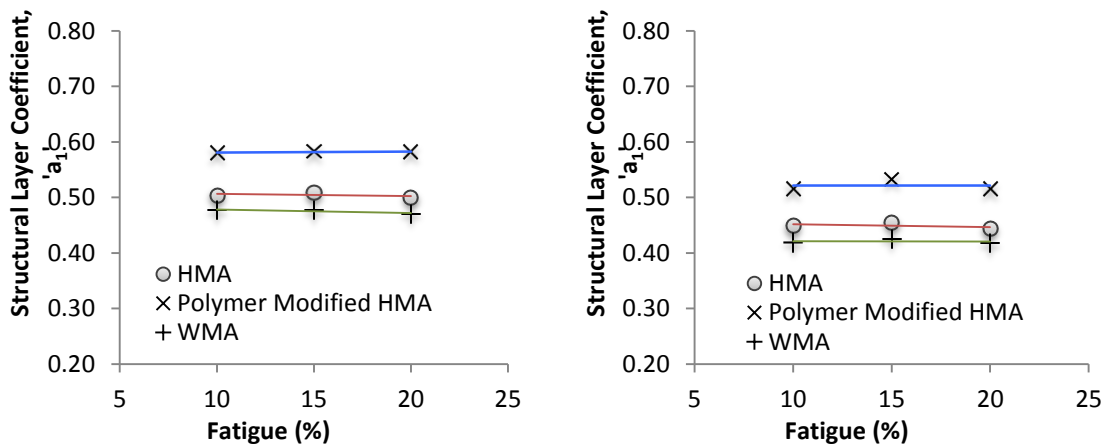


Figure 5.11: Sensitivity of structural layer coefficient to % fatigue cracking in cold climate (Chicago) (left), and moderate to hot climate (Dallas) (right).

ii. Sensitivity to Traffic Volume

The sensitivity of the structural layer coefficient to traffic volume was examined by varying average annual daily truck traffic (AADTT) from 10,000 to 20,000 by increments of 5,000 for two climatic conditions: cold (represented by Chicago), and moderate to hot (represented by Dallas). The graphs in Figure 5.12 show that the layer coefficient is independent of traffic volume.

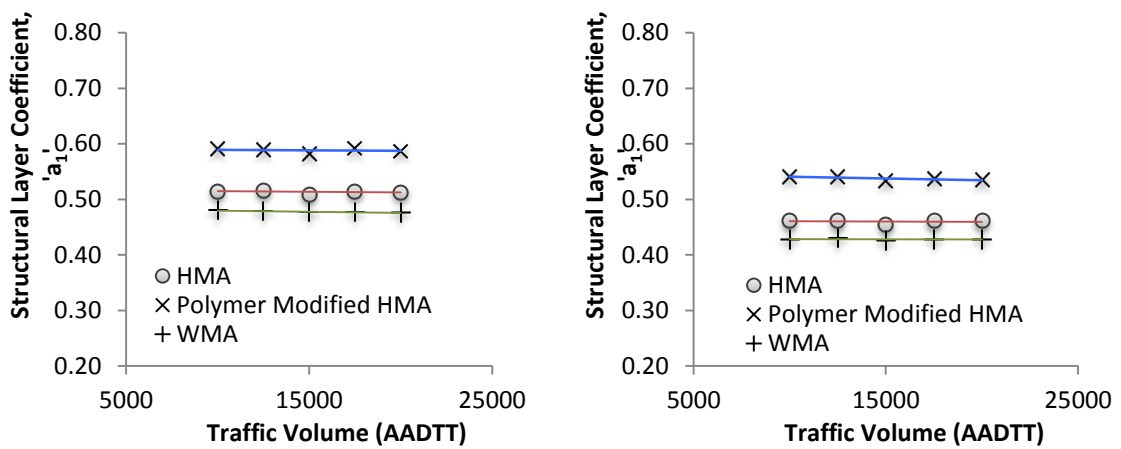


Figure 5.12: Sensitivity of structural layer coefficient to traffic volume in cold climate (Chicago) (left), and moderate to hot climate (Dallas) (right).

iii. Sensitivity to Thickness of Base

The sensitivity of the structural layer coefficient to the thickness of the aggregate base layer was examined by varying it from 13 to 17 in. (~33 to 43 cm) by increments of 2 in. (~5 cm) for two climatic conditions: cold (represented by Chicago), and moderate to hot (represented by Dallas). The graphs in Figure 5.13 show that the layer coefficient is relatively insensitive to the thickness of the aggregate base layer.

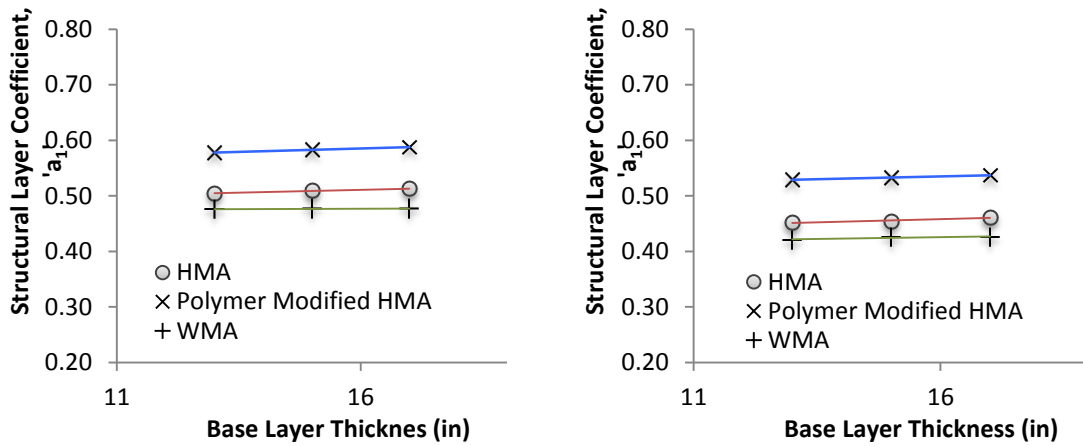


Figure 5.13: Sensitivity of structural layer coefficient to base thickness in cold climate (Chicago) (left), and moderate to hot climate (Dallas) (right).

iv. Sensitivity to Resilient Modulus of Subgrade

The sensitivity of the structural layer coefficient to the resilient modulus of the subgrade was examined by varying the it from 15,000 to 25,000 psi (~103 to 172 MPa) by increments of 5,000 psi (~34.5 MPa) for two climatic conditions: cold (represented by Chicago), and moderate to hot (represented by Dallas). The graphs in Figure 5.14 show that the for polymer modified mixes, the structural layer coefficient is insensitive to the resilient modulus of the subgrade, whereas mixes with unmodified binder are slightly sensitive to it. The effect of subgrade resilient modulus may be masked by the thickness and modulus of the base layer, and therefore, at this stage, it was decided to neglect it. Nevertheless, sensitivity of the structural layer coefficient of the asphalt layer to the resilient modulus of the subgrade must be investigated in future studies.

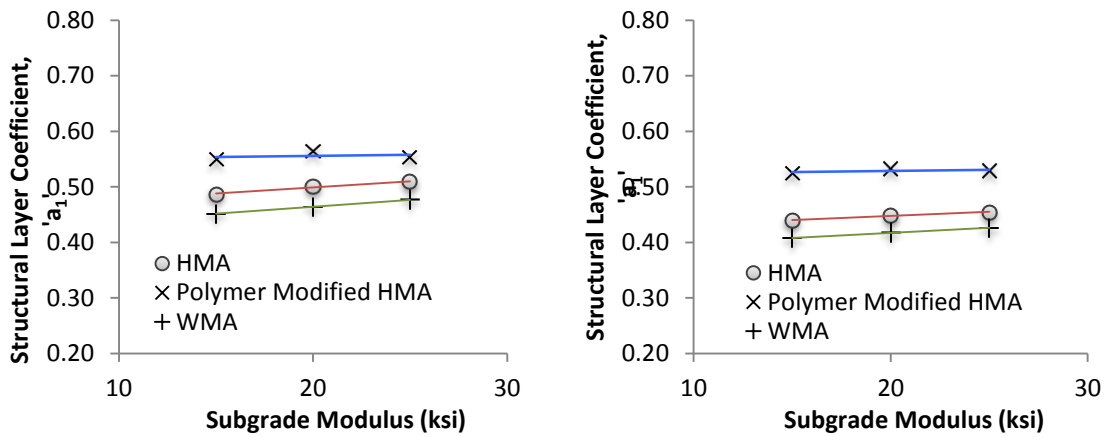


Figure 5.14: Sensitivity of structural layer coefficient to subgrade modulus in cold climate (Chicago) (left), and moderate to hot climate (Dallas) (right).

v. Sensitivity to Resilient Modulus of Aggregate Base

The sensitivity of the structural layer coefficient to the resilient modulus of the aggregate base layer was examined by varying the modulus (20,000, 22,500, 25,000, 27,500, 30,000, and 35,000 psi (138, 155, 172, 190, 207, and 241 respectively)) for two climatic conditions: cold (represented by Chicago), and moderate to hot (represented by Dallas). Figure 5.15 shows the effect of base modulus on the back-calculated structural layer coefficient. It is evident that the assumed modulus has a significant effect on value of the back-calculated structural layer coefficient. The structural layer coefficient of the asphalt layer decreases as resilient modulus of the base layer increases.

On average, the structural layer coefficient decreases by 0.0055 for every increment in modulus of the base layer of 1 ksi. This is reasonable since the modulus of the aggregate base has a central effect on the pavement's structural number in the 1993 design guide (Equation 3.3), and the stress-strain response of the asphalt layer. Here, it is important to distinguish between asphalt *layer* (structural property) and asphalt

material. By definition, the layer coefficient is a combined structural and material indicator. It not only indicates the integrity of the material, but also its ability to act as a structural component in the given pavement. Therefore, it is expected that the structural coefficient be not only dependent on the asphalt material type and material properties, but also on the layer's boundary conditions, represented here by the modulus of the base layer.

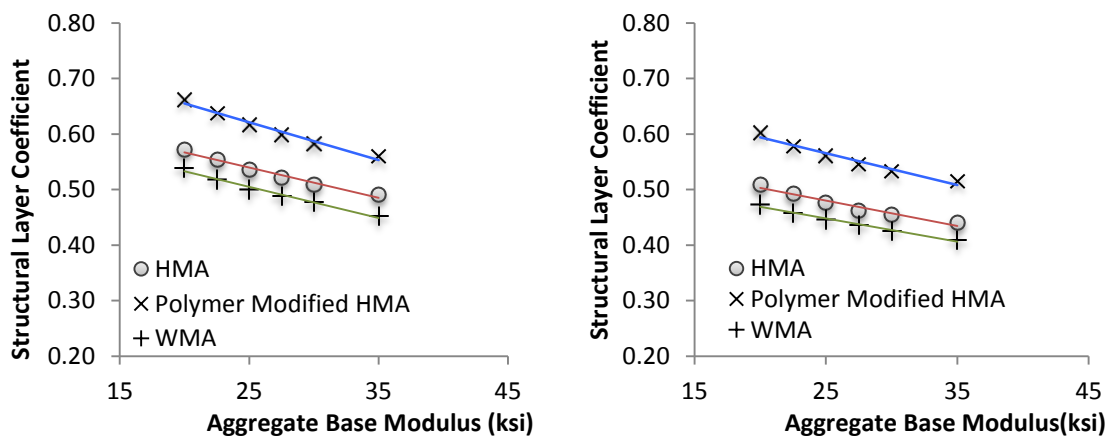


Figure 5.15: Sensitivity of structural layer coefficient to aggregate base modulus in cold climate (Chicago) (left), and moderate to hot climate (Dallas) (right).

5.5 $a_1-|E^*|_{\text{eff.}}-E_{\text{base}}$ Relationship and Discussion

Based on the sensitivity analysis, particularly the effect of the modulus of the aggregate base layer on ' a_1 ', it can be concluded that the curve developed in Figure 5.15 is specific to the assumed aggregate base modulus of 30,000 psi. Thus, it is important to account for other values of the aggregate base modulus and the subsequent effect on the structural coefficient of the asphalt layer. To do so, the base moduli of 20,000, 22,500, 25,000, 27,500, 30,000, and 35,000 psi (138, 155, 172, 190, 207, and 241 respectively)

included in the sensitivity are considered. By applying linear regression to the three mix types (conventional HMA, polymer modified HMA, and WMA), the final regression equation was found to be as shown in Equation 5.2, where the structural layer coefficient of the asphalt layer is a function of $|E^*|_{\text{eff}}$ and the logarithm of the aggregate base modulus (through Box-Cox transformation analysis).

$$a_1 = m|E^*_{\text{eff}}| + n \log(E_{\text{base}}) + \text{int.} \quad (5.2)$$

where a_1 = structural coefficient of the asphalt layer,
 $|E^*_{\text{eff}}|$ = effective dynamic modulus of the asphalt mix,
 m = slope (unit change in a_1 for every unit change in $|E^*_{\text{eff}}|$),
 n = slope (unit change in a_1 for every unit change in $\log(E_{\text{base}})$), and
 int. = intercept.

Based on the three mixes considered, it was found that the effect of the base modulus is fairly independent of mix type, and is represented by an average slope of -0.32. As such, for every unit increase in $\log(E_{\text{base}})$, i.e., E_{base} increases by 10 times, the layer coefficient decreases by 0.32 given that $|E^*|_{\text{eff}}$ is constant.

To portray the relationship between $|E^*|_{\text{eff}}$, E_{base} , and the structural coefficient of the asphalt layer, a nomograph was developed based on the relationship of a representative conventional HMA mix (Figure 5.16). To demonstrate its use, the following example is taken. Assuming a pavement structure consists of an asphalt layer with an effective dynamic modulus of 17,000 MPa, laid on top of an aggregate base with a modulus of 20 ksi, then the structural layer coefficient of the asphalt layer is approximately 0.51.

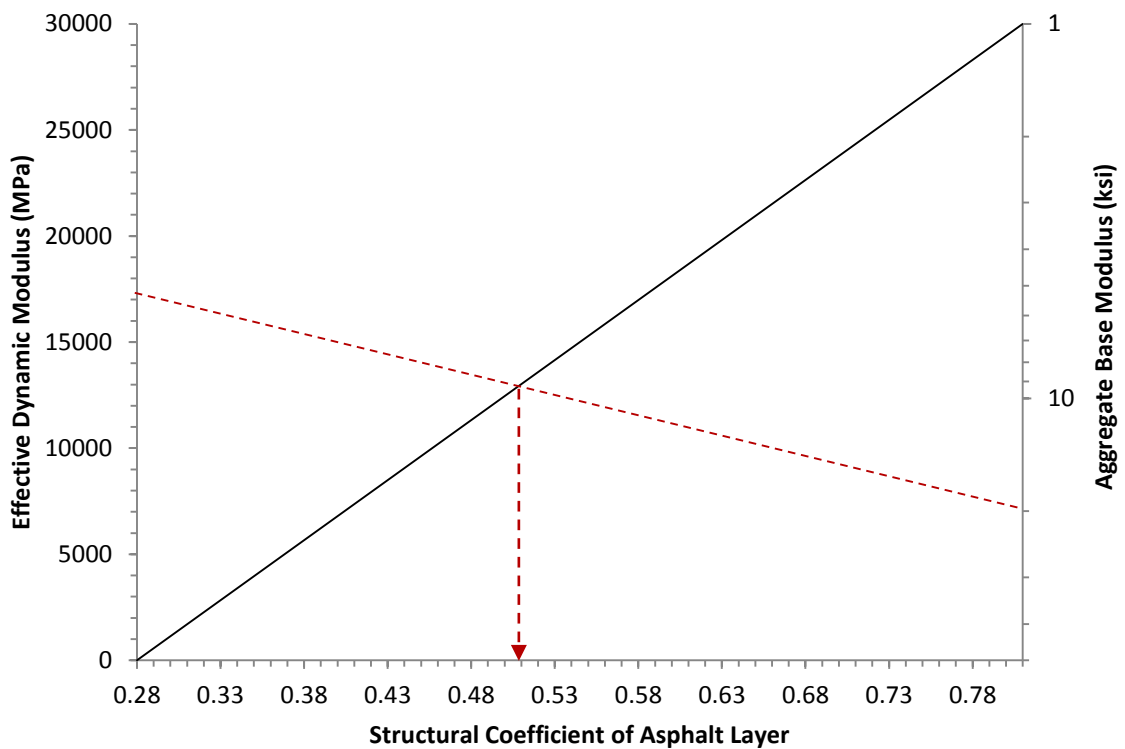


Figure 5.16: Sample nomograph for calculating the structural layer coefficient of an average conventional HMA mix bas based on $|E^*|_{\text{eff.}}$ and E_{base} .

5.6 Implications of Research Findings

The importance of the $a_1-|E^*|_{\text{eff.}}$ relationship lies in the fact it allows for material properties, climate, and traffic speed to be accounted for in pavement design. This in turn leads to a more accurate design thickness of the asphalt layer. A new ‘ a_1 ’ value greater than 0.44 means that designing the pavement using the recommended value of 0.44, i.e., neglecting mix type and climate/traffic, yields a pavement that is over-designed. On the other hand, a new ‘ a_1 ’ value that is less than 0.44 means that designing the pavement using the recommended value of 0.44 yields a pavement that is under-designed. Both these scenarios can hold serious economic and environmental

implications, depending on the magnitude of the difference between the new ‘ a_I ’ value and 0.44.

To study such implications, four cases are considered: (1) polymer-modified HMA in a moderate climate (St Louis), (2) HMA with RAP in a moderate climate (St Louis), (3) conventional HMA in a cold climate (Chicago), and (4) conventional HMA in a hot climate (Phoenix). To portray the examples, a traffic level of 15 Million ESALs, a base modulus of 30,000 psi, a design reliability of 90%, change in PSI of 1.2, and standard deviation of 0.4 are considered. The structural coefficient for each of the asphalt mixes is found using the final $a_I-|E^*|_{\text{eff}}$ relationships (Equation 5.2), and the design thickness was acquired accordingly based on the equations of the 1993 guide (Table 5.2).

Constructing an optimal pavement in terms of design thickness results in savings in material quantities, which leads to life cycle cost reductions, and reduced environmental impacts (for ‘ a_I ’ > 0.44). On the other hand, designing for a thicker pavement in order to meet performance criteria leads to reduction in economic and environmental costs associated with maintenance and rehabilitation (for ‘ a_I ’ < 0.44).

Table 5.2: Design Thicknesses Using $a_I-|E^*|_{\text{eff}}$ Curves Compared to Design Thicknesses Using $a_I=0.44$

Mix Type	Climate	Traffic Speed (mph)	New ‘ a_I ’	Design thickness based on new ‘ a_I ’ (in)	Design thickness based on $a_I=0.44$ (in)	% Savings in material quantities
Polymer-modified HMA	St Louis	60	0.56	5.9	7.5	21.2
HMA with RAP	St Louis	60	0.48	6.9	7.5	6.6
Conventional HMA	Chicago	60	0.54	6.1	7.5	18.7
Conventional HMA	Phoenix	60	0.44	7.5	7.5	0
Conventional HMA	Chicago	40	0.53	6.2	7.5	17.3

5.7 Conclusions

The research resulted in the development of a relationship between the structural layer coefficient, the effective dynamic modulus of the asphalt mix, and the resilient modulus of the aggregate base layer. As a result, the empirical nature of the asphalt layer coefficient is significantly reduced, which is now correlated to fundamental material properties ($|E^*|_{\text{eff}}$ and E_{base}). The developed relationship is thus believed to yield an improvement in the accuracy of the estimated structural layer coefficient of any given mix and structure, compared to the default value of 0.44. Moreover, the developed relationship may be generalized to include various mixes types, climatic conditions, traffic speeds, and structural configurations, which is a significant improvement in the area of empirical pavement design.

Chapter 6

DESIGN SUPPORT TOOL

6.1 Introduction

The main objective of this study is to propose a simple, practical model that accommodates the incorporation of asphalt mixture properties in the 1993 AASHTO design methodology. Chapter 5 presented the main research findings that primarily entailed establishing a relationship between the structural layer coefficient ' a_1 ', the effective dynamic modulus ($|E^*|$), and the resilient modulus of the base layer (E_{base}). This chapter presents a primer of a design support tool to complement the objective of the study. The tool, which was developed using VBA in Microsoft Excel, employs the a_1 - $|E^*|_{eff}$ - E_{base} relationship (Figure 5.9) and the design methodology of the 1993 guide to provide a more accurate estimate of the structural layer coefficient of asphalt and resultant design thickness.

6.2 Features of Design Support Tool

At the core of the design tool is the various a_1 - $|E^*|_{eff}$ - E_{base} relationships that were developed for the various mix categories in the scope of this study. The interface of the tool is shown in Figure 6.1. The computation methodology used in the tool is summarized in the flowchart in Figure 6.2.

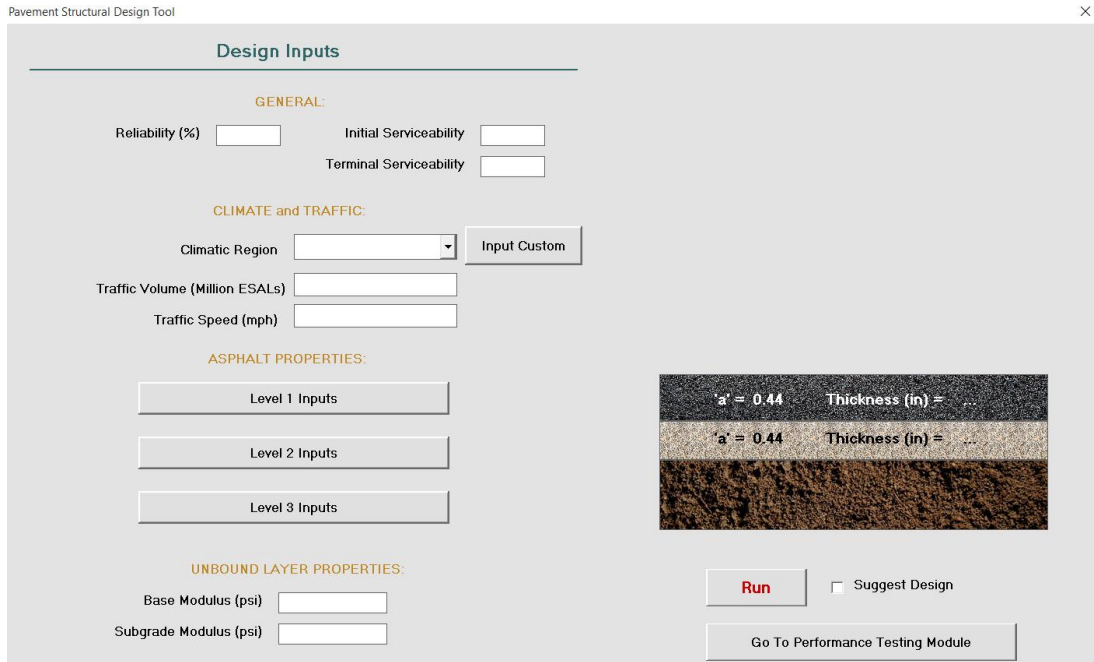


Figure 6.1: Interface of structural design tool.

The tool requires the following inputs:

- **General:** The general inputs include design reliability (%), and the assumed initial and terminal serviceability.
- **Climate:** The user has the option to select a pre-defined climatic location, or input custom climatic data. This data consists of the mean annual air temperature ($^{\circ}\text{F}$), the mean monthly standard deviation ($^{\circ}\text{F}$), wind speed (mph), sunshine (%), and cumulative annual rainfall (in), as shown in Figure 6.3. These climatic parameters are required to calculate the effective temperature for fatigue cracking and asphalt rutting (Equation 3.7 and Equation 3.8).
- **Traffic:** The required inputs are traffic volume (ESALs) and traffic speed (mph).

- **Unbound Layer Moduli:** The inputs entail the modulus of the aggregate base material and the subgrade material (psi).
- **Asphalt Materials:** The basis of asphalt material inputs is the dynamic modulus mastercurve. The user may select one of three input levels:

Level 1: The user inputs the sigmoidal and shift factor coefficients of the dynamic modulus mastercurve (Figure 6.4 (a)).

Level 2: If mastercurve data is not available, the user may select the mix type and NMAS (Figure 6.4 (b)). In this case, the software selects a mix from the tool's database that best represents the user's input. The selection process is optimized to account for the given traffic volume and mean temperature.

Level 3: The user may input mix volumetrics. The software then uses the data to calculate the effective E^* based on the Witczak predictive equation (Equation 3.15). The inputs are shown in Figure 6.4 (c). The user enters the PG grade of the binder, from which G^* and delta are calculate based on the Witczak database [121].

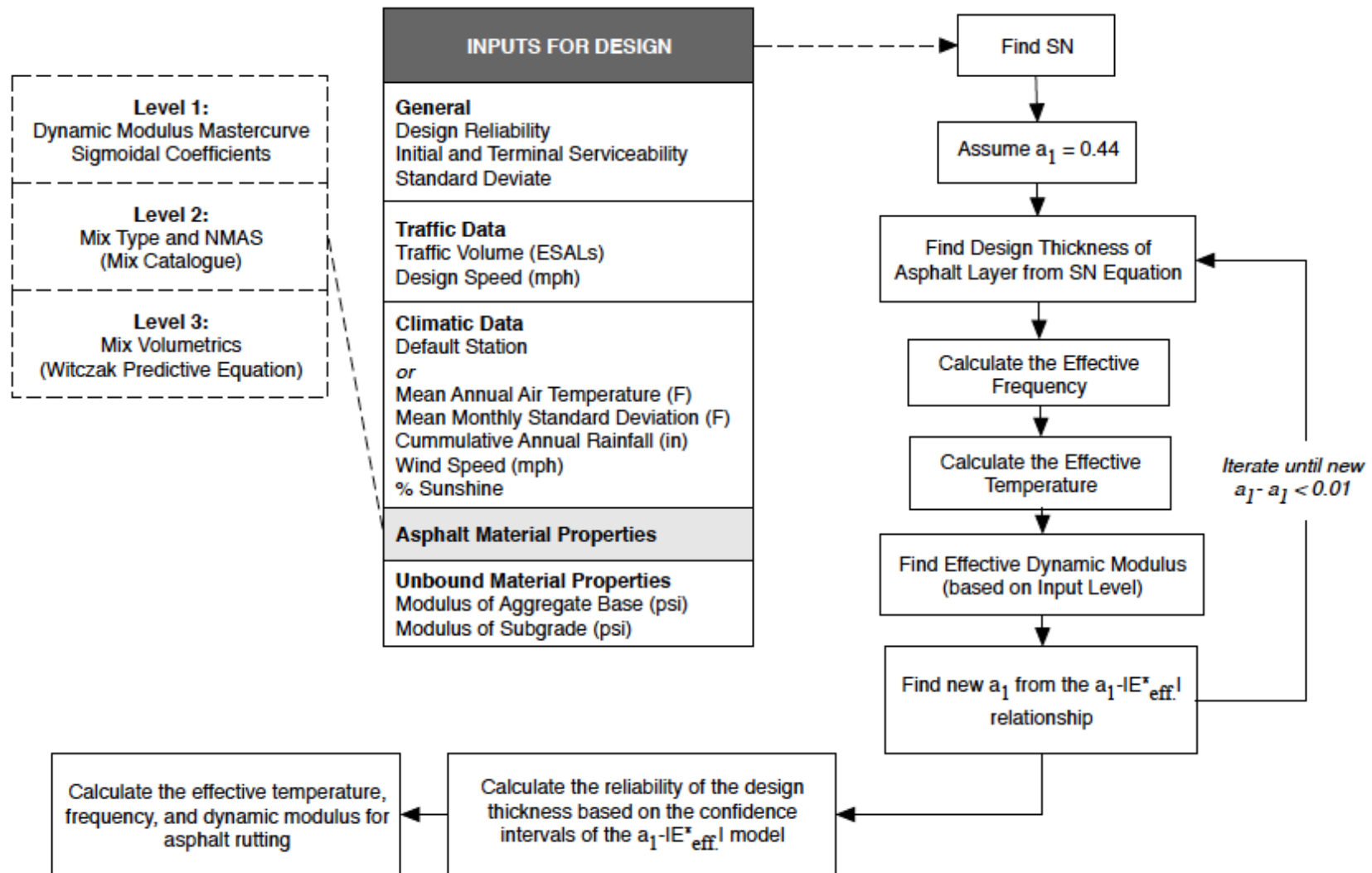


Figure 6.2: Computation methodology adopted in design tool.

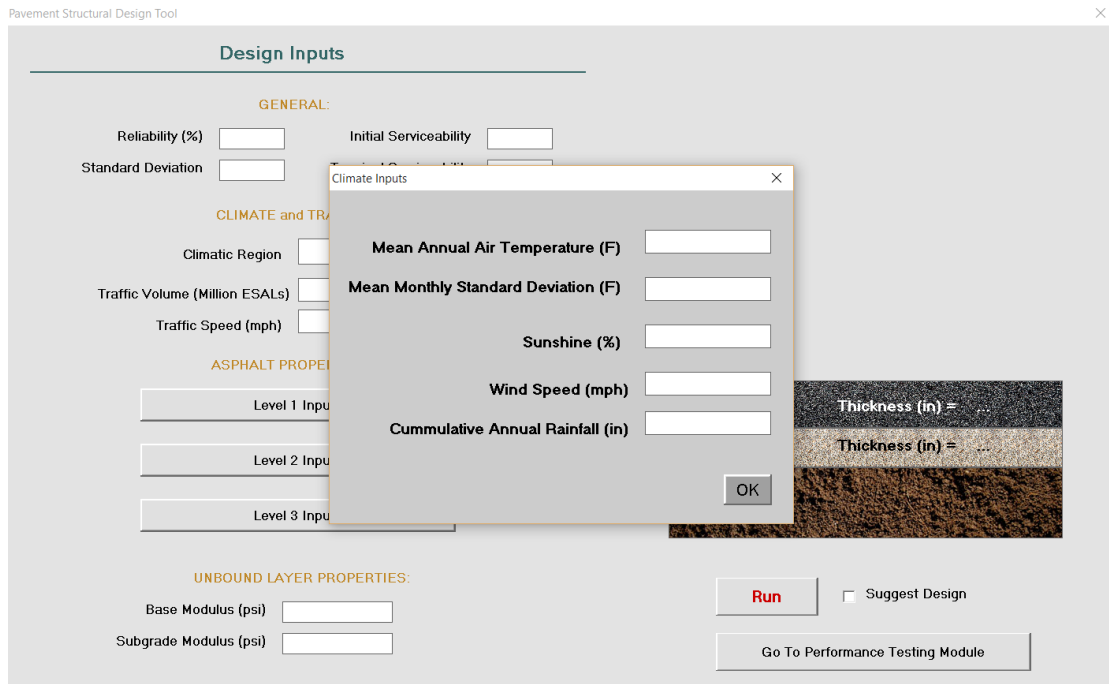
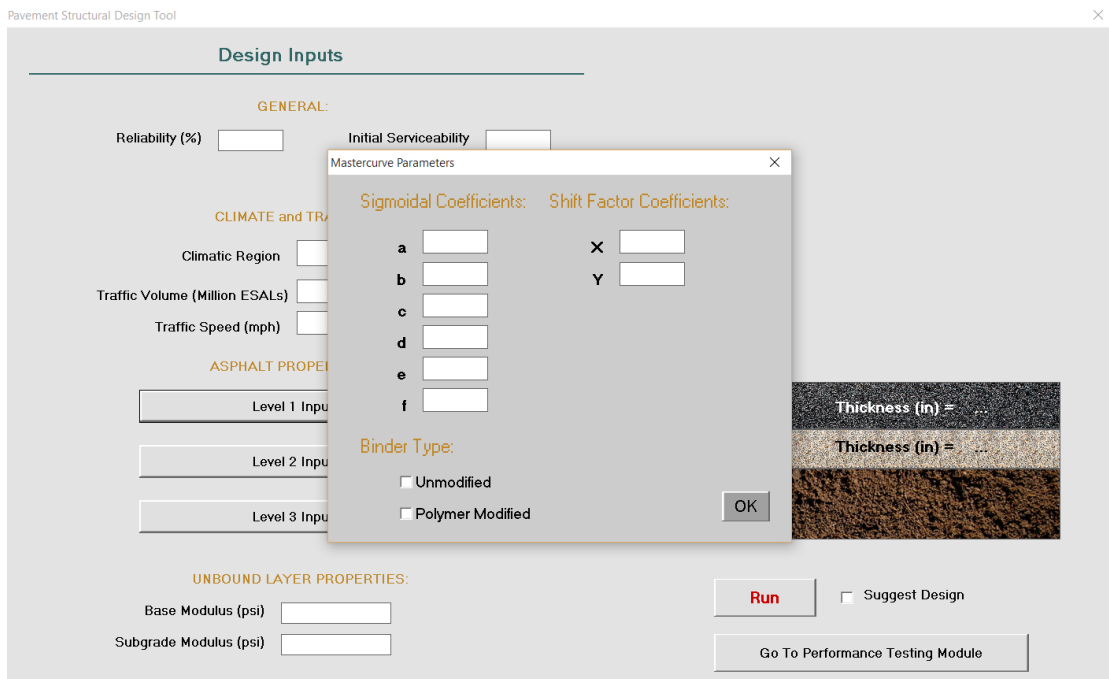
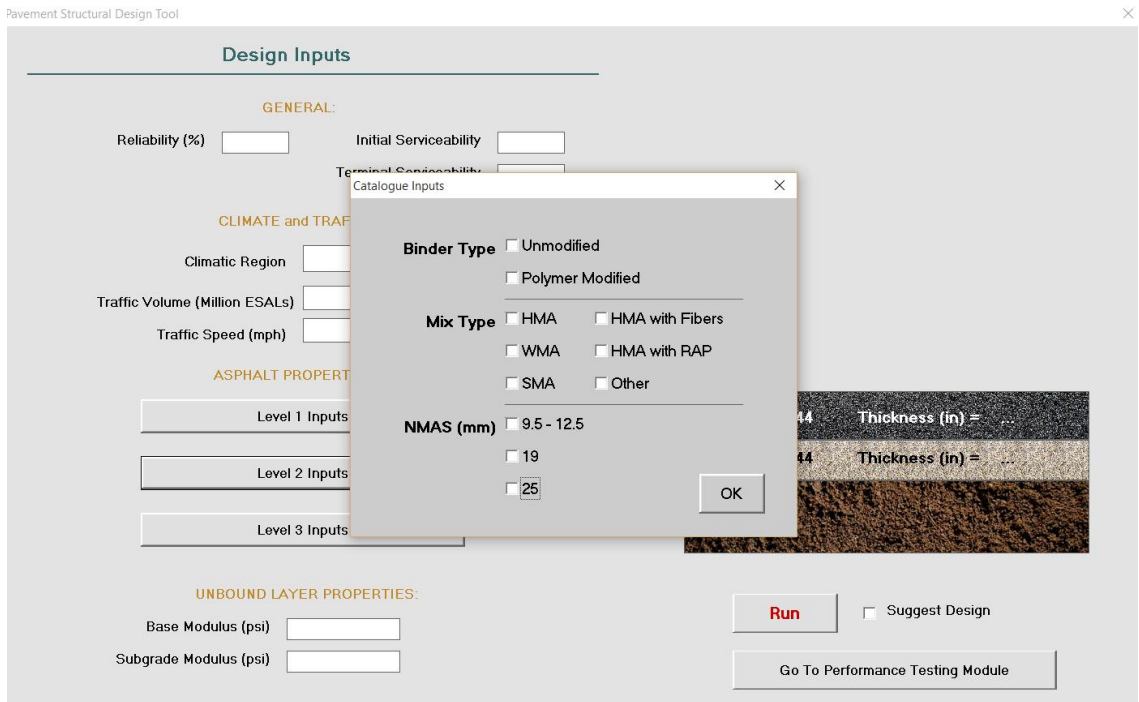


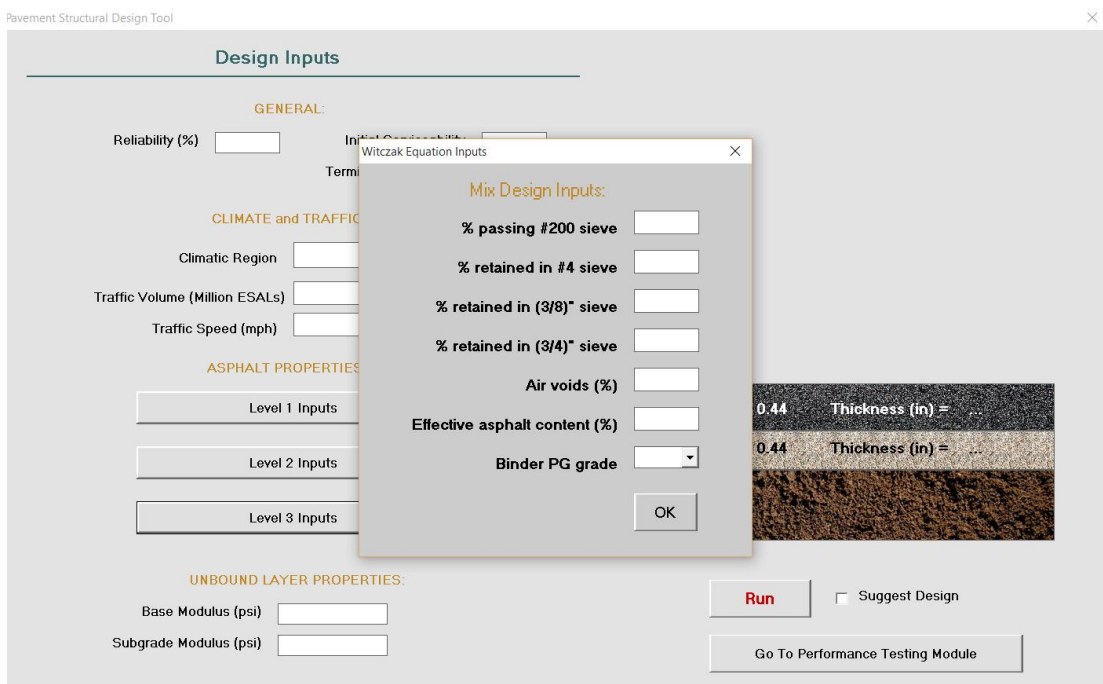
Figure 6.3: Climatic data inputs for structural design tool.



(a)



(b)



(c)

Figure 6.4: Design tool material inputs: (a) Level 1, (b) Level 2, (c) Level 3.

The tool then generates the design thicknesses based on the improved structural layer coefficient from the $a-|E^*|-E_{base}$ relationship, and displays the reliability of the design thickness based on the reliability of the regressed $a-|E^*|-E_{base}$ relationship (Figure 6.6). The tool has two additional options:

1. The tool generates the effective dynamic modulus for fatigue and for rutting which may be used for testing during mix design or during quality assurance/quality control (QA/QC) (Figure 6.5).
2. The tool also includes a “suggest design” option, which is based on an algorithm that suggests an asphalt mix, and subsequent structural design, based on the climate and traffic level. This option may be used for benchmarking.

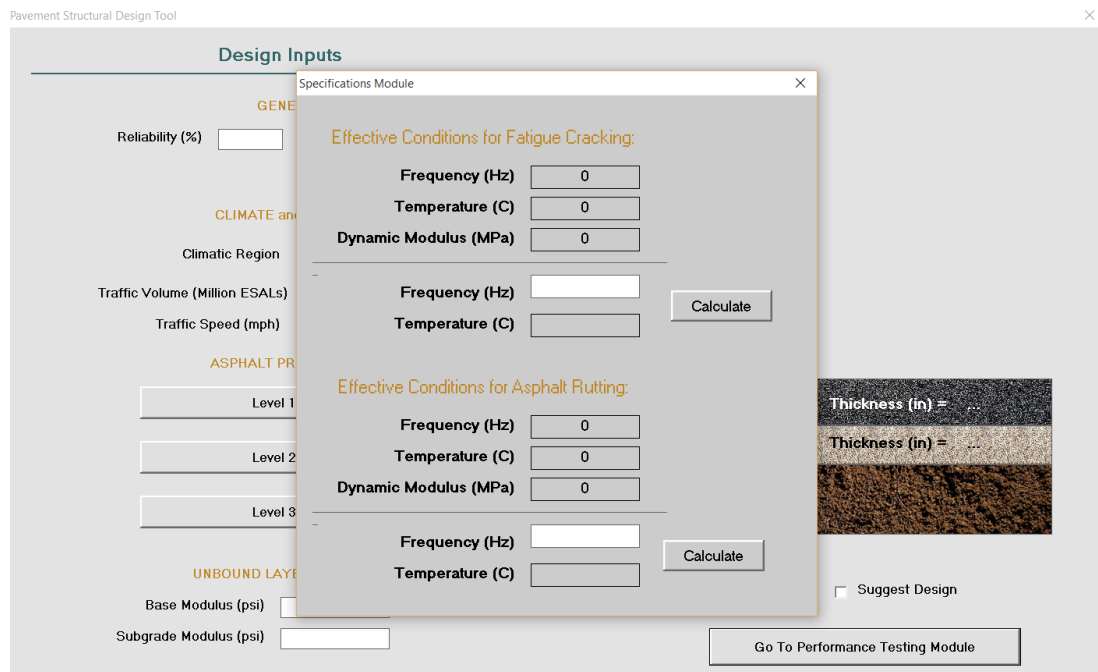


Figure 6.5: Effective conditions for fatigue and rutting.

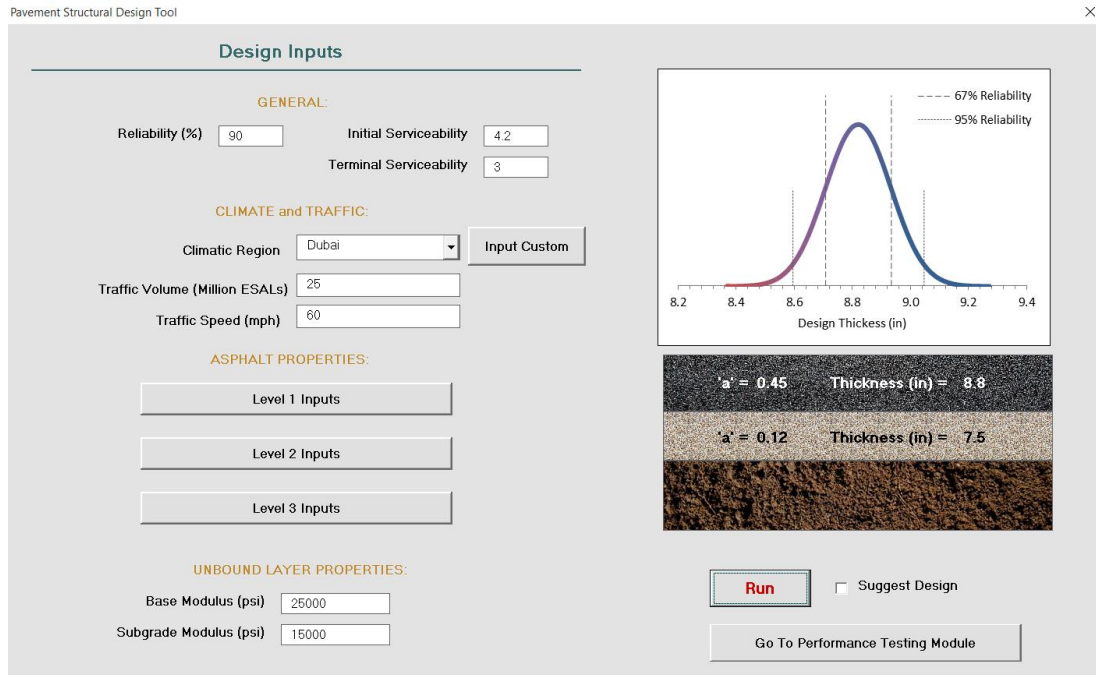


Figure 6.6: Sample input and output.

6.3 Comparison of Developed Tool Against 1993 AASHTO and MEPDG

To assess the tool, 32 scenarios of different asphalt mix types, climatic locations, traffic volumes and speeds, and aggregate base moduli are considered (Table 6.1). The design thicknesses acquired by the tool are compared to those acquired by the 1993 AASHTO (assuming $a_1 = 0.44$) as well as those resulting from analysis using the MEPDG (Pavement-ME). The results, summarized in Table 6.1, Figure 6.7, and Figure 6.8, reveal that the tool is more reliable than the 1993 design guide, and yields design thicknesses that closer to those acquired using the MEPDG (Pavement-ME). The 1993 design guide tends to over-predict the design thickness compared to the MEPDG (Figure 6.7). It is evident that the tool, which incorporates the $a_1 - |E^*| - E_{base}$ relationship developed in this research, efficiently accounts for material properties (asphalt mix type and aggregate base modulus), and climatic and traffic conditions. Further analysis of the outputs of the tool is necessary in the future.

6.4 Limitations

The tool has two main limitations: (1) the integrated a_1 - $|E^*|$ - E_{base} relationship, as well as the mix database, is limited by the number of mixes and mix types included in the scope of the study. Therefore, the results of the tool are as reliable as the developed model, (2) the tool does not accommodate more than one asphalt layer.

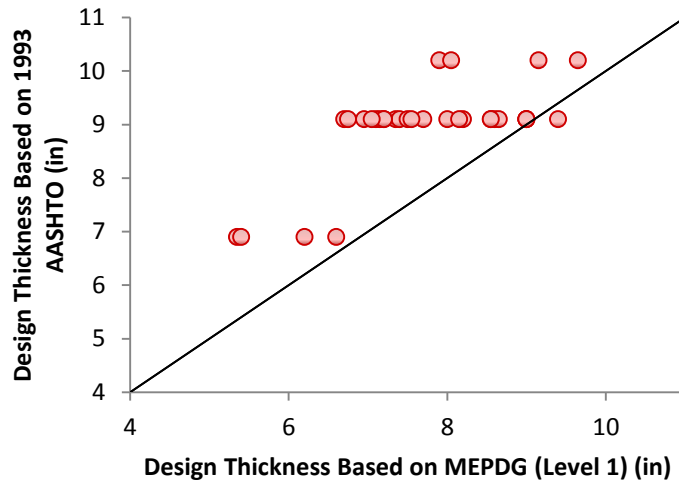


Figure 6.7: Design thicknesses acquired using the 1993 design guide compared to those acquired using the MEPDG (Level 1) based on the scenarios in Table 6.1.

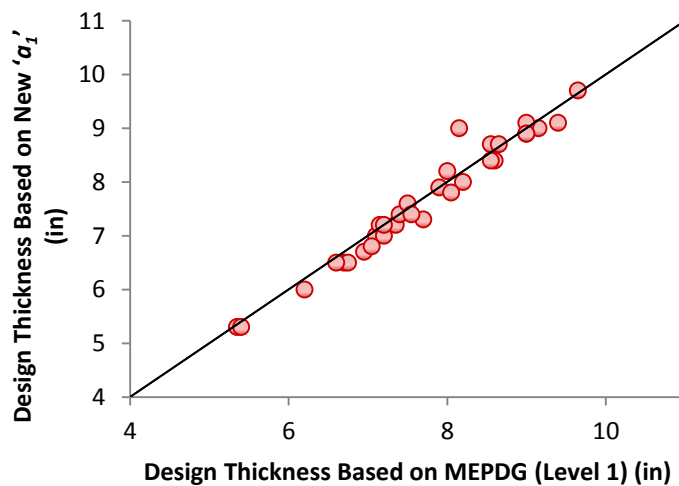


Figure 6.8: Design thicknesses acquired using the developed tool (new a_1) compared to those acquired using the MEPDG (Level 1) based on the scenarios in Table 6.1.

Table 6.1: Comparison of output of design tool to design thicknesses using 1993 AASHTO and MEPDG*.

Mix Type	Climate	Traffic Volume (AADTT)	Traffic Speed (mph)	Base Modulus (psi)	New ' a_1 '	Design thickness based on new ' a_1 ' (in)	Design thickness based on 1993 AASHTO ($a_1=0.44$) (in)	Design thickness based on MEPDG (Level 1)
Conventional HMA	St Louis	5,000	60	25,000	0.5	6	6.9	6.2
Conventional HMA	St Louis	20,000	60	25,000	0.5	8	9.1	8.2
Conventional HMA	St Louis	35,000	60	25,000	0.5	9	10.2	9.15
Conventional HMA	St Louis	20,000	30	25,000	0.48	8.4	9.1	8.6
Conventional HMA	Houston	20,000	60	25,000	0.46	8.7	9.1	8.55
Conventional HMA	Houston	20,000	30	25,000	0.44	9.1	9.1	9
Conventional HMA	Muncie	20,000	60	25,000	0.53	8.2	9.1	8
Conventional HMA	St Louis	20,000	60	35,000	0.51	7.3	9.1	7.7
Polymer Modified HMA	St Louis	5,000	60	25,000	0.57	5.3	6.9	5.35
Polymer Modified HMA	St Louis	20,000	60	25,000	0.57	7	9.1	7.1
Polymer Modified HMA	St Louis	35,000	60	25,000	0.57	7.9	10.2	7.9
Polymer Modified HMA	St Louis	20,000	30	25,000	0.56	7.2	9.1	7.35
Polymer Modified HMA	Houston	20,000	60	25,000	0.55	7.2	9.1	7.15
Polymer Modified HMA	Houston	20,000	30	25,000	0.54	7.4	9.1	7.4
Polymer Modified HMA	Muncie	20,000	60	25,000	0.6	6.7	9.1	6.95
Polymer Modified HMA	St Louis	20,000	60	35,000	0.54	6.5	9.1	6.7
WMA with PMB	St Louis	5,000	60	25,000	0.58	5.3	6.9	5.4
WMA with PMB	St Louis	20,000	60	25,000	0.57	7	9.1	7.2
WMA with PMB	St Louis	35,000	60	25,000	0.57	7.8	10.2	8.05
WMA with PMB	St Louis	20,000	30	25,000	0.56	7.6	9.1	7.5
WMA with PMB	Houston	20,000	60	25,000	0.55	7.2	9.1	7.2
WMA with PMB	Houston	20,000	30	25,000	0.54	7.4	9.1	7.55

WMA with PMB	Muncie	20,000	60	25,000	0.59	6.8	9.1	7.05
WMA with PMB	St Louis	20,000	60	35,000	0.53	6.5	9.1	6.75
HMA with RAP	St Louis	5,000	60	25,000	0.46	6.5	6.9	6.6
HMA with RAP	St Louis	20,000	60	25,000	0.46	8.7	9.1	8.65
HMA with RAP	St Louis	35,000	60	25,000	0.46	9.7	10.2	9.65
HMA with RAP	St Louis	20,000	30	25,000	0.45	8.9	9.1	9
HMA with RAP	Houston	20,000	60	25,000	0.45	8.9	9.1	9
HMA with RAP	Houston	20,000	30	25,000	0.44	9.1	9.1	9.4
HMA with RAP	Muncie	20,000	60	25,000	0.48	8.4	9.1	8.55
HMA with RAP	St Louis	20,000	60	35,000	0.43	9	9.1	8.15

**Subgrade modulus = 15,000 psi*

6.5 Potential Applications of the Design Support Tool

The tool, though primarily designed to support the structural design of roadway pavements, may be used for other applications, notably for airfield pavement design, and for promoting performance-based quality assurance/quality control. The following sections offer a brief overview of these applications.

6.5.1 Airfield Pavement Design

There is an added challenge when it comes to airfield pavement design, particularly in considering aircraft traffic. FAARFIELD, the airfield pavement design software adopted by the Federal Aviation Administration (FAA) and the most commonly used worldwide, is based on a linear analysis of the pavement structure. It assumes a default modulus of the asphalt layer of 200 ksi, which may be over-conservative in some cases. It also assumes that the aggregate base and subgrade layers have linear elastic material properties, and does not consider effects of asphalt concrete mix types, temperature, and speed.

Empirical pavement design procedures require equivalent single axle loads (ESALs) as traffic inputs, and cannot directly incorporate aircraft traffic. The MEPDG, on the other hand, accommodates a range of truck types and loads, as well as special axle configurations that can be inputted by the user. Based on a pilot study, inputting aircraft axle configurations into the MEPDG was sometimes found to yield illogical results. Therefore, a methodology is proposed to convert airfield traffic to ESALs for use in the pavement design tool developed in this study. This methodology is explained through a case study.

i. Case Study

The case study refers to an airport in one of the countries in the Middle East. The estimated annual aircraft movement for the runway in question constitutes an average of 92,500 departures, with a predicted annual growth of 12.4%. To convert aircraft traffic to equivalent highway ESALs for fatigue cracking considerations, the equivalent axle load factors (EALF) for each of the design aircraft types must be acquired. For the purpose of this case study, three design aircraft types are selected: Boeing 777, Boeing 737, and Airbus 330.

The methodology to acquire the EALF is as follows:

1. Acquiring the damage ratio for one 18-kip ESAL using KENPAVE or any other equivalent finite element software,
2. Acquiring the damage ratio for one axle for each of the aircraft types using KENPAVE or any other equivalent finite element software,
3. Calculating the EALF, where:

$$EALF = \frac{\text{damage ratio for aircraft axle}}{\text{damage ratio for 18-kip ESAL}} \quad (6.1)$$

For the purpose of calculating the EALF, an estimate of the structure, i.e., an estimate of layer thicknesses, can be used. In this case, the as-built structure is known, so the actual thicknesses were used. The damage ratios and EALF for fatigue for each aircraft type for this particular case are presented in Table 6.2.

Table 6.2: Damage ratio and EALF for fatigue for B777, B737 and A330

	Damage Ratio	EALF
18-kip ESAL	1.225 x 10 ⁻⁸	1
B777	8.1 x 10 ⁻⁶	661
B737	7.838 x 10 ⁻⁶	640
A330	6.567 x 10 ⁻⁶	536

Assuming an aircraft traffic profile consisting of 40% B777, 30% B737 and 30% A330, the calculation of the equivalent *annual* highway ESALS is demonstrated in Equation 7.2.

$$\begin{aligned}
 & \text{Equivanlent } \mathbf{annual} \text{ highway ESALs (EHEs)} \\
 & = 95,200 (0.4 \times 661 + 0.3 \times 640 + 0.3 \times 536) \\
 & = 57,000,000 \tag{6.2}
 \end{aligned}$$

Considering the 12.4% growth factor, EHEs at the end of the 10-year design life is calculated as shown in Equation 7.3.

$$\begin{aligned}
 \text{Total equivalent highway ESALs (EHEs)} & = 10 \times (57,000,000) \times 1.124^{10} \\
 & = 1,835,000,000 \tag{6.3}
 \end{aligned}$$

Using the developed design support tool, and inputting the climate data, asphalt mix data, and unbound layer properties, the design thickness of the asphalt layer is found to be 12.3 inches, which is very close to the design thickness of 12.5 inches that was implemented in actual construction. It is important to note that the actual design consists of two asphalt layers: a surface layer and a base layer; whereas, the thickness acquired from the tool is based on a one-layer system.

6.5.2 Performance-Based Specifications

Proper pavement quality assurance/quality control (QA/QC) is essential to limit pavement distresses over its service life. Deteriorated pavement conditions lead to increased user costs (e.g. vehicle maintenance costs, traffic delay), and threaten passenger safety (accidents). Moreover, premature rehabilitation and/or reconstruction lead to waste of resources (materials, money, time, workmanship) and closure of roadway, which causes traffic stoppage (vehicle or aircraft) and/or imposes work-zone user costs (e.g. work-zone traffic delay, work-zone accidents, work-zone vehicle maintenance) [122].

The pavement QA/QC process may rely on simple volumetric parameters or thorough material characterization. Performance-related specifications rely on materials and construction quality characteristics that have been found to correlate with fundamental engineering properties affecting performance, such as air void percentage and binder content [123]. Those typically require simple, quick tests, data of which are easy to analyze. Performance-based specifications elevate pavement QA/QC to a new level by relying on fundamental engineering properties (e.g. full $|E^*|$ characterization) to predict the performance of the mix over its service life [123]. These predictions typically include rut values (depths) and fatigue percentages. Because most fundamental engineering properties are associated with timely and costly testing and more complex data analysis, performance-based specifications are not yet widely used in pavement construction [123].

Pavement QA/QC is an integrated material and structural problem. Relying on the 1993 design method, which does not incorporate material properties, inhibits the

adoption of performance-based specifications. Deteriorated pavements could be a result of structural failures or poor mix design, but neither can be directly accountable since the mix properties are not incorporated in the structural design. It is difficult to “control” the quality in such cases. Therefore, including material properties early on in the planning and design phase is essential for effective QC/QA. When the material properties are well known during design, enforcing the specification criteria to meet these properties becomes relatively straightforward in the construction phase.

The design methodology and design tool presented in this thesis help promote performance-based specifications, through the use of the effective dynamic modulus in the design process. Being confident about the reliability of the structural design, and basing it on predefined fundamental material properties and an anticipated distress level at the end of the service life, shifts the responsibility of construction quality to the contractor. As a result, contractor warranties become a viable option, where the contractor is held liable for the quality of the construction for a certain period of time. In addition, the specifications module in the tool (Figure 6.5) generates material properties, namely the effective dynamic modulus ($|E^*|_{\text{eff.}}$), that could be used for decision making in the design phase, and also in the construction (QC/QA) phase, similar to the NCHRP 9-19 and NCHRP 9-22 tools. For QC/QA, the effective dynamic modulus of samples from construction can be compared to that of the mix used for structural design. The $|E^*|_{\text{eff.}}$ of samples from construction can then be used as input in linear-elastic analysis software to acquire the strains in the asphalt layer. These strains, and the $|E^*|_{\text{eff.}}$, can be used in transfer functions (e.g. Equation 3.4) and the acquired performance compared to the design criteria. Additional work will be conducted in the future to expand the possibilities and capabilities of the tool in this regard.

Chapter 7

CONCLUSIONS AND FUTURE WORK

7.1 Conclusions

With numerous obstacles preventing the implementation of the MEPDG, the 1993 AASHTO empirical pavement design guide remains to date one of the most widely used pavement design methodologies around the world. The main shortcoming of the 1993 design guide is the assumed asphalt layer coefficient of 0.44. This value (0.44) is based on a vastly empirical relationship that was developed almost five decades ago as a result of the AASHO road test under strictly limited material, climatic, traffic, and structural conditions. The objective of the research presented in this thesis is to improve the estimate of the asphalt layer coefficient in order to cater for a wider range of mix types, and incorporate the effect of climate and traffic speed on the layer coefficient.

The layer coefficient of the asphalt layer is initially found to be dependent on two main factors: the mix type, and the temperature-frequency combination that the pavement is subjected to. As a result, a relationship is developed between the layer coefficient and the effective dynamic modulus, which is chosen as a material property that represents the two factors. Upon exploring the developed relationship, it is then found that the layer coefficient is also dependent on the resilient modulus of the base layer. By definition, the layer coefficient is a combined structural and material indicator. It not only indicates the integrity of the material, but also its ability to act as a structural component in the given pavement. Therefore, it is understandable that the structural

coefficient be also on the layer's boundary conditions, represented by the modulus of the base layer.

The research resulted in the development of a multi-linear relationship between the structural layer coefficient, the effective dynamic modulus of the asphalt mix, and the resilient modulus of the aggregate base layers. Acquiring the structural number from the developed relationship is proven to yield design thicknesses that are generally close to those acquired using the MEPDG. A Microsoft-Excel-based pavement structural design tool was also built to support the developed relationship, and simplify calculations.

7.2 Limitations and Future Work

The main limitations of the research are summarized below.

- The research is based on an underlying assumption that using the MEPDG for pavement design gives close-to-optimal design thicknesses, which may be debatable. Therefore, the accuracy of the developed $a_1-|E^*|-E_{\text{base}}$ is directly dependent on the reliability of MEPDG's performance predictions.
- The $a_1-|E^*|-E_{\text{base}}$ relationship and design support tool are limited by the number and types of mixes included within the scope of the study.
- The developed $a_1-|E^*|-E_{\text{base}}$ relationship and design support tool do not cater for pavements that have more than one asphalt layer.
- The developed model is yet to be validated across field performance data.

Future work includes expanding the scope of the research to include a wider array of mix types and structural design scenarios, and continuously enhancing the a_I - $|E^*|$ - E_{base} relationship. Future work also entails improving the design support tool to accommodate multiple asphalt layers, and validating the design thicknesses acquired from the tool across measured performance data.

REFERENCES

- [1] G. E. Elkins, P. Schmalzer, T. Thompson, and A. Simpson, “Long-term pavement performance information management system pavement performance database user reference guide,” 2003.
- [2] M. W. Witczak, K. Kaloush, T. Pellinen, M. El-Basyouny, and H. Von Quintus, “Simple performance test for superpave mix design, NCHRP Report 465,” *Transp. Res. Board, Washington, DC, USA*, 2002.
- [3] ARA.Inc., “Guide for Mechanistic-Empirical Design of New and Rehabilitated Pavement Structures,” *Final Report, NCHRP 1-37A*, 2004. [Online]. Available: <http://www.trb.org/mepdg/guide.htm>.
- [4] S. Mun, M. Guddati, and Y. Richard Kim, “Fatigue cracking mechanisms in asphalt pavements with viscoelastic continuum damage finite-element program,” *Transp. Res. Rec. J. Transp. Res. Board*, no. 1896, pp. 96–106, 2004.
- [5] B. Underwood, C. Baek, and Y. Kim, “Simplified viscoelastic continuum damage model as platform for asphalt concrete fatigue analysis,” *Transp. Res. Rec. J. Transp. Res. Board*, no. 2296, pp. 36–45, 2012.
- [6] S. Munl, G. R. Chehab, T. Kumar, and Y. R. Kim, “Modeling Fatigue Cracking of Asphalt Concrete Mixtures Using Viscoelastic Continuum Damage Theory and Finite Element Analysis,” *Int. J. Pavement Res. Technol.*, vol. 1, no. 3, p. 76, 2008.
- [7] M. S. Medeiros Jr, J. S. Daniel, and G. R. Chehab, “Framework for Low-Temperature Cracking Analysis of Asphalt Mixtures Using a Viscoelastic Continuum Damage Model,” *J. Mater. Civ. Eng.*, vol. 27, no. 10, p. 4014265, 2014.
- [8] A. Scarpas, R. Al-Khoury, C. Van Gorp, and S. Erkens, “Finite element simulation of damage development in asphalt concrete pavements,” in *Eighth International Conference on Asphalt Pavements*, 1997, no. Volume I.
- [9] A. Collop, A. Scarpas, C. Kasbergen, and A. de Bondt, “Development and finite element implementation of stress-dependent elastoviscoplastic constitutive model with damage for asphalt,” *Transp. Res. Rec. J. Transp. Res. Board*, no. 1832, pp. 96–104, 2003.
- [10] C.-W. Huang, R. K. Abu Al-Rub, E. A. Masad, and D. N. Little, “Three-dimensional simulations of asphalt pavement permanent deformation using a nonlinear viscoelastic and viscoplastic model,” *J. Mater. Civ. Eng.*, vol. 23, no. 1, pp. 56–68, 2010.
- [11] E. Masad, L. Tashman, D. Little, and H. Zbib, “Viscoplastic modeling of asphalt mixes with the effects of anisotropy, damage and aggregate characteristics,” *Mech. Mater.*, vol. 37, no. 12, pp. 1242–1256, 2005.
- [12] E. Masad, R. A. Al-Rub, and D. N. Little, “Recent Developments and Applications of Pavement Analysis Using Nonlinear Damage (PANDA) Model,” in *7th RILEM International Conference on Cracking in Pavements*, 2012, pp.

399–408.

- [13] G. C. Hurley and B. D. Prowell, “Evaluation of potential processes for use in warm mix asphalt,” *J. Assoc. Asph. Paving Technol.*, vol. 75, pp. 41–90, 2006.
- [14] K. E. Kaloush, K. P. Biligiri, W. A. Zeiada, M. C. Rodezno, and J. X. Reed, “Evaluation of fiber-reinforced asphalt mixtures using advanced material characterization tests,” *J. Test. Eval.*, vol. 38, no. 4, p. 1, 2010.
- [15] Y. H. Huang, *Pavement analysis and design*. 1993.
- [16] G. R. Chehab and K. A. Galal, “The ME Pavement Design Guide: A Case Study on HMA Overlays over Fractured PCC Slabs,” *J. Asph. Pavement Technol.*, 2005.
- [17] J. Li, J. S. Uhlmeier, J. P. Mahoney, and S. T. Muench, “Use of the 1993 AASHTO Guide, MEPDG and Historical Performance to Update the WSDOT Pavement Design Catalog,” 2011.
- [18] H. Ceylan, B. J. Coree, and K. Gopalakrishnan, “Strategic plan for implementing mechanistic-empirical pavement design guide in iowa,” in *Transportation Research Board 85th Annual Meeting*, 2006, no. 06–2784.
- [19] M. I. Darter, L. Titus-Glover, and H. L. Von Quintus, “Implementation of the Mechanistic-Empirical Pavement Design Guide in Utah: validation, calibration, and development of the UDOT MEPDG User’s Guide,” 2009.
- [20] F. Bayomy, S. M. El-Badawy, and A. Awed, “Implementation of the MEPDG for Flexible Pavements in Idaho,” 2012.
- [21] H. Sadek, E. Masad, O. Sirin, H. Al-Khalid, and D. Little, “The implementation of mechanistic-empirical pavement design method to evaluate asphalt pavement design in Qatar,” in *5th Eurasphalt & Eurobitume Congress*, 2012, pp. 13–15.
- [22] M. Ameri and A. Khavandi, “Development of Mechanistic-Empirical Flexible Pavement Design in Iran,” *J. Appl. Sci.*, vol. 9, no. 2, pp. 354–359, 2009.
- [23] D. H. Timm, M. M. Robbins, N. Tran, and C. Rodezno, “Flexible Pavement Design–State of the Practice,” 2014.
- [24] T. Nantung, G. Chehab, S. Newbolds, K. Galal, S. Li, and D. Kim, “Implementation initiatives of the mechanistic-empirical pavement design guides in Indiana,” *Transp. Res. Rec. J. Transp. Res. Board*, no. 1919, pp. 142–151, 2005.
- [25] D. Ayyala, G. R. Chehab, and J. S. Daniel, “Sensitivity of ME PDG level 2 and 3 inputs using statistical analysis techniques for New England states,” in *Transportation Research Board 89th Annual Meeting*, 2010, no. 10–3694.
- [26] A. A. of S. Highway and T. Officials, *AASHTO Guide for Design of Pavement Structures*, 1993, vol. 1. AASHTO, 1993.
- [27] M. El-Basyouny and M. Jeong, “Effective temperature for analysis of permanent deformation and fatigue distress on asphalt mixtures,” *Transp. Res. Rec. J. Transp. Res. Board*, no. 2127, pp. 155–163, 2009.
- [28] M. El-Basyouny and M. G. Jeong, “Probabilistic Performance-Related

- Specifications Methodology Based on *Mechanistic-Empirical Pavement Design Guide*,” *Transp. Res. Rec. J. Transp. Res. Board*, vol. 2151, no. -1, pp. 93–102, 2010.
- [29] M. G. Jeong, “Manual of practice HMA quality assurance spreadsheet program using measured values of E^* and d .” Transportation Research Board, 2010.
- [30] Austroads, “Guide to Pavement Technology,” *Part 2 Pavement Struct. Des.*, 2012.
- [31] SANRA, “South African Pavement Engineering Manual,” *Chapter 10*, 2014.
- [32] A. Das, “Structural Design of Asphalt Pavements: Principles and Practices in Various Design Guidelines,” *Transp. Dev. Econ.*, vol. 1, no. 1, pp. 25–32, 2015.
- [33] FHWA, “Geotechnical Aspects of Pavements Reference Manual,” 2015. [Online]. Available: <http://www.fhwa.dot.gov/engineering/geotech/pubs/05037/03b.cfm>.
- [34] “MEPDG Guide: A Manual of Practice,” *Am. Assoc. State Highw. Transp. Off.*, 2008.
- [35] M. Darter, “NCHRP project 1-40D (02), technical assistance to NCHRP and NCHRP project 1-40A: Versions 0.9 and 1.0 of the ME pavement design software,” *Transp. Res. Board*, 2006.
- [36] P. Wilke, “Impact of Energy Developments on Low Volume Roads,” *Slideshare*, 2012. [Online]. Available: <http://www.slideshare.net/mecocca5/impacts-of-energy-development-on-low-volume-roads-paul-wilke-pe>.
- [37] HRB, “The AASHO Road Test,” 1962.
- [38] K. Peters-Davis and D. H. Timm, “Recalibration of the asphalt layer coefficient,” 2009.
- [39] AASHTO, “Interim Design Guide,” 1972.
- [40] M. Pologruto, “Procedure for use of falling weight deflectometer to determine AASHTO layer coefficients,” *Transp. Res. Rec. J. Transp. Res. Board*, no. 1764, pp. 11–19, 2001.
- [41] Y. R. Kim, S. R. Ranjithan, J. D. Troxler, and B. Xu, “NCHRP Research Results Digest 254: Assessing Pavement Layer Condition Using Deflection Data. NCHRP Project 10-48 Final Report. TRB, National Research Council, Washington, D. C., June 2001.”
- [42] X. Qi, P. E. Sebaaly, and J. A. Epps, “Evaluation of polymer-modified asphalt concrete mixtures,” *J. Mater. Civ. Eng.*, vol. 7, no. 2, pp. 117–124, 1995.
- [43] M. Hossain, A. Habib, and T. Latorella, “Structural layer coefficients of crumb rubber-modified asphalt concrete mixtures,” *Transp. Res. Rec. J. Transp. Res. Board*, no. 1583, pp. 62–70, 1997.
- [44] B. Marquis, D. Peabody, R. Mallick, and T. Soucie, “Determination of structural layer coefficient for roadway recycling using foamed asphalt,” *Durham, NH Recycl. Mater. Resour. Cent.*, 2003.
- [45] J. MacGregor, W. Hightler, and D. DeGroot, “Structural numbers for reclaimed

- asphalt pavement base and subbase course mixes,” *Transp. Res. Rec. J. Transp. Res. Board*, no. 1687, pp. 22–28, 1999.
- [46] S. Bin-Shafique, T. B. Edil, C. H. Benson, and A. Senol, “Incorporating a fly-ash stabilised layer into pavement design,” *Proc. ICE-Geotechnical Eng.*, vol. 157, no. 4, pp. 239–249, 2004.
- [47] S. Romanoschi, M. Hossain, A. Gisi, and M. Heitzman, “Accelerated pavement testing evaluation of the structural contribution of full-depth reclamation material stabilized with foamed asphalt,” *Transp. Res. Rec. J. Transp. Res. Board*, no. 1896, pp. 199–207, 2004.
- [48] A. Misra, S. Kumar, S. Patel, and F. Gustin, “Resilient Moduli and Structural Layer Coefficient of Flyash Stabilized Recycled Asphalt Base,” in *World of Coal Ash (WOCA) Conference*, 2007, pp. 7–10.
- [49] A. J. Puppala, L. R. Hoyos, and A. K. Potturi, “Resilient moduli response of moderately cement-treated reclaimed asphalt pavement aggregates,” *J. Mater. Civ. Eng.*, vol. 23, no. 7, pp. 990–998, 2011.
- [50] K. A. Galal and G. R. Chehab, “Considerations for implementing the 2002 ME design procedure using a HMA rehabilitated pavement section in Indiana,” in *Presented and published at the Transportation Research Board (TRB) 84th Annual Meeting, Washington, DC*, 2005.
- [51] D. Ayyala, “Sensitivity Analysis of Pavement Performance Prediction Using the MEPDG.” The Pennsylvania State University, 2009.
- [52] K. Galal and G. Chehab, “Implementing the mechanistic-empirical design guide procedure for a Hot-Mix Asphalt-rehabilitated pavement in Indiana,” *Transp. Res. Rec. J. Transp. Res. Board*, no. 1919, pp. 121–133, 2005.
- [53] J. Bari and M. W. Witzak, “Development of a new revised version of the Witzak E* predictive model for hot mix asphalt mixtures (with discussion),” *J. Assoc. Asph. Paving Technol.*, vol. 75, 2006.
- [54] M. Witzak and O. Fonseca, “Revised predictive model for dynamic (complex) modulus of asphalt mixtures,” *Transp. Res. Rec. J. Transp. Res. Board*, no. 1540, pp. 15–23, 1996.
- [55] R. Olson, “Mechanistic-Empirical Pavement Design Guide in Indiana,” *ACEC Indiana Short List*, vol. 5, no. 5, 2009.
- [56] F. G. Fernando, J. Oh, and D. Ryu, “Phase I of MEPDG Program Implementation in Florida,” *Rep. D004491/PR15281-1. Texas Transp. Institute, Coll. Station. Tx*, 2007.
- [57] “Pavement Resource Program Quarterly Progress Report,” *Center for Advanced Infrastructure & Transportation, Rutgers, the State University of New Jersey*, 2006. [Online]. Available: http://www.state.nj.us/transportation/refdata/research/pdf/caitqrep/cait_06_q1_pavement_resource.pdf.
- [58] R. Kim and N. Muthadi, “Implementation Plan for the New Mechanistic Empirical Pavement Design Guide,” *NCDOT Proj. 2005-28. North Carolina State Univ. Raleigh, NC*, 2007.

- [59] C. Schwartz, "Implementation of the NCHRP 1-37A Design Guide," *Rep. No. SP0077B41. Maryland State Highw. Adm. Lutherville, MD*, 2007.
- [60] "VDOT Preparation Plan for the Implementation of the Mechanistic-Empirical Guide for Design of New and Rehabilitated Pavement Structures," 2007. .
- [61] G. Cochran, N. Funk, K. Hoegh, L. Khazanovich, M. Marasteanu, and R. Velasquez, "Implementation of the MEPDG for New and Rehabilitated Pavement Structures for Design of Concrete and Asphalt Pavements in Minnesota," *Rep. MN/RC 2009-06. Minnesota Dep. Transp. St. Paul, MN*, 2009.
- [62] L. Pierce, "New Pavement Design Guide," *Washington State Department of Transportation, Olympia, WA*, 2007. [Online]. Available: http://resources/07Fall_NewPavemtDesignGuide.pdf.
- [63] "Montana Department of Transportation Performance Prediction Models," 2007. [Online]. Available: http://mdt.mt.gov/research/docs/research_proj/pave_model/final_presentation.pdf .
- [64] C. R. Williams, C. J. Robinette, J. Bausano, and T. Breakah, "Testing of Wisconsin Asphalt Mixtures for the Forthcoming AASHTO Mechanistic-Empirical Pavement Design Procedure," *Rep. No. WHRP 07-06. Wisconsin Dep. Transp. Madison, WI*, 2007.
- [65] A. M. Khattab, S. M. El-Badawy, A. A. Al Hazmi, and M. Elmwafi, "Evaluation of Witczak E* predictive models for the implementation of AASHTOWare-Pavement ME Design in the Kingdom of Saudi Arabia," *Constr. Build. Mater.*, vol. 64, pp. 360–369, 2014.
- [66] H. A. Sadek, E. A. Masad, O. Sirin, H. Al-Khalid, M. A. Sadeq, and D. Little, "Implementation of mechanistic-empirical pavement analysis in the State of Qatar," *Int. J. Pavement Eng.*, vol. 15, no. 6, pp. 495–511, 2014.
- [67] "Road Collapses after Rains in Saudi Arabia," 2015. [Online]. Available: <http://www.emirates247.com/news/region/road-collapses-after-rains-in-saudi-arabia-2015-11-27-1.612092>.
- [68] "Dubai's Palm Jumeirah 'safe' after road collapse, says Nakheel," 2013.
- [69] L. Carroll, "Building Evacuated After Road Collapses in Abu Dhabi," 2014. [Online]. Available: <http://www.thenational.ae/uae/building-evacuated-after-road-collapses-in-abu-dhabi>.
- [70] PavementInteractive, "Rutting," 2008. [Online]. Available: <http://www.pavementinteractive.org/article/rutting/>.
- [71] PavementInteractive, "Fatigue Cracking," 2009. [Online]. Available: <http://www.pavementinteractive.org/article/fatigue-cracking/>.
- [72] J. Uzan, "Influence of the interface condition on stress distribution in a layered system (abridgement)," *Transp. Res. Rec.*, no. 616, 1976.
- [73] C. W. Schwartz, R. Li, S. Kim, H. Ceylan, and K. Gopalakrishnan, "Sensitivity evaluation of MEPDG performance prediction," 2011.
- [74] M. C. Lee, *Mechanistic-Empirical Pavement Design Guide: Evaluation of*

Flexible Pavement Inputs. 2004.

- [75] S. A. Masad, "Sensitivity analysis of flexible pavement response and AASHTO 2002 design guide for properties of unbound layers." Texas A&M University, 2004.
- [76] M. M. El-Basyouny and M. W. Witzcak, "Verification of the Calibrated Fatigue Cracking Models for the 2002 Design Guide (With Discussion)," *J. Assoc. Asph. Paving Technol.*, vol. 74, 2005.
- [77] M. El-Basyouny and M. Witzcak, "Part 2: Flexible Pavements: Calibration of Alligator Fatigue Cracking Model for 2002 Design Guide," *Transp. Res. Rec. J. Transp. Res. Board*, no. 1919, pp. 76–86, 2005.
- [78] M. M. El-Basyouny, M. W. Witzcak, and S. El-Badawy, "Verification for the calibrated permanent deformation models for the 2002 design guide (with discussion)," *J. Assoc. Asph. Paving Technol.*, vol. 74, 2005.
- [79] C. W. Schwartz, "Evaluation of the Witzcak dynamic modulus prediction model," in *Proceedings of the 84th Annual Meeting of the Transportation Research Board, Washington, DC*, 2005, no. 05–2112.
- [80] S. F. Brown, M. Darter, G. Larson, M. Witzcak, and M. M. El-Basyouny, "Independent Review of the 'Mechanistic-Empirical Pavement Design Guide' and Software," *NCHRP Res. results Dig.*, no. 307, 2006.
- [81] R. Carvalho and C. Schwartz, "Comparisons of flexible pavement designs: AASHTO empirical versus NCHRP project 1-37A mechanistic-empirical," *Transp. Res. Rec. J. Transp. Res. Board*, no. 1947, pp. 167–174, 2006.
- [82] G. Chehab and J. Daniel, "Evaluating recycled asphalt pavement mixtures with mechanistic-empirical pavement design guide level 3 analysis," *Transp. Res. Rec. J. Transp. Res. Board*, no. 1962, pp. 90–100, 2006.
- [83] R. Graves and K. Mahboub, "Part 2: flexible pavements: pilot study in sampling-based sensitivity analysis of NCHRP design guide for flexible pavements," *Transp. Res. Rec. J. Transp. Res. Board*, no. 1947, pp. 123–135, 2006.
- [84] R. C. Graves and K. C. Mahboub, "A Pilot Study in Sampling Based Sensitivity Analysis of the NCHRP 1-37A Design Guide for Flexible Pavements," in *TRB Annual Meeting. January*, 2005.
- [85] L. Khazanovich, C. Celauro, B. Chadbourn, J. Zollars, and S. Dai, "Evaluation of subgrade resilient modulus predictive model for use in mechanistic-empirical pavement design guide," *Transp. Res. Rec. J. Transp. Res. Board*, no. 1947, pp. 155–166, 2006.
- [86] H. Ceylan, S. Kim, M. Heitzman, and K. Gopalakrishnan, "Sensitivity Study of Iowa Flexible Pavements Using Mechanistic-Empirical Pavement Design Guide," in *Transportation Research Board 85th Annual Meeting*, 2006, no. 06–2139.
- [87] L. Mohammad, Z. Wu, S. Obulareddy, S. Cooper, and C. Abadie, "Permanent deformation analysis of hot-mix asphalt mixtures with simple performance tests and 2002 mechanistic-empirical pavement design software," *Transp. Res. Rec. J. Transp. Res. Board*, no. 1970, pp. 133–142, 2006.

- [88] H. Yin, G. R. Chehab, and S. M. Stoffels, "A case study: assessing the sensitivity of the coefficient of thermal contraction of AC mixtures on thermal crack prediction," in *Asphalt Concrete Simulation, Modeling, and Experimental Characterization. R. Lytton Symposium on Mechanics of Flexible Pavements*, 2006.
- [89] S. Zaghoul, A. Ayed, A. El Halim, N. Vitillo, and R. Sauber, "Investigations of environmental and traffic impacts on mechanistic-empirical pavement design guide predictions," *Transp. Res. Rec. J. Transp. Res. Board*, no. 1967, pp. 148–159, 2006.
- [90] T. E. Hoerner, K. A. Zimmerman, K. D. Smith, and L. A. Cooley, "Mechanistic-Empirical Pavement Design Guide Implementation Plan," 2007.
- [91] S. Kim, H. Ceylan, and K. Gopalakrishnan, "Effect of ME design guide inputs on flexible pavement performance predictions," *Road Mater. Pavement Des.*, vol. 8, no. 3, pp. 375–397, 2007.
- [92] N. Buch, K. Chatti, S. W. Haider, and A. Manik, "Evaluation of the 1-37A design process for new and rehabilitated JPCP and HMA pavements, final report," *Michigan Dep. Transp. Constr. Technol. Div. PO Box*, vol. 30049, 2008.
- [93] L. Khazanovich, S. F. Wojtkiewicz, and R. Velasquez, "MEPDG-RED: Framework for Reliability Analysis with Mechanistic-Empirical Pavement Design Procedure," in *Transportation Research Board 87th Annual Meeting*, 2008, no. 08–3142.
- [94] J. P. Aguiar-Moya, A. Banerjee, and J. A. Prozzi, "Sensitivity analysis of the MEPDG using measured probability distributions of pavement layer thickness," in *Transportation Research Board 88th Annual Meeting*, 2009, no. 09–0412.
- [95] S. Ahn, S. Kandala, J. Uzan, and M. M. El-Basyouny, "Comparative analysis of input traffic data and MEPDG output for flexible pavements in state of Arizona," in *Transportation Research Board 88th Annual Meeting*, 2009, no. 09–2875.
- [96] C. W. Schwartz, "Influence of unbound materials on flexible pavement performance: a comparison of the AASHTO and MEPDG methods," in *Bearing Capacity of Roads, Railways and Airfields. 8th International Conference (BCR2A'09)*, 2009.
- [97] S. Thyagarajan, N. Sivaneswaran, B. Muhunthan, and K. Petros, "Statistical Analysis of Critical Input Parameters in Mechanistic Empirical Pavement Design Guide," *J. Assoc. Asph. Paving Technol.*, vol. 79, 2010.
- [98] K. D. Hall, X. Xiao, and K. C. P. Wang, "Thickness estimation of existing pavements using nondestructive techniques: matching accuracy to application," in *Transportation Research Board 89th Annual Meeting*, 2010, no. 10–2480.
- [99] C. W. Schwartz and R. Li, "Sensitivity of predicted flexible pavement performance to unbound material hydraulic properties," in *GeoFlorida 2010@ Advances in Analysis, Modeling & Design*, 2010, pp. 2672–2681.
- [100] H. Yin, G. R. Chehab, S. M. Stoffels, T. Kumar, and L. Premkumar, "Use of creep compliance interconverted from complex modulus for thermal cracking prediction using the M–E pavement design guide," *Int. J. Pavement Eng.*, vol.

- 11, no. 2, pp. 95–105, 2010.
- [101] PavementInteractive, “Equivalent Single Axle Load,” 2007. [Online]. Available: <http://www.pavementinteractive.org/article/equivalent-single-axle-load/>.
- [102] PavementInteractive, “Roughness,” 2007. [Online]. Available: <http://www.pavementinteractive.org/article/roughness/>.
- [103] B. Al-Omari and M. I. Darter, “Relationships between International Roughness Index and Present Serviceability Rating,” *Transp. Res. Rec. 1435, Transp. Res. Board, Washingt. D.C.*, 1994.
- [104] S. Gulen, R. Woods, J. Weaver, and V. L. Anderson, “Correlation of present serviceability ratings with international roughness index,” *Transp. Res. Rec.*, vol. 1435, p. 27, 1994.
- [105] K. Hall and C. Muñoz, “Estimation of present serviceability index from international roughness index,” *Transp. Res. Rec. J. Transp. Res. Board*, no. 1655, pp. 93–99, 1999.
- [106] “Guide for Mechanistic-Empirical Design of New and Rehabilitated Pavement Structures,” *NCHRP*, vol. Appendix I, 2003.
- [107] L. Tashman and M. A. Elangovan, “Dynamic Modulus Test-Laboratory Investigation and Future Implementation in the State of Washington,” 2008.
- [108] M. W. Witczak, *Simple performance tests: Summary of recommended methods and database*, vol. 46. Transportation Research Board, 2005.
- [109] H. Azari, G. Al-Khateeb, A. Shenoy, and N. Gibson, “Comparison of Simple Performance Test| E*| of Accelerated Loading Facility Mixtures and Prediction| E*|: Use of NCHRP 1-37A and Witczak’s New Equations,” *Transp. Res. Rec. J. Transp. Res. Board*, 2007.
- [110] M. W. Witczak, *Specification criteria for simple performance tests for rutting*, vol. 1. Transportation Research Board, 2007.
- [111] N. S. Kahil, S. S. Najjar, and G. Chehab, “Probabilistic Modeling of Dynamic Modulus Master Curves for Hot-Mix Asphalt Mixtures,” in *Transportation Research Board 94th Annual Meeting*, 2015, no. 15–4392.
- [112] A. A. of S. Highway, T. Officials, A. S. University, F. C. (Firm), and N. C. H. R. Program, *A Performance-related Specification for Hot-mixed Asphalt*, vol. 704. Transportation Research Board, 2011.
- [113] M. W. Witczak, M. El-Basyouny, and J. Uzan, *Adapting Specification Criteria for Simple Performance Tests to HMA Mix Design*. National Cooperative Highway Research Program, Transportation Research Board of the National Academies, 2011.
- [114] M. W. Witczak and J. Uzan, “NCHRP Web-Only Document 172: Adapting Specification Criteria for Simple Performance Tests to HMA Mix Design,” no. January, 2011.
- [115] M. El-Basyouny and M. G. Jeong, “Effective Temperature for Analysis of Permanent Deformation and Fatigue Distress on Asphalt Mixtures,” *Transp. Res. Rec. J. Transp. Res. Board*, vol. 2127, no. -1, pp. 155–163, 2010.

- [116] D. Z. Al Hassanieh, "Use of fine recycled concrete aggregates in asphalt mixtures." 2014.
- [117] J. S. Daniel and G. R. Chehab, "Use of RAP mixtures in mechanistic empirical pavement design guide," in *Transportation Research Board 87th Annual Meeting*, 2008, no. 08–2890.
- [118] J. S. Daniel, G. R. Chehab, and D. Ayyala, "Sensitivity of RAP binder grade on performance predictions in the MEPDG," *J. Assoc. Asph. Paving Technol.*, vol. 78, 2009.
- [119] A. K. Apeagyei and S. D. Diefenderfer, "Asphalt Material Design Inputs for Use with the Mechanistic-Empirical Pavement Design Guide in Virginia," 2011.
- [120] Rs. Team, "RStudio: integrated development for R," *RStudio, Inc., Boston, MA*. URL <http://www.RStudio.com/ide>, 2014.
- [121] D. Andrei, M. W. Witczak, and M. W. Mirza, "Development of Revised Predictive Model for the Dynamic Complex Modulus of Asphalt Mixtures (NCHRP 1-37A)." University of Maryland, College Park, Maryland, 2005.
- [122] Y. Hamdar, H. Kassem, I. Srour, and G. Chehab, "Performance-Based Specifications for Sustainable Pavements: A Lean Engineering Analysis," *Energy Procedia*, vol. 74, pp. 453–461, 2015.
- [123] Transport Research Board, "Glossary of highway quality assurance terms," no. May, p. 40, 2005.

APPENDIX

MEPDG DESIGN INPUTS FOR ASPHALT MIXES

This Appendix presents the MEPDG design inputs of the mixes included in the scope (Table 4.1) from Source 1, Source 1, Source 2, and Source 3. Those acquired from Source 4 can be found in reference [119].

M-HMA-1

Asphalt Mix: Dynamic Modulus Table

Temperature (°F)	Mixture E* (psi)					
	0.1 Hz	0.5 Hz	1 Hz	5 Hz	10 Hz	25 Hz
14	3208099	3522599	3647269	3910542	4012657	4137506
40	2117522	2496374	2657080	3016684	3163665	3349119
70	930637	1230921	1373608	1728913	1889364	2105179
100	262275	392797	462902	661646	763410	912928
130	50355	82100	100938	160878	195271	250385

Asphalt Binder: Superpave Binder Test Data

Temperature (°F)	Angular Freq. = 10 rad/s	
	G* (Pa)	Delta (degrees)
168.8	1948.05	66.058
179.6	1212.26	64.151
190.4	808.26	60.891

Asphalt General: Volumetric Properties as Built

Effective Binder Content (%)	9.2
Air Voids (%)	6
Total Unit Weight (pcf)	157.6

M-HMA-2

Asphalt Mix: Dynamic Modulus Table

Temperature (°F)	Mixture E* (psi)					
	0.1 Hz	0.5 Hz	1 Hz	5 Hz	10 Hz	25 Hz
14	3279589	3593912	3719218	3985764	4090017	4218268
40	2145328	2525728	2686909	3048160	3196346	3384031
70	895182	1197940	1341633	1698802	1859902	2076602
100	220664	341671	407912	598482	697071	842662
130	36359	61227	76402	126177	155517	203395

Asphalt Binder: Superpave Binder Test Data

Angular Freq. = 10 rad/s		
Temperature (°F)	G* (Pa)	Delta (degrees)
168.8	1948.05	66.058
179.6	1212.26	64.151
190.4	808.26	60.891

Asphalt General: Volumetric Properties as Built

Effective Binder Content (%)	9.0
Air Voids (%)	6
Total Unit Weight (pcf)	157.8

HMA-Fib

Asphalt Mix: Dynamic Modulus Table

Temperature (°F)	Mixture E* (psi)					
	20 Hz	10 Hz	5 Hz	1 Hz	0.5 Hz	0.1 Hz
20	4543544	4392096	4228303	3800447	3596606	3084723
40	3207679	2979533	2745406	2192506	1957292	1440471
70	1276038	1086253	913142	581527	469410	274234
100	399723	317442	249915	139843	108169	59453
125	192884	150619	117150	64982	50502	28598

Asphalt Binder: Superpave Binder Test Data

Angular Freq. = 10 rad/s		
Temperature (°F)	G* (Pa)	Delta (degrees)
125.6	5940.29	86.342
136.4	2578.88	87.511
147.2	1176.28	88.371
158	569.84	88.907
168.8	294.42	89.14

Asphalt General: Volumetric Properties as Built

Effective Binder Content (%)	9.9
Air Voids (%)	6
Total Unit Weight (pcf)	157.6

HMA-1

Asphalt Mix: Dynamic Modulus Table

Temperature (°F)	Mixture E* (psi)					
	20 Hz	10 Hz	5 Hz	1 Hz	0.5 Hz	0.1 Hz
20	4791307	4625657	4447113	3983278	3763398	3213749
40	3341834	3095905	2844282	2253050	2002802	1455754
70	1289850	1089380	907376	561810	446331	248348
100	392638	305659	234936	122213	90921	45010
125	184162	138717	103524	51238	37703	18773

Asphalt Binder: Superpave Binder Test Data

Temperature (°F)	Angular Freq. = 10 rad/s	
	G* (Pa)	Delta (degrees)
125.6	5940.29	86.342
136.4	2578.88	87.511
147.2	1176.28	88.371
158	569.84	88.907
168.8	294.42	89.14

Asphalt General: Volumetric Properties as Built

Effective Binder Content (%)	9.9
Air Voids (%)	6
Total Unit Weight (pcf)	157.6

M-HMA-3

Asphalt Mix: Dynamic Modulus Table

Temperature (°F)	Mixture E* (psi)					
	20 Hz	10 Hz	5 Hz	1 Hz	0.5 Hz	0.1 Hz
20	4686698	4519579	4343059	3898384	3693090	3190689
40	3352774	3128752	2900966	2367964	2141729	1640637
70	1431145	1243935	1070779	728274	607248	384978
100	461185	376190	304496	181766	144337	83561
125	189873	150548	118924	68309	53816	31274

Asphalt Binder: Superpave Binder Test Data

Angular Freq. = 10 rad/s		
Temperature (°F)	G* (Pa)	Delta (degrees)
168.8	1948.05	66.058
179.6	1212.26	64.151
190.4	808.26	60.891

Asphalt General: Volumetric Properties as Built

Effective Binder Content (%)	9.7
Air Voids (%)	6
Total Unit Weight (pcf)	157.7

M-WMA-O

Asphalt Mix: Dynamic Modulus Table

Temperature (°F)	Mixture E* (psi)					
	20 Hz	10 Hz	5 Hz	1 Hz	0.5 Hz	0.1 Hz
20	4413808	4282664	4140952	3770541	3593554	3146186
40	3254115	3052222	2843680	2344195	2127878	1641266
70	1444049	1258527	1086045	743072	621556	398399
100	507592	417667	341542	210492	170249	104341
125	244146	197637	159827	98149	80063	51201

Asphalt Binder: Superpave Binder Test Data

Angular Freq. = 10 rad/s		
Temperature (°F)	G* (Pa)	Delta (degrees)
168.8	2415.59	64.41
179.6	1503.2	62.55
190.4	1002.24	59.37

Asphalt General: Volumetric Properties as Built

Effective Binder Content (%)	9.7
Air Voids (%)	6
Total Unit Weight (pcf)	157.7

M-WMA-C

Asphalt Mix: Dynamic Modulus Table

Temperature (°F)	Mixture E* (psi)					
	20 Hz	10 Hz	5 Hz	1 Hz	0.5 Hz	0.1 Hz
20	4057713	3961272	3853496	3555560	3405521	3006447
40	3080735	2893071	2694326	2201387	1982204	1482701
70	1266272	1077971	905521	575387	464541	273690
100	373905	297000	234712	135125	106961	63980
125	167953	132474	104902	62863	51354	33903

Asphalt Binder: Superpave Binder Test Data

Angular Freq. = 10 rad/s		
Temperature (°F)	G* (Pa)	Delta (degrees)
168.8	1363.635	66.058
179.6	848.582	64.151
190.4	565.782	60.891

Asphalt General: Volumetric Properties as Built

Effective Binder Content (%)	10.3
Air Voids (%)	6
Total Unit Weight (pcf)	156.6

M-WMA-F

Asphalt Mix: Dynamic Modulus Table

Temperature (°F)	Mixture E* (psi)					
	20 Hz	10 Hz	5 Hz	1 Hz	0.5 Hz	0.1 Hz
20	4975324	4823426	4656024	4205426	3984916	3417929
40	3550912	3292688	3025212	2387462	2115326	1521092
70	1293183	1083202	895500	549324	437348	250360
100	344184	270040	211006	118700	93083	54369
125	144524	112965	88680	52004	42006	26812

Asphalt Binder: Superpave Binder Test Data

Temperature (°F)	Angular Freq. = 10 rad/s	
	G* (Pa)	Delta (degrees)
168.8	1948.05	66.06
179.6	1212.26	64.15
190.4	808.26	60.89

Asphalt General: Volumetric Properties as Built

Effective Binder Content (%)	9.8
Air Voids (%)	6
Total Unit Weight (pcf)	156.6

HMA-2

Asphalt Mix: Dynamic Modulus Table

Temperature (°F)	Mixture E* (psi)					
	20 Hz	10 Hz	5 Hz	1 Hz	0.5 Hz	0.1 Hz
20	5426812	5268411	5096279	4641844	4422501	3861992
40	4078316	3825250	3561389	2919628	2637671	1995891
70	1732340	1484946	1255317	803743	647327	370623
100	443303	343544	262771	135029	99870	48570
125	130324	96003	70288	33717	24602	12071

Asphalt Binder: Superpave Binder Test Data

Angular Freq. = 10 rad/s		
Temperature (°F)	G* (Pa)	Delta (degrees)
125.6	5940.29	86.342
136.4	2578.88	87.511
147.2	1176.28	88.371
158	569.84	88.907
168.8	294.42	89.14

Asphalt General: Volumetric Properties as Built

Effective Binder Content (%)	8.5
Air Voids (%)	6
Total Unit Weight (pcf)	159.3

WMA-O

Asphalt Mix: Dynamic Modulus Table

Temperature (°F)	Mixture E* (psi)					
	20 Hz	10 Hz	5 Hz	1 Hz	0.5 Hz	0.1 Hz
20	4220073	4115158	3998704	3680244	3521377	3102134
40	3235066	3042147	2837660	2327743	2098829	1569088
70	1534061	1316494	1110765	696400	550589	293180
100	633233	497078	381705	189371	134898	56993
125	447244	344301	259419	123389	86375	35136

Asphalt Binder: Superpave Binder Test Data

Temperature (°F)	Angular Freq. = 10 rad/s	
	G* (Pa)	Delta (degrees)
125.6	7365.95	84.18
136.4	3197.81	85.32
147.2	1458.59	86.16
158	706.6	86.68
168.8	365.08	86.91

Asphalt General: Volumetric Properties as Built

Effective Binder Content (%)	8.3
Air Voids (%)	6
Total Unit Weight (pcf)	159.4

WMA-C

Asphalt Mix: Dynamic Modulus Table

Temperature (°F)	Mixture E* (psi)					
	20 Hz	10 Hz	5 Hz	1 Hz	0.5 Hz	0.1 Hz
20	4773229	4630291	4472106	4043422	3832332	3286406
40	3414389	3162658	2900748	2272370	2003002	1413922
70	1335380	1112937	912349	539752	419474	221891
100	481894	371953	283241	144434	106835	52775
125	319485	241692	180953	90081	66447	33226

Asphalt Binder: Superpave Binder Test Data

Temperature (°F)	Angular Freq. = 10 rad/s	
	G* (Pa)	Delta (degrees)
125.6	7365.95	86.34
136.4	3197.81	87.51
147.2	1458.59	88.37
158	353.3	88.91
168.8	182.54	89.14

Asphalt General: Volumetric Properties as Built

Effective Binder Content (%)	8.3
Air Voids (%)	6
Total Unit Weight (pcf)	159.4

WMA-F

Asphalt Mix: Dynamic Modulus Table

Temperature (°F)	Mixture E* (psi)					
	20 Hz	10 Hz	5 Hz	1 Hz	0.5 Hz	0.1 Hz
20	4660498	4531551	4388795	4000585	3808217	3305245
40	3481905	3253764	3013647	2423460	2163058	1573679
70	1415914	1189785	982311	586180	454837	235223
100	377604	285129	211738	100265	71253	31402
125	154862	112786	81127	36403	25542	11258

Asphalt Binder: Superpave Binder Test Data

Temperature (°F)	Angular Freq. = 10 rad/s	
	G* (Pa)	Delta (degrees)
125.6	5940.29	86.34
136.4	2578.88	87.51
147.2	1176.28	88.37
158	569.84	88.91
168.8	294.42	89.14

Asphalt General: Volumetric Properties as Built

Effective Binder Content (%)	8.4
Air Voids (%)	6
Total Unit Weight (pcf)	159.4

HMA-3

Asphalt Mix: Dynamic Modulus Table

Temperature (°F)	Mixture E* (psi)					
	20 Hz	10 Hz	5 Hz	1 Hz	0.5 Hz	0.1 Hz
20	3609002	3555416	3495307	3327229	3241149	3005748
40	2997382	2879109	2750899	2416274	2257827	1865732
70	1416610	1246475	1082929	741962	616302	380522
100	295159	232191	181023	99164	76143	41469
125	60734	46761	36174	20535	16366	10136

Asphalt Binder: Superpave Binder Test Data

Angular Freq. = 10 rad/s		
Temperature (°F)	G* (Pa)	Delta (degrees)
136.4	2152.115	86.96
147.2	1024.59	87.98
158	507.94	88.725
168.8	260.485	89.205
179.6	141.29	89.395
190.4	81.875	89.4

Asphalt General: Volumetric Properties as Built

Effective Binder Content (%)	10.6
Air Voids (%)	6
Total Unit Weight (pcf)	146.5

HMA-RA-1

Asphalt Mix: Dynamic Modulus Table

Temperature (°F)	Mixture E* (psi)					
	20 Hz	10 Hz	5 Hz	1 Hz	0.5 Hz	0.1 Hz
20	4505943	4423809	4332965	4085078	3961124	3630743
40	3569771	3405699	3230896	2787856	2584003	2093891
70	1558940	1360755	1172821	788817	649908	393178
100	344610	270024	209230	111673	84258	43311
125	98359	74439	56056	28790	21659	11457

Asphalt Binder: Superpave Binder Test Data

Angular Freq. = 10 rad/s		
Temperature (°F)	G* (Pa)	Delta (degrees)
136.4	2152.115	86.96
147.2	1024.59	87.98
158	507.94	88.725
168.8	260.485	89.205
179.6	141.29	89.395
190.4	81.875	89.4

Asphalt General: Volumetric Properties as Built

Effective Binder Content (%)	10.1
Air Voids (%)	6
Total Unit Weight (pcf)	146.1

HMA-RA-2

Asphalt Mix: Dynamic Modulus Table

Temperature (°F)	Mixture E* (psi)					
	20 Hz	10 Hz	5 Hz	1 Hz	0.5 Hz	0.1 Hz
20	4272818	4198887	4116739	3890783	3776913	3470910
40	3459532	3308869	3147329	2733620	2541385	2074931
70	1637113	1441248	1253626	863900	720462	450713
100	428636	342401	270830	152549	118141	64936
125	125403	96795	74665	41236	32206	18727

Asphalt Binder: Superpave Binder Test Data

Angular Freq. = 10 rad/s		
Temperature (°F)	G* (Pa)	Delta (degrees)
136.4	2152.115	86.96
147.2	1024.59	87.98
158	507.94	88.725
168.8	260.485	89.205
179.6	141.29	89.395
190.4	81.875	89.4

Asphalt General: Volumetric Properties as Built

Effective Binder Content (%)	10.5
Air Voids (%)	6
Total Unit Weight (pcf)	144.5

HMA-RA-3

Asphalt Mix: Dynamic Modulus Table

Temperature (°F)	Mixture E* (psi)					
	20 Hz	10 Hz	5 Hz	1 Hz	0.5 Hz	0.1 Hz
20	3803427	3740303	3669703	3473386	3373445	3102170
40	3033825	2894940	2745784	2363398	2185897	1757028
70	1340767	1166141	1000817	665296	545281	326706
100	348635	275357	215376	118450	90940	49266
125	129079	99749	76940	42285	32894	18901

Asphalt Binder: Superpave Binder Test Data

Angular Freq. = 10 rad/s		
Temperature (°F)	G* (Pa)	Delta (degrees)
136.4	2152.115	86.96
147.2	1024.59	87.98
158	507.94	88.725
168.8	260.485	89.205
179.6	141.29	89.395
190.4	81.875	89.4

Asphalt General: Volumetric Properties as Built

Effective Binder Content (%)	10.9
Air Voids (%)	6
Total Unit Weight (pcf)	143.2

HMA-4

Asphalt Mix: Dynamic Modulus Table

Mixture E* (psi)					
Temperature (°F)	0.1 Hz	1 Hz	5 Hz	10 Hz	20 Hz
14	2042248	2401625	2660185	2629291	2730767
32	1103230	1614329	2001256	2234427	2240292
50	348977	725202	1073379	1243976	1340271
68	103164	274268	514848	653430	767041
86	27218	76004	159345	233969	346456
131	10000	15363	32354	45236	63391

Asphalt Binder: Superpave Binder Test Data

Angular Freq. = 10 rad/s		
Temperature (°F)	G* (Pa)	Delta (degrees)
136.4	6750	77.6
147.2	3270	80.1
158	1590	82.3

Asphalt General: Volumetric Properties as Built

Effective Binder Content (%)	10.5
Air Voids (%)	6
Total Unit Weight (pcf)	154.4

HMA-RAP-1

Asphalt Mix: Dynamic Modulus Table

Mixture E* (psi)					
Temperature (°F)	0.1 Hz	1 Hz	5 Hz	10 Hz	20 Hz
14	2087443	2478274	2739177	2797299	2671795
32	1203543	1678954	1978952	1949184	1900163
50	484174	869841	1211053	1246477	1661107
68	165332	388293	640245	786766	999318
86	59351	145327	283426	383186	510125
131	49568	134511	258074	333821	424520

Asphalt Binder: Superpave Binder Test Data

Angular Freq. = 10 rad/s		
Temperature (°F)	G* (Pa)	Delta (degrees)
136.4	6750	77.6
147.2	3270	80.1
158	1590	82.3

Asphalt General: Volumetric Properties as Built

Effective Binder Content (%)	10.5
Air Voids (%)	6
Total Unit Weight (pcf)	155.0

HMA-RAP-2

Asphalt Mix: Dynamic Modulus Table

Mixture E* (psi)					
Temperature (°F)	0.1 Hz	1 Hz	5 Hz	10 Hz	20 Hz
14	2393371	2705771	2921260	3019173	2453416
32	1469594	1928551	2236964	2394778	2302709
50	788353	1159118	1537259	1705726	1999689
68	300735	566906	843035	981117	1165093
86	92384	217822	405777	524012	581912
131	29990	78929	151865	198251	255657

Asphalt Binder: Superpave Binder Test Data

Angular Freq. = 10 rad/s		
Temperature (°F)	G* (Pa)	Delta (degrees)
135.5	10310	67.6
146.1	5480	70.3
156.6	3039	72.9

Asphalt General: Volumetric Properties as Built

Effective Binder Content (%)	10.5
Air Voids (%)	6
Total Unit Weight (pcf)	154.4

HMA-RAP-3

Asphalt Mix: Dynamic Modulus Table

Temperature (°F)	Mixture E* (psi)				
	0.1 Hz	1 Hz	5 Hz	10 Hz	20 Hz
14	2249242	2753567	3047687	3005649	2670748
32	1571405	1953848	2206776	2191162	2345823
50	873591	1273048	1596426	1742522	1614686
68	352946	655022	941305	1102959	1111204
86	135116	280157	477064	585646	642566
131	33268	90421	168128	214630	270089

Asphalt Binder: Superpave Binder Test Data

Angular Freq. = 10 rad/s		
Temperature (°F)	G* (Pa)	Delta (degrees)
168.8	3510	59
179.6	2200	59.6
190.4	1390	60.9

Asphalt General: Volumetric Properties as Built

Effective Binder Content (%)	10.5
Air Voids (%)	6
Total Unit Weight (pcf)	155.2

